Functional assistive devices to support the impaired shoulder and hand

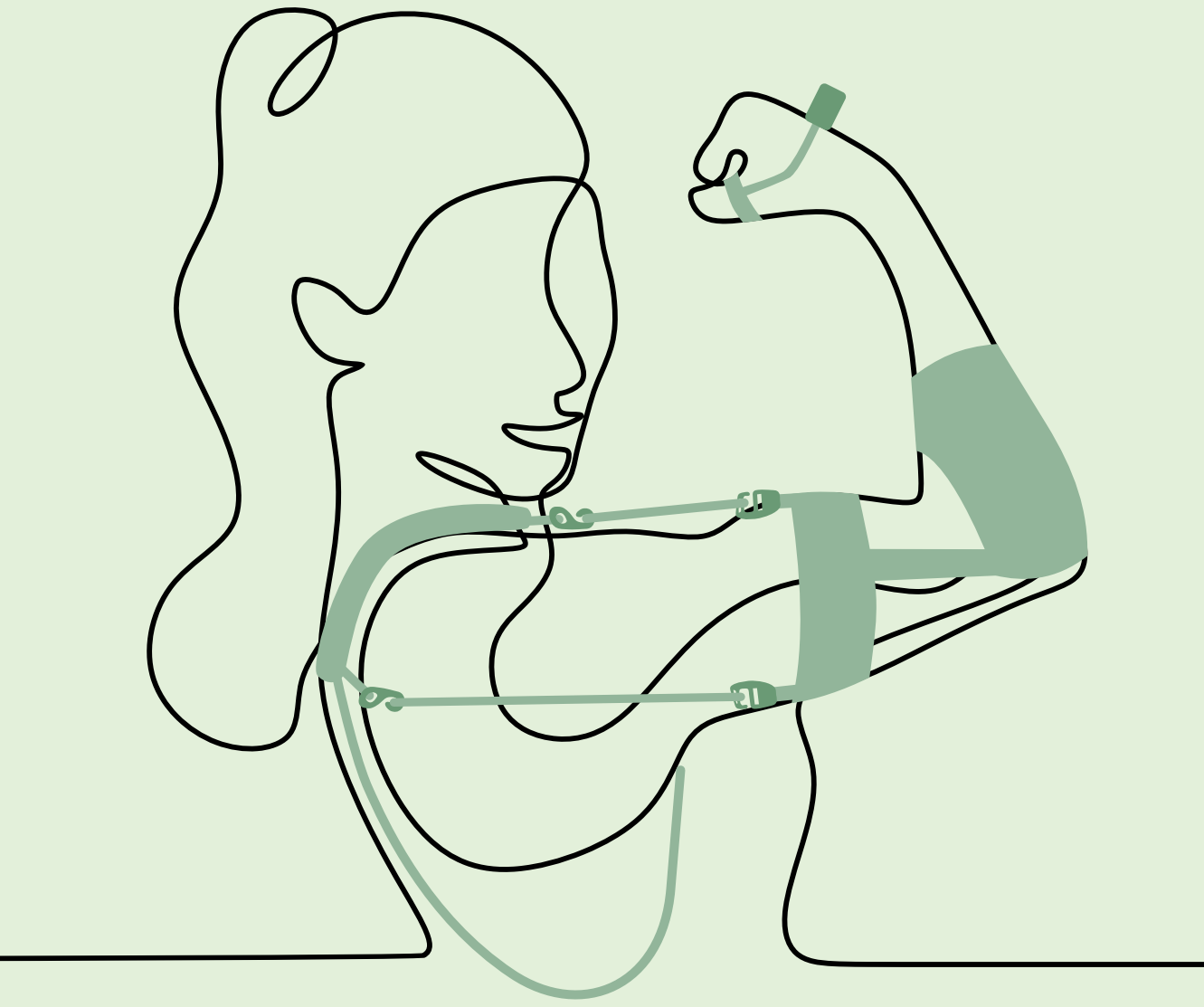

Claudia Haarman

FUNCTIONAL ASSISTIVE DEVICES TO SUPPORT THE IMPAIRED SHOULDER AND HAND

Claudia Haarman

FUNCTIONAL ASSISTIVE DEVICES TO SUPPORT THE IMPAIRED SHOULDER AND HAND

DISSERTATION

to obtain

the degree of doctor at the University of Twente,
on the authority of the rector magnificus,
prof. dr. ir. A. Veldkamp,
on account of the decision of the Doctorate Board
to be publicly defended
on Thursday 29 September 2022 at 12.45 hours

Claudia Josephina Wilhelmina Haarman

born on the 18th of November, 1987
in Raalte, The Netherlands

This dissertation has been approved by:

Supervisors

prof. dr. ir. H. van der Kooij
prof. dr. J.S. Rietman

This work was partly supported by the European Unions Horizon 2020 research and innovation programme under Grant 688857 (SoftPro).

This work has benefited from the advice and financial support of the following companies, whose support is thankfully acknowledged.

Cover design: Claudia Haarman

Printed by: Gildeprint – The Netherlands

Lay-out: Claudia Haarman

ISBN: 978-90-365-5437-4

DOI: 10.3990/1.9789036554374

Graduation Committee:

Chair / secretary:	prof.dr.ir. H.F.J.M. Koopman
Supervisors:	prof.dr.ir. H. van der Kooij Universiteit Twente
	prof.dr. J.S. Rietman Universiteit Twente
Committee Members:	prof.dr.ir. G.J.M. Tuijthof Universiteit Twente
	prof.dr.ir. G.D.S. Ludden Universiteit Twente
	prof. dr. R.W. Selles Erasmus MC
	prof.em. K. Postema Rijksuniversiteit Groningen
	dr. J.F.M. Fleuren Roessingh

In his capacity as daily supervisor ir. E.E.G. Hekman has significantly contributed to the creation of this thesis.

Contents

1. Introduction

Functional use of the arms and hands is important in daily life and promotes the autonomy of humans. Patients with upper extremity impairments may benefit from assistive devices that support their affected body function during the execution of daily activities to increase their independence. However, existing assistive technologies often do not meet basic user requirements regarding effectiveness and comfort, leading to high rejection rates of these devices. Therefore, a new generation of assistive devices supporting the impaired upper extremity during daily activities is required.

This thesis describes the research that has been performed to develop and evaluate three assistive devices, one to reduce disability caused by impaired shoulder function and two to reduce disability caused by impaired hand function. This introduction starts with a description of the healthy upper extremity. Then, a theoretical model for describing disability is presented, followed by a paragraph on upper extremity impairments. Next, an overview of existing assistive devices is presented, including their shortcomings. Finally, the research objectives and the thesis outline are discussed.

1.1. The upper extremity

The upper extremity plays an essential role in daily functioning as it is involved in reaching and grasping. A redundant number of degrees of freedom in the kinematic chain of the upper extremity allows the human to select the best combination of joint motions for a particular task [1,2]. The shoulder and elbow bring the hand to a position where objects are within reach, so that they can be grasped by the hand. To limit the scope, this thesis focuses on the shoulder (reaching) and the hand (grasping).

The shoulder complex entails three joints, acromioclavicular (AC) joint, sternoclavicular (SC) joint and glenohumeral (GH) joint. The SC joint connects the shoulder complex to the trunk. The scapulothoracic articulation together with stabilizing muscles trapezius, serratus anterior and rhomboid contributes to stability of the scapula. The GH joint contributes the most to the mobility of the arm [3]. This joint, between the humeral head and the scapula, is a ball-and-socket joint with three degrees of freedom, and allows for abduction/adduction, flexion/extension and internal/external rotation movements. As the articulating surface between the glenoid of the scapula and the humeral head is shallow, static structures (i.e. capsule and ligaments) and dynamic structures (i.e. rotator cuff muscles) are required to stabilize the GH joint. Four basic mechanical characteristics define normal shoulder function: motion, stability, strength and smoothness [4]. Many shoulder pathologies affect the GH joint and compromise one or more of these mechanical characteristics. Even though most daily activities do not require maximum mobility [5] and strength [6], still it is crucial that a functional range of motion and sufficient stability and strength of the GH joint can be maintained.

The hand is a complex interplay of many bones, ligaments, tendons and muscles [7]. Each finger has four degrees of freedom: three for flexion/extension and one for

abduction/adduction. The thumb has five degrees of freedom. This large number of degrees of freedom allows the human to employ many different grasp types in their daily activities including power or precision grasps [8]. Power grasps are associated with gross finger movements, whereas precision grasps are associated with fine finger movements.

Hand grasps consist of two phases: pre-shaping and grasping [9]. During pre-shaping the hand is adapted to the object's size and shape. This occurs in parallel to the reaching movement of the arm. Typically the fingers move from a closed initial position to a maximum aperture. After approximately 60-70% of the reaching movement, the fingers begin to close and adapt to the size and shape of the object [10]. Three overlapping sets of constraints determine the feasible grasp space for a particular task during the grasping phase, see also Fig. 1.1 [11]. These are: task constraints (forces, motions), objects constraints (shape, fragility) and hand constraints (maximum grasp force, maximum hand opening). Choosing a grasp from this feasible grasp space involves the optimization of an objective function that considers quality measures such as stability, resistance to slipping and internal forces, etcetera [11]. However, if the set of constraints do not overlap, for example due to lack of muscle force, then no grasp is feasible and the task cannot be performed.

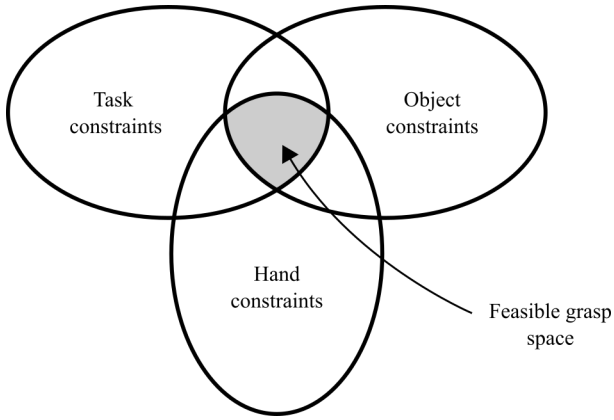

Fig. 1.1 – The intersection between task, object and hand constraints determines the feasible grasp space. (Adapted from [11])

1.2. International Classification of Functioning, Disability and Health

The International Classification of Functioning, Disability and Health (ICF) is a framework for describing health and disability [12]. According to the ICF biopsychosocial model (see Fig. 1.2), disability involves dysfunction on one or more levels: (1) impairments in body function (physiological) or body structure (anatomy), (2) activity limitations, and (3) participation restrictions [13]. From the model follows that the degree of disability is not only determined by the health condition, but contextual factors should also be considered. Contextual factors include external, environmental factors (e.g. legal and social structures, climate, etc.) and internal, personal factors (e.g. gender, age, education, profession etc.). As long as the disability can be managed effectively such that activities are not limited and

participation in society is not restricted, the effects of disability may not pose real problems in daily life. However, solutions may be required if this is not possible. Assistive devices can contribute to reducing the effect of disability [14].

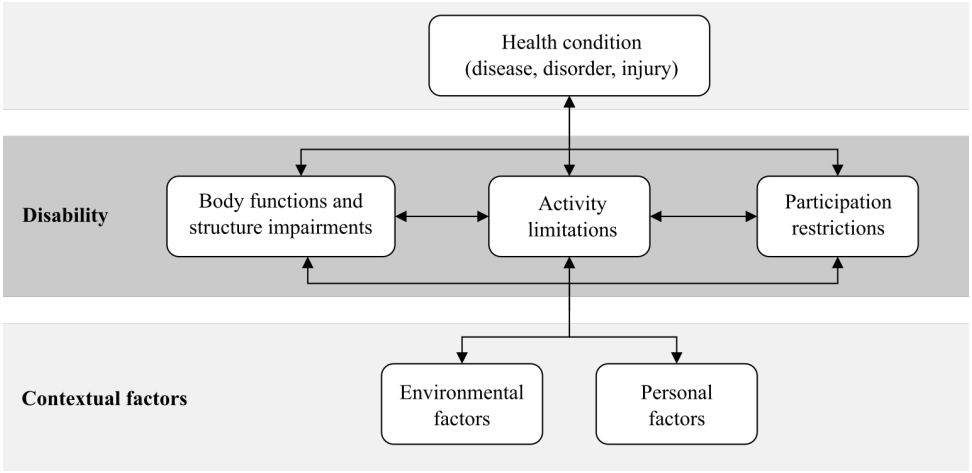

Fig. 1.2 – The biopsychosocial model of disability. Disability is defined on an impairments, activity and participation level. Interaction between health conditions and contextual factors determine the degree of impairment. (Adapted from [13])

1.3. The impaired upper extremity

Impairments of body function and structure can manifest themselves as motor, sensory or cognitive impairments. In this research, only motor impairments will be considered. Symptoms arising from motor impairments can either be 'positive' or 'negative' [15]. Positive symptoms refer to the release of abnormal behavior, such as increased muscle tone (hypertonicity) or pain (myalgias). Negative symptoms refer to the loss of normal behavior, for instance due to limited muscle activation [16].

Impaired shoulder function may be caused by a decreased tone of the rotator cuff muscles (negative symptom) due to for example shoulder trauma or neuromuscular disorders [17-18]. This may lead to glenohumeral instability and subluxation, which is defined as a partial dislocation of the glenohumeral joint [19]. The subsequent stretch of the passive structures around this joint may provoke shoulder pain [20]. Patients suffering from shoulder pain often still have the capacity to successfully execute tasks, but pain is preventing them from actively engaging their affected shoulder in daily activities, leading to a decreased performance (activity and participation level). Active engagement of the arm is associated with the preservation of glenohumeral alignment [21].

Neurological disorders such as stroke, or musculoskeletal conditions such as traumatic injuries or muscular disorders are common causes of hand impairments [22]. Depending on

their impairment(s), patients may require support of the impaired hand during grasping, hand opening, or both. Two common patterns of impaired hand function are discussed below.

Movement deficits associated with stroke may include abnormal, increased muscle tone of the finger flexor muscles (positive symptom). This leads to increased joint stiffness and a loss of joint mobility [23]. As a result, stroke patients will not be able to sufficiently extend their fingers during the pre-shaping phase, and objects cannot be grasped [24]. Depending of the severity of their impairment, the forces required to extend the fingers of these patients can be high [25].

Movement deficits associated with cervical spinal cord injury may include muscle weakness due to a lack of voluntary muscle control (negative symptom). Muscle weakness in turn leads to increased stiffness and immobility, which can introduce other problems that contribute to motor impairments [26]. Spinal cord injury patients with lack of voluntary control of the finger flexors typically have problems generating sufficient grip strength which negatively affects their performance during activities of daily living [27].

1.4. Assistive devices

Assistive devices are examples of physical environmental interventions that can: (1) reduce the effects of impairments by restoring body function, (2) reduce activity limitations and participation restrictions by mitigating performance barriers, or (3) do both in varying degrees [14]. In the context of this research only assistive devices are considered that mitigate both the impact of impairments as well as performance barriers. These body-related assistive devices are commonly referred to as orthoses or exoskeletons. The terms orthoses and exoskeletons will be used interchangeably in this dissertation.

Contrary to devices commonly used in a clinical setting during rehabilitation therapy, assistive devices are specifically designed for use in a home environment to assist with daily activities [28]. This poses strict requirements on their design. Personal factors such as needs, abilities, preferences and past experiences may affect the level of engagement of patients to use assistive devices, or the cognitive burden of a device [29]. Non-use (abandonment) concerns up to one third of all devices provided, and occurs mostly within the first three months [30]. Device abandonment is strongly related to device performance and the degree to which the user's expectations are met regarding effectiveness, reliability, durability, comfort and ease of use [29]. Device development should therefore closely consider the users' needs to enhance their quality of life. We emphasize the importance of improving the performance (i.e. on the activity and participation level) rather than restoring capacity (i.e. on the impairment level). As a consequence, all functionality that does not contribute to this goal shall be omitted from the design.

1.4.1. Assistive devices to support the shoulder

Assistive devices to support the shoulder aim to decrease shoulder pain by reducing the gravitational pull on the passive structures surrounding the shoulder complex and stabilize the joint [31]. The major shortcoming of commercially available shoulder orthoses is that

they limit the remaining motion of the shoulder. For example, the GivMohr sling (Fig. 1.3A) supports the upper extremity by using the extended arm to create an upward force [32]. It requires the use of a hand piece to provide the counteracting force. The device is aimed at patients with a flaccid upper extremity and supports the arm during standing and ambulation. The Omo Neurexa (Fig. 1.3B) (Otto Bock, Germany) and NeuroLux (Fig. 1.3C) (Sporlastic, Germany) provide an upward force and stabilize the shoulder by tensioning non-elastic straps between the arm cuff and a shoulder sleeve. Both devices can stabilize and reposition the humeral head, but restrict arm movements. As a consequence, patients will not be able to functionally use their arm during reaching tasks, unless the tension of the straps (and thus upward force) is reduced. The restriction of arm movements needs to be addressed in a new device to improve performance during daily activities.

Fig. 1.3. – Left: GivMohr sling [32]. Middle: Omo Neurexa Plus (Otto Bock, Germany). Right: NeuroLux (Sporlastic, Germany).

1.4.2. Assistive devices to support the hand

In recent years numerous assistive devices have been developed to support impaired hand function [28,33]. Many of these devices are active, while some are passive (spring-based). They typically support several degrees of freedom to restore hand opening, grasping, or both.

Commercially available assistive devices to support hand opening of patients with increased voluntary muscle tone are mostly passive (i.e. spring-based). The SaeboGlove (Saebo, USA) consists of a glove and a wrist support, see Fig. 1.4A. Individual tensioners located above the finger joints assist the phalanxes with extending. Although the resulting design is slim, the tensioners cannot provide large extension torques that are required to support patients with high finger joint stiffness. The SaeboFlex (Fig. 1.4B) (Saebo, USA) can provide much larger extension torques. It consists of a forearm support and a dorsal hand platform that anchors two spring attachments. Individual finger sleeves are attached to the springs to assist with finger extension. This device was originally designed for training purposes and not for daily activities. As a result, the SaeboFlex is considered too heavy for long-term use and encompasses a large volume. Also, high voluntary flexion torques are required to overcome the spring stiffness [34]. Devices under development to support hand opening mainly concern active, cable-driven systems [35-37], see Fig. 1.4C for an example. In these systems, cables are routed on the dorsal side of the hand through a glove. However, a general drawback of gloves is that they are difficult to put on and limit touch sensation of the finger tips [38].

Fig. 1.4 – Left: SaeboGlove (Saebo, USA). Middle: SaeboFlex (Saebo, USA). Right: Hand Extension Robot Orthosis (HERO) Grip Glove [37].

Other systems under development use gloves with inflatable chambers to extend the finger [39-40], but this requires heavy and bulky actuators [28]. In conclusion, the state of the art lacks a portable device, that is capable of providing large torques to extend the fingers within a small volume. Reducing the size and weight of assistive devices that support hand opening are steps towards a higher degree of acceptability.

Exoskeletons that support grasping typically consist of tendon-driven gloves (cables), jointless structures (pneumatics) or linkages to provide finger flexion [22]. Commercially available active hand exoskeletons that support grasping include cable-driven systems such as NeoMano (Fig. 1.5A) (Neofect, South Korea) and Carbonhand (Fig. 1.5B) (BioServo, Sweden). Both devices use electric motors to control cables that are routed through a glove that support grasping. The exoskeletons provide combined actuation of multiple degrees of freedom. The underactuated approach of both exoskeletons has resulted in compact designs. NeoMano has the most limited functionality as only the thumb, index and middle finger are supported by a single motor to enable a cylindrical grasp. In case of the Carbonhand, the thumb, middle and ring finger are remotely actuated, each with their own motor. The added functionality of the Carbonhand comes at the cost of added weight of two additional motors. Increased compliance and a large number of degrees of freedom are among the biggest advantages of these designs. However, their compliant nature also allows for unwanted movements that may compromise safe operation. Devices currently under development partly solve this problem. For instance, the RELab tenoexo [41], see Fig. 1.5C, contains both rigid and soft structures that help to stabilize the fingers as well as guarantee safe human-machine interaction. Their lightweight, underactuated design features a three-layered sliding spring mechanism that flexes the fingers. The thumb can be manually put into pad and side opposition. The authors claim that their device can generate the four most frequently used

Fig. 1.5 – Left: NeoMano (Neofect, South Korea). Middle: Carbonhand (BioServo, Sweden). Right: RELab tenoexo [41].

grasp types and cover up to 80% of daily grasping activities. The resulting exoskeleton however, consists of many (fragile) components, which makes it difficult to guarantee important user requirements regarding reliability and durability.

Significant advances can be made to the state of the art of assistive hand exoskeletons if the design focuses on the core the functionality that will contribute the most to the performance in daily life. By doing so, hardware complexity will be reduced which will eventually improve reliability and durability and increase the uptake of technology in daily life.

1.5. Objectives

The main contribution of this thesis is to develop and evaluate novel assistive devices that support patients with impaired shoulder or hand function. The focus of this research lies on improving the state of the art, by exploring and iteratively testing alternative mechanical design strategies that can provide functional benefit to the user during daily activities which in turn promote the person's independence [14]. We believe that device development should not consider restoring normal (healthy) function, but should rather tackle limiting factors that prevent patients from engaging their affected upper limb in daily life. Several functional requirements are currently not sufficiently addressed in the state of the art. The context in which the technology is used, plays an important role during the design of assistive devices. The environment, together with the user's characteristics largely determine the perceived benefit. Devices that work well in one context, e.g. when used by a stroke patient with unilateral hand function, may not adequately address the user's needs when used in a different context, e.g. when used a bimanually affected spinal cord injury patient in a wheelchair.

In case of a shoulder orthosis that supports the shoulder of patients with chronic shoulder pain, the objective is therefore to develop a mechanism that supports the arm without impeding residual movements. In case of a hand orthosis that supports hand opening of stroke patients with increased flexor muscle tone, the objective is to develop a mechanical structure that is capable of providing large extension torques, and allows for easy donning and doffing by the patient. In case of a hand orthosis that supports grasping of spinal cord injury patients, the objective is to develop a system that allows users to complete basic activities of daily living by supporting the impaired hand. To this end, we adopt a user-centered, iterative design approach that enables us to capture basic user requirements and gather user feedback during the evaluation of prototypes. Interviews, observations and questionnaires aim to find gaps between the users' current and desired level of shoulder and hand function, and capture past experiences with other technologies.

Problem simplification will help to maintain the overall design goal of developing effective, reliable, durable, comfortable and easy to use assistive devices. Functionality that does not contribute to this goal will not be included in the design.

Effectiveness and comfort are often not only determined by the assistive devices itself, but also the fitting procedure plays an important role. For example, misalignment of orthoses can create undesired forces acting on the body that may contribute to discomfort or compromise

functionality. Additionally, knowledge about the actual wear time could to help understand (the lack of) device efficacy.

1.6. Thesis outline

The thesis consists of two parts. The first part focuses on the impaired shoulder, whereas the second part relates to the impaired hand. All chapters (except the introduction and discussion) of this thesis were written as journal or conference publications.

Part I: the Shoulder. In the first part the steps related to the development and evaluation of an assistive device to support the shoulder are described. This part consists of four chapters.

Chapter 2 focuses on the conceptual design of a dynamic shoulder orthosis. The dynamic shoulder orthosis aims to reduce the stress on the structures around shoulder joint, thereby reducing pain without impeding the remaining range of motion of the shoulder. This orthosis works by statically balancing the arm with two elastic bands. If these elastic bands are not aligned correctly, a net moment around the joint is introduced that could lead to discomfort or a restriction of arm movements. Proper alignment of the orthosis will always direct the upward force towards the glenohumeral joint thus creating no net moment.

For an optimal functioning of the balancing principle of the shoulder orthosis, the device must be aligned with the glenohumeral joint. There is currently no easy method to do this. Therefore, in **Chapter 3**, a novel method is presented to determine the center of rotation of the glenohumeral joint using only one camera and two printed markers.

An orthosis can only be effective if it is worn by the user. To be able to assess the effectiveness of the device, it is important to determine the wearing time reliably. Subjective methods such as diaries or questionnaires are often used in the current clinical practice, but are unreliable and lead to an overestimation of the actual use. In **Chapter 4** an algorithm is developed that provides an objective estimate of the wearing time of upper extremity orthoses using miniature temperature loggers.

To conclude the first part, **Chapter 5** presents the clinical evaluation of the dynamic shoulder orthosis. In a clinical study with 10 patients, the immediate and clinical effects of the orthosis on shoulder pain and arm function were investigated after two weeks of use.

Part II: the Hand. In order to perform grasping tasks, it is important that the hand can be opened far enough, and then sufficient force can be applied to grasp the object. The second part of this thesis focuses on the development of two assistive devices that support the impaired hand of different target groups. This part consists of two chapters.

Hand opening may be compromised if stroke patients do not have sufficient extensor muscle strength to overcome the effects of hypertonia of the finger flexors. In these cases, it may be necessary to support the hand opening with an assistive device. In **Chapter 6** the mechanical design and feasibility of a hand orthosis is presented that supports finger extension of stroke patients.

Performing grasping tasks is complicated if patients do not have sufficient muscle strength to grasp objects. **Chapter 7** presents the design and evaluation of a hand orthosis that supports a single, frequently used grasp (lateral pinch grip) of spinal cord injury patients.

Finally, **Chapter 8** provides a general discussion.

References

[1] Bernstein, N. A. (1967). The co-ordination and regulation of movements. Oxford: Pergamon Press.

[2] Latash, M. L. (2012). The bliss (not the problem) of motor abundance (not redundancy). Experimental Brain Research, 217(1), 1–5.

[3] Kempf, J. F., Lacaze, F., Nerisson, D., & Bonnomet, F. (1999). Biomechanics of the Shoulder BT - Shoulder Arthroplasty (G. Walch & P. Boileau, eds.). Berlin, Heidelberg: Springer Berlin Heidelberg.

[4] Lippitt, S. B., Matsen, F. A., Harryman, D. T., & Sidles, J. A. (1994). Practical Evaluation and Management of the Shoulder (First). Saunders.

[5] Namdari, S., Yagnik, G., Ebaugh, D. D., Nagda, S., Ramsey, M. L., Williams, G. R., & Mehta, S. (2012). Defining functional shoulder range of motion for activities of daily living. Journal of Shoulder and Elbow Surgery, 21(9), 1177–1183.

[6] Rantanen, T., Avlund, K., Suominen, H., Schroll, M., Frändin, K., & Pertti, E. (2002). Muscle strength as a predictor of onset of ADL dependence in people aged 75 years. Aging Clinical and Experimental Research, 14(3 Suppl), 10–15.

[7] Duncan, S. F. M., Saracevic, C. E., & Kakinoki, R. (2013). Biomechanics of the Hand. Hand Clinics, 29(4), 483–492.

[8] Cutkosky, M. R., & Howe, R. D. (1990). Human Grasp Choice and Robotic Grasp Analysis. Dextrous Robot Hands, 1, 5–31.

[9] Scano, A., Chiavenna, A., Tosatti, L. M., Müller, H., & Atzori, M. (2018). Muscle synergy analysis of a hand-grasp dataset: A limited subset of motor modules may underlie a large variety of grasps. Frontiers in Neurorobotics, 12(September), 1–14.

[10] Hu, Y., Osu, R., Okada, M., Goodale, M. A., & Kawato, M. (2005). A model of the coupling between grip aperture and hand transport during human prehension. Experimental Brain Research, 167(2), 301–304.

[11] Cutkosky, M. R. (1989). On Grasp Choice, Grasp Models, and the Design of Hands for Manufacturing Tasks. IEEE Transactions on Robotics and Automation, 5(3), 269–279.

[12] World Health Organization. (2001). International Classification on Function Disability and Health: ICF.

[13] World Health Organization. (2002). Towards a Common Language for Functioning , Disability and Health ICF. 1149, 1–22. Retrieved from http://www.who.int/classifications/icf/training/icfbeginnersguide.pdf

[14] Jette, A. M., Spicer, C. M., & Flaubert, J. L. (Eds.). (2017). The Promise of Assistive Technology to Enhance Activity and Work Participation.

[15] Foerster, O. (1936). The motor cortex in man in the light of Hughlings Jackson's doctrines. Brain, 59(2), 135–159.

[16] Shumway-Cook, A., & Woollacott, M. H. (2012). Motor control: Translating research into clinical practice. Philadelphia: Lippincott Williams & Wilkins.

[17] Pritchett, J. W. (1997). Inferior subluxation of the humeral head after trauma or surgery. Journal of Shoulder and Elbow Surgery, 6(4), 356–359.

[18] Vitoonpong, T., & Chang, K. (2022). Shoulder subluxation. StatPearls Publishing [Internet]. Retrieved from https://www.ncbi.nlm.nih.gov/books/NBK507847/
[19] Paci, M., Nannetti, L., & Rinaldi, L. A. (2005). Glenohumeral subluxation in hemiplegia: An overview. The Journal of Rehabilitation Research and Development, 42(4), 557.
[20] Turner-Stokes, L., & Jackson, D. (2002). Shoulder pain after stroke: a review of the evidence base to inform the development of an integrated care pathway. Clinical Rehabilitation, 16(3), 276–298.
[21] van Bladel, A., Lambrecht, G., Oostra, K. M., Vanderstraeten, G., & Cambier, D. (2017). A randomized controlled trial on the immediate and long-term effects of arm slings on shoulder subluxation in stroke patients. European Journal of Physical and Rehabilitation Medicine, 53(3), 400–409.
[22] Noronha, B., & Accoto, D. (2021). Exoskeletal Devices for Hand Assistance and Rehabilitation: A Comprehensive Analysis of State-of-the-Art Technologies. IEEE Transactions on Medical Robotics and Bionics, 3(2), 525–538.
[23] Kamper, D. G., & Rymer, W. Z. (2001). Impairment of voluntary control of finger motion following stroke: Role of inappropriate muscle coactivation. Muscle and Nerve, 24(5), 673–681.
[24] Lang, C. E., DeJong, S. L., & Beebe, J. A. (2009). Recovery of thumb and finger extension and its relation to grasp performance after stroke. Journal of Neurophysiology, 102(1), 451–459.
[25] Kamper, D. G., & Rymer, W. Z. (2000). Quantitative features of the stretch response of extrinsic finger muscles in hemiparetic stroke. Muscle and Nerve, 23(6), 954–961.
[26] Raghavan, P. (2015). Upper Limb Motor Impairment After Stroke. Physical Medicine and Rehabilitation Clinics of North America, 26(4), 599–610.
[27] Kim, D. (2016). The effects of hand strength on upper extremity function and activities of daily living in stroke patients, with a focus on right hemiplegia. Journal of Physical Therapy Science, 28(9), 2565–2567.
[28] du Plessis, T., Djouani, K., & Oosthuizen, C. (2021). A review of active hand exoskeletons for rehabilitation and assistance. Robotics, 10(1).
[29] Scherer, M. J. (1996). Outcomes of assistive technology use on quality of life. Disability and Rehabilitation, 18(9), 439–448.
[30] Scherer, M., & Galvin, J. (1994). Matching people with technology. Rehabilitation Management, 7(2), 128–130.
[31] Li, K., Murai, N., & Chi, S. (2013). Clinical reasoning in the use of slings for patients with shoulder subluxation after stroke: a glimpse of the practice phenomenon in california. OTJR: Occupation, Participation and Health, 33(4), 228–235.
[32] Dieruf, K., Poole, J. L., Gregory, C., Rodriguez, E. J., & Spizman, C. (2005). Comparative effectiveness of the GivMohr sling in subjects with flaccid upper limbs on subluxation through radiologic analysis. Archives of Physical Medicine and Rehabilitation, 86(12), 2324–2329.
[33] Bos, R. A., Haarman, C. J. W., Stortelder, T., Nizamis, K., Herder, J. L., Stienen, A. H. A., & Plettenburg, D. H. (2016). A structured overview of trends and technologies used in dynamic hand orthoses. Journal of NeuroEngineering and Rehabilitation, 13(1), 62.

[34] Sanders, Q., Okita, S., Lobo-Prat, J., De Lucena, D. S., Smith, B. W., & Reinkensmeyer, D. J. (2018). Design and Control of a Novel Grip Amplifier to Support Pinch Grip with a Minimal Soft Hand Exoskeleton. Proceedings of the IEEE RAS and EMBS International Conference on Biomedical Robotics and Biomechatronics, 2018-Augus(April 2019), 1089–1094.

[35] In, H., & Cho, K. (2015). Exo-Glove : Soft wearable robot for the hand using soft tendon routing system. IEEE Robotics & Automation, 22(March 2015), 97–105.

[36] Popov, D., Gaponov, I., & Ryu, J. (2017). Portable Exoskeleton Glove With Soft Structure for Hand Assistance in Activities of Daily Living. IEEE/ASME Transactions on Mechatronics, 22(2), 865–875.

[37] Yurkewich, A., Kozak, I. J., Hebert, D., Wang, R. H., & Mihailidis, A. (2020). Hand Extension Robot Orthosis (HERO) Grip Glove: Enabling independence amongst persons with severe hand impairments after stroke. Journal of NeuroEngineering and Rehabilitation, 17(1), 1–17.

[38] Proulx, C. E., Higgins, J., & Gagnon, D. H. (2021). Occupational therapists' evaluation of the perceived usability and utility of wearable soft robotic exoskeleton gloves for hand function rehabilitation following a stroke. Disability and Rehabilitation: Assistive Technology, 0(0), 1–10.

[39] Connelly, L., Jia, Y., Toro, M. L., Stoykov, M. E., Kenyon, R. V., & Kamper, D. G. (2010). A pneumatic glove and immersive virtual reality environment for hand rehabilitative training after stroke. IEEE Transactions on Neural Systems and Rehabilitation Engineering, 18(5), 551–559.

[40] Coffey, A. L., Leamy, D. J., & Ward, T. E. (2014). A novel BCI-controlled pneumatic glove system for home-based neurorehabilitation. 2014 36th Annual International Conference of the IEEE Engineering in Medicine and Biology Society, EMBC 2014, 3622–3625.

[41] Bützer, T., Lambercy, O., Arata, J., & Gassert, R. (2021). Fully Wearable Actuated Soft Exoskeleton for Grasping Assistance in Everyday Activities. Soft Robotics, 8(2), 128–143.

Part I
the Shoulder

2. A new shoulder orthosis to dynamically support glenohumeral subluxation

Abstract—Objective: In this paper we presented a novel shoulder subluxation support that aims to reduce the stress on the passive structures around the shoulder of patients with glenohumeral subluxation and glenohumeral related shoulder pain. The device applies a force to the upper arm without impeding the functional range of motion of the arm. Our design contains a mechanism that statically balances the arm with two elastic bands. Methods: A technical evaluation study was conducted to assess the performance of the orthosis. Additionally, two patients evaluated the orthosis. Results: The results of the technical validation confirm the working of the balancing mechanism. The pilot study demonstrated that the shoulder support increased the feeling of stability of the shoulder joint and, to a lesser extent, decreased shoulder pain. Furthermore, both patients reported that the orthosis did not impede their range of motion. Conclusion: In this research we developed a shoulder orthosis based on two statically balanced springs that support the shoulder of patients with glenohumeral subluxation that have residual shoulder muscle force. Compared to existing shoulder supports, our design does not impede the range of motion of the arm, and continues to provide a stabilizing force to the shoulder, even if the arm is moved away from the neutral position. Tests with two participants showed promising results. Significance: The device presented in this work could have a significant impact on the shoulder function which may improve rehabilitation outcome and improve the quality of life of patients suffering from glenohumeral subluxation and shoulder pain.

Published as: Haarman, C. J. W., Hekman, E. E. G., Haalboom, M. F. H., van der Kooij, H., & Rietman, J. S. (2021). A New Shoulder Orthosis to Dynamically Support Glenohumeral Subluxation. IEEE Transactions on Biomedical Engineering, 68(4), 1142–1153. https://doi.org/10.1109/TBME.2020.3021521

2.1. Introduction

The shoulder complex contributes to the mobility necessary to perform reaching tasks. The glenohumeral joint (GHJ) is one of the four joints that together form the shoulder complex. The GHJ is a ball and socket joint that allows for a large range of motion of the upper arm. As a consequence, this joint is relatively unstable [1]. For its stability the GHJ heavily relies on the posterior deltoid and the supraspinatus, together with the other rotator cuff muscles (infraspinatus, teres minor, and subscapularis) and capsule and ligaments [2]. Without normal tone of (one or more of) these muscles, the contribution of the relatively weak inferior and anterior capsule and ligaments to the stabilization of the shoulder is increased. These structures are easily overstretched due to the weight of the arm [3]. An inferior displacement of the humeral head from glenoid fossa may occur, also referred to as glenohumeral subluxation (GHS). The continuous stretching of the capsule and ligaments can be painful [4]. GHS often leads to a reduction of the painless range of motion of the shoulder, thus inhibiting the functional recovery of the upper limb and compromising the arm function during daily activities [5].

Shoulder supports, also known as braces or orthoses, are frequently prescribed to patients with GHS [6]–[8]. Clinical reasons to prescribe a shoulder brace include, among others, a reduction of stress in the passive structures from gravitational pull during standing or walking, maintenance of a proper glenohumeral alignment and shoulder pain reduction [9]. Several orthoses are commercially available, including: Omo Neurexa (Ottobock, Germany) [10], Neuro-Lux (Sporlastic GmbH, Germany) [11] and GivMohr (GivMohr Corporation, US) [12]. The aim of these orthoses is to reduce stress from the gravitational pull by applying an external force between the humerus and scapula that pulls the arm upwards. Stress reduction is closely related to proper GHJ alignment. A recent review by Nadler et al. concluded that, on average, shoulder orthoses are able to reduce the vertical subluxation with at least 5 to 10 mm in neutral position [6]. This instantaneous mechanical effect of shoulder braces is often assessed by measuring the humeral head position relative to the scapula from an X-ray with the arm in neutral position after initial fitting.

Several studies assessed the effect of a shoulder brace on shoulder pain reduction [10-11, 13]. Across these studies, only a modest improvement in pain measures is reported by 57% of the patients who used the orthosis for a few weeks.

Besides the low evidence for efficacy of shoulder supports [8,12,14], other commonly observed disadvantages include a reduction of the functional range of motion of the arm, due to the use of non-elastic straps in many braces. These straps create an upward force on the upper arm in resting position, but resist arm movement and thus limit the remaining range of motion. Van Bladel et al. stress the importance of actively engaging the arm in muscle activity to preserve glenohumeral alignment [13].

In this paper we present the concept of a new shoulder sub- luxation orthosis that reduces the stress on the soft tissue around the shoulder complex of patients with GHS and GHS-related shoulder pain without limiting the retaining range of motion of the arm, such that the functional recovery of patients with remaining arm function is not inhibited and shoulder

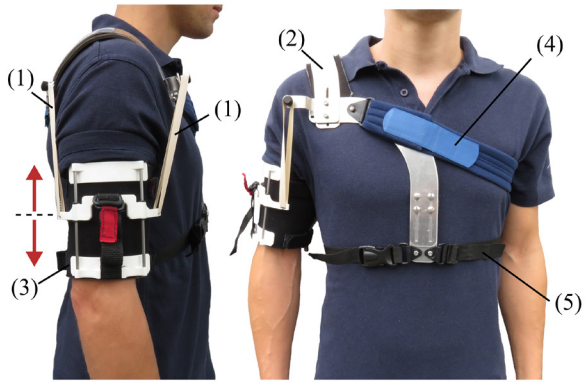

Fig. 2.1 – Sagittal and frontal view of the prototype of the shoulder orthosis, consisting of five components: (1) Anterior and posterior elastic bands. (2) Shoulder bracket that provides a stable base for the two proximal elastic band attachment points. (3) An upper arm cuff with tensioning mechanism provides a stable base for the two distal elastic band attachment points. The amount of force applied to the upper arm is controlled by adjusting the length and/or number of the elastic bands. Sliding of the arm cuff with respect to the skin is prevented by gel liner material on the inside of the arm cuff. Users will be instructed how to properly put on the arm cuff. The arrows indicate the allowed movement of the white 3D printed slider. (4) Strap to the contralateral shoulder, and (5) strap around the waist that keeps the shoulder bracket in place.

pain is reduced. The orthosis is suitable for, but not limited to, patients suffering from rotator cuff injury, stroke or brachial plexus injury.

We propose a design that consists of a trunk part and an upper arm cuff, connected only by two elastic bands (there is no hinge). It applies a force to the upper arm, directed towards the center of rotation (CoR) of the glenoid across the entire functional range of motion. Our proposed mechanism uses static balancing of two elastic bands to achieve this (Fig. 2.1).

2.2. Design criteria

The aim of the shoulder subluxation support is to reduce shoulder pain by reducing the stress on the passive structures surrounding the shoulder complex without impeding the functional range of motion of the arm.

In order to take over the function of the passive structures surrounding the shoulder joint, the shoulder orthosis should be able to apply an upward force with a magnitude of at most one times the mass of the arm. This equals a supporting force that completely reduces the gravitational pull on the arm and is considered as a worst-case scenario. Depending on the condition of the patient (e.g., residual muscle force) and individual preferences, less supporting force may be required. Therefore, the user must be able to easily adjust the magnitude of this upward force.

To not impede the functional range of motion of the arm, the supportive force should be directed towards the center of rotation of the glenoid. Several studies investigated arm movements (frequency and elevation levels) of healthy individuals during daily activities [15–17]. On average, about 90% of the arm movements during daily activities involve flexion angles less than 90°. Also, the time spent below a flexion angle of 90° was approximately

96% of the time [18-19]. The brace should therefore allow for an elevation angle of at least 90°.

The brace should not obstruct normal arm swing, since disturbed arm swing increases the metabolic cost of walking [20-21]. Maximum shoulder extension angles of approximately 20° are seen during normal walking [20]. The device should therefore allow for a shoulder extension angle of at least 20°.

The achieved pain reduction with existing braces is modest. 57% of the patients across three studies show an improvement of shoulder pain [6]. Most of the commercially available braces feature two non-elastic straps on the anterior and posterior part of the arm. From a mechanical viewpoint it can be seen that these straps resist arm motion in case they have been fitted tight with the arm in a neutral position. Fitting the straps loosely in neutral arm position allows arm motion but does not provide sufficient upward force. In the latter case, the reduction of the stress on the passive structures is low, especially in this neutral position. In order to further reduce the stress on the structures around the shoulder complex, a restoring force in the direction of the glenoid should be present throughout the entire range of motion.

GHS is associated with a decreased muscle tone of the rotator cuff [22]. The residual strength of unaffected muscles should be optimally deployed. Additional effort by the patients to overcome any added resistance during movements with the shoulder brace is undesirable and should be prevented as much as possible.

The orthosis should not restrict elbow movement, to not impede functional use of the arm, and to prevent synergistic flexion patterns and soft tissue contractures of the elbow [7,9].

Considerations when designing an orthosis include, among others, the optimization of cosmesis [23]. In order to minimize the visibility, the brace should preferably be worn under clothing. This requires a slim design that closely follow the contours of the patient's body.

In Table 2.1 a summary of the main requirements is listed.

Requirements

• Allowed range of motion by mechanism:
  - Up to 90° shoulder elevation (or higher)
  - Up to 20° shoulder extension (or higher)
• Force applied to the upper arm:
  ▪ In the direction of the glenoid
  ▪ Up to 100% of arm weight
  ▪ During entire allowed range of motion
• Prevent added resistance by brace during movement
• Prevent synergistic flexion patterns and soft tissue contractures
• Minimize visibility

Table 2.1 – Main requirements of the shoulder subluxation brace

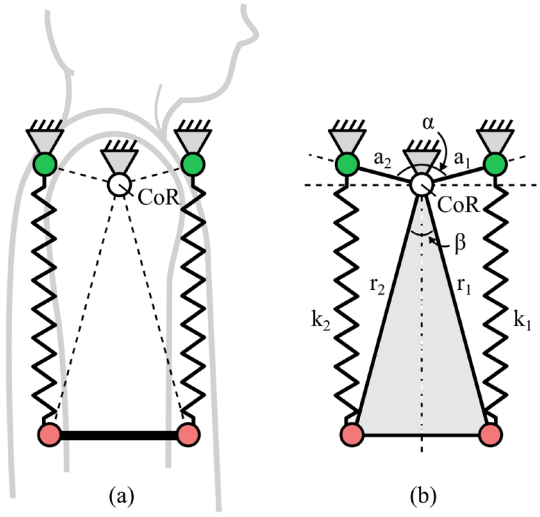

Fig 2.2 – A) Principle of spring to spring balancing using a rotated spring balancer. B) The spring balancer mechanism applied to the shoulder. Two zero-free-length springs are placed between attachment points located on the trunk and upper arm to create a force towards the center of rotation.

2.3. Conceptual design

An upward (restoring and stabilizing) force on the upper arm that will not impede the functional range of motion of the arm can be generated using two springs attached between the upper arm and the shoulder. Fig. 2.2A shows a schematic overview of this spring balancing mechanism. The proximal spring attachment points are fixed to the trunk and the distal spring attachment points are fixed to the upper arm.

2.3.1. Static Balance

Mechanically, the shoulder-arm-spring system resembles a spring-loaded lever, where the glenohumeral joint forms the rotation point. If the springs are balanced, the resulting force is directed towards the center of rotation of the glenohumeral joint, and no joint moment is introduced. Perfect balance of this rotated spring balancer is achieved when the following conditions are met [24]:

$$\alpha + \beta = \pi \tag{2.1}$$

$$k_1 a_1 r_1 = k_2 a_2 r_2 \tag{2.2}$$

Where k_1 and k_2 are the spring stiffnesses, a_1 and a_2 are the distances from the center of rotation to the proximal spring attachment points, and r_1 and r_2 the distances from the rotation center to the distal spring attachment points. α and β are the angles between a_1 and a_2, resp. r_1 and r_2. In Fig. 2.2B the parameters are shown.

Additionally, the spring force F must be proportional to its length x:

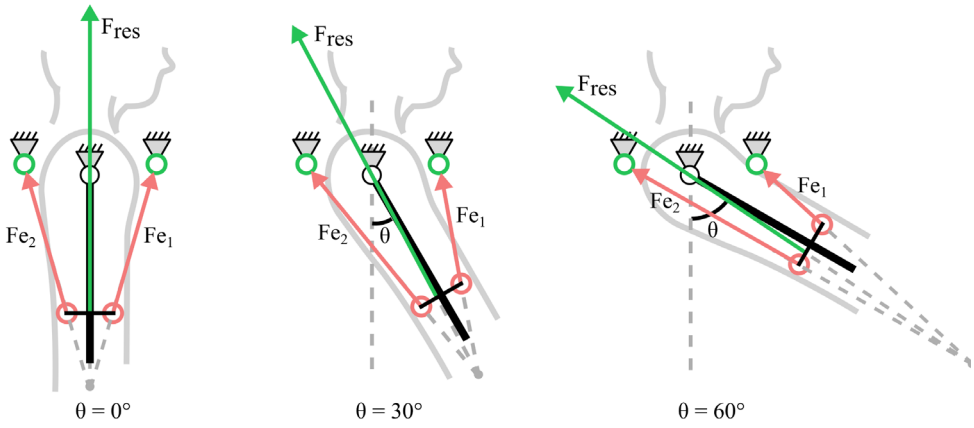

Fig. 2.3 – The force vectors (Fe_1 and Fe_2) created by the elastic bands are shown for different upper arm flexion angles (θ = 0°, 30° and 60°). It can be seen that in each situation, the resultant force (F_{RES}) travels through the center of rotation of the glenohumeral joint.

$$F = kx \tag{2.3}$$

Springs that exhibit this behavior are called "ideal springs" or "zero-free-length springs".

2.3.2. Direction Resultant Force

The resulting force F_{RES} is in any configuration directed towards the center of rotation. In Fig. 2.3 three examples (upper arm flexion angles of 0°, 30° and 60°) are shown to illustrate this. Since the resultant force crosses the center of rotation, the resulting moment that the elastic bands apply to the GHJ is equal to zero. Arm movements in the sagittal plane are therefore not impeded by the brace. Note: since the system is always balanced under the stated conditions, regardless of position, there is no requirement for symmetry of the attachment points in vertical arm position. The direction of the resultant force cannot be changed by the user. The elastic band attachment points will be aligned only once during the initial fitting process by the orthotist.

2.3.3. Spring Tensioning Mechanism

The magnitude of this supporting force can be manually adjusted by the user with the elastic band tensioning mechanism mounted on the arm cuff, see also Fig. 2.1. Pulling on a strap with their unaffected hand will allow users to move a carriage containing the distal spring attachment points over two linear guides. The distal spring attachment points can be moved approximately 5 cm up and down. This will alter the supportive (upward) force of the elastic bands.

2.3.4. Zero-Free-Length Springs

Zero-free-length springs, necessary to achieve balance (see also Eq. 2.3), have a force proportional to their length. Elastic bands made from natural rubber or synthetic polyisoprene (nonlatex rubber) are a practical implementation of zero-free-length springs when used in their linear range, which is typically between 150% and 350% of their initial length [25]. The

	Elastic band 1	Elastic band 2
Material	Natural rubber (latex)	Synthetic polyisopropene (non-latex)
Free length	88.9×10^{-3} m	88.9×10^{-3} m
Width	12.7×10^{-3} m	6.4×10^{-3} m
Thickness	8×10^{-4} m	8×10^{-4} m

Table 2.2 – Characteristics of elastic bands 1 and 2 used in this study.

characteristics of the two types of elastic bands used in this study are summarized in Table 2.2. These commercially available bands are composed of different materials and have a different stiffness. The selected stiffness of the elastic bands can, together with their length adjustment, provide a wide range of supportive forces. For example, elastic band I can support between 31% and 50% of the arm weight of a 50th percentile male, whereas elastic band II can support between 44% and 71% of the arm weight. The elastic bands are chosen such that their ranges overlap. If required, a combination of multiple springs can increase the supportive force range even further. In the section about the elastic bands their lifetime, stiffness and linearity over time are further characterized.

2.4. Methods

In this section, we propose methods to validate the technical performance of the orthosis and evaluate the orthosis with patients.

2.4.1. Attachment Point Locations

The attachment point locations of the elastic bands should respect the conditions for static balance, remain close to the body, and not impede the functional range of motion of the upper arm (between -20° and 90° arm flexion). The latter means that the arm should not touch the proximal attachment points within the allowed range of motion. In order to wear the brace under clothing, the brace should have maximum height of 3 cm (R_{MAX}) added to the skin surface. The constraints are summarized in Table 2.3 and visually depicted in Fig. 2.4. Note that the constraints resulting from the conditions for static balance are not included in this table.

Constraint	Symbol	Value
Maximum distance from skin surface	R_{MAX}	30×10^{-3} m
Minimum shoulder flexion angle	θf	90°
Minimum shoulder extension angle	θe	20°
Distance from CoR to distal spring attachment point	L	0.2 m
Elastic bands		Should have minimal contact with the skin

Table 2.3 – Constraints of the elastic band attachment point locations.

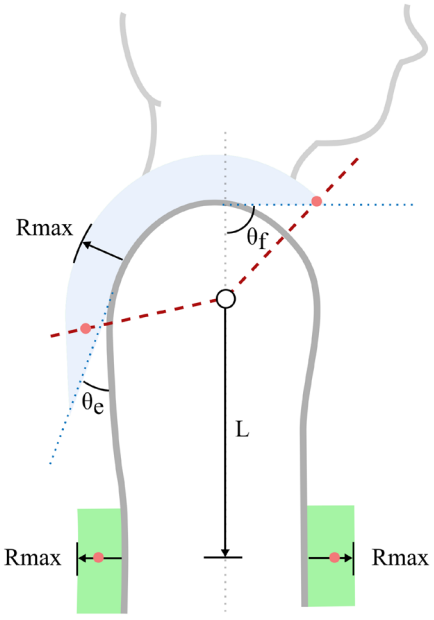

Fig. 2.4 – Sagittal view of the upper arm. The shaded arc around the shoulder joint shows the valid area for the proximal spring attachment locations and is bounded by the allowable distance from the skin surface (Rmax) and shoulder flexion (θf) and extension (θe) angles. The shaded area anterior and posterior of the upper arm shows the valid area for the distal spring attachment locations and is bounded by Rmax. The dots show a possible solution of the attachment point locations for the 50th percentile male. For 90 percent of the adult population, the proximal spring attachment points P_1 and P_2 are always located on the dashed line.

A custom Matlab script was used (MathWorks, USA) to search for attachment point locations that satisfy the conditions for balance and constraints. Preferably, solutions are chosen where the elastic band does not touch the arm, to reduce friction between the elastic bands and the skin. Feasible combinations of model parameters that respect all constraints are investigated for similarity to obtain a shoulder brace design that is easily customizable to 90 percent (5th to 95th percentile) of the adult population. Anthropometric models of this population were constructed using normative data from multiple sources [26-27].

2.4.2. Conditions for Balance

The shoulder brace should be properly aligned to minimize the added resistance by the brace to arm movements. A sensitivity analysis is performed to investigate the sources of misalignment that potentially degrade the balance of the system. For this analysis a fixed reference geometry (50th percentile male) is used and only mechanism parameters are changed.

Static balance is compromised if Eq. 2.1 or Eq. 2.2 are violated, or if the elastic bands are used outside their zero-free-length range such that Eq. 2.3 is no longer valid. In the following paragraphs we investigated the influence of changing these parameters on the conditions for balance. In Fig. 2.5 a graphical overview of all possible types of misalignment is presented.

1) *Potential Energy*: Eq. 2.2 relies on the correct positioning of the center of rotation of the mechanism with the anatomical center of rotation. We investigated the influence of misalignment between the anatomical and mechanism center of rotation (Fig. 2.5A) by shifting the center of rotation ± 2 cm in x- and y-direction. Also, the misalignment between the theoretical and implemented elastic band attachment points is investigated by varying a1 ± 20% with respect to a_2 (Fig. 2.5B), and varying k_1 ± 20% with respect to k_2 (Fig. 2.5C). Since r_1 and r_2 are equal as both distal attachment points are always moved simultaneously along the linear slider, we will not investigate the influence of ratio r_1 and r_2 on the balance.

2) *Enclosed Angles*: Eq. 2.1 is compromised if either angle α and/or β is changed such that the addition of these angles is not equal to π. In Fig. 2.5D the angle α is changed between ±20%. In Fig. 2.5E the vertical location of the distal attachment points on the upper arm is changed between ± 20%. This influences angle β.

3) *Zero-Free Length*: If the force-length relationship of the elastic bands changes over time, for example due to degradation of the elastomeric chains, the elastic bands may not have a zero-free length anymore. This will distort the balance of the system since Eq. 2.3 is violated. We measure the force-length characteristics with the experimental test setup described in the next paragraph. A linear regression model is fitted to the force-length data according to:

$$F = \beta_0 + kx \tag{2.4}$$

Here, β_0 is the intercept, k the slope of the linear fit and F and x are respectively the measured force and elastic band length.

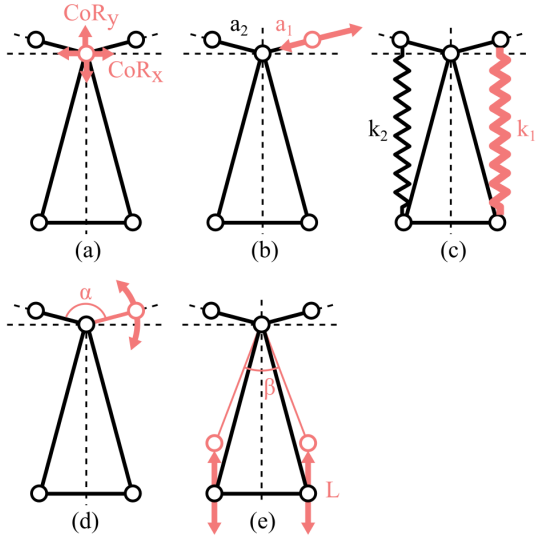

Fig. 2.5 – Parameters that are changed to investigate static balance of the system. A) Mechanism center of rotation shifted in x- and y-direction. B) Changing distance a1 with respect to a2. C) Changing stiffness k1 with respect to k2. D) Changing angle α. E) Changing angle β by varying length L.

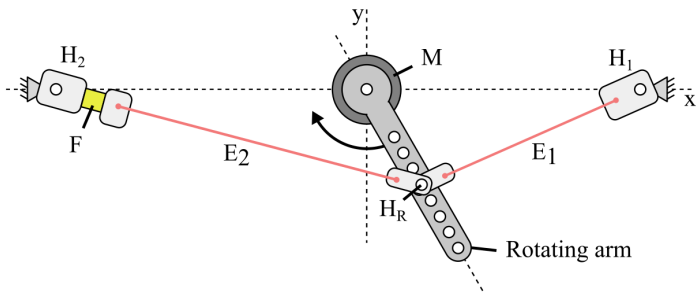

Fig. 2.6 – Schematic top view of the experimental test rig to perform lifetime and stiffness measurements of elastic bands. A rotating arm is connected to the motor (M) to continuously elongate and shorten two elastic bands (E1 and E2) between limits lmin and lmax. These limits can set by moving H1 and H2 along the x-axis and by moving the HR along the rotating arm. A force sensor (F) is connected to measure the force-length characteristic at predefined intervals.

We calculated the 95% confidence intervals of the intercept β_0 of the linear fit. The elastic bands show zero-free-length behavior if the value 0 is included in the confidence intervals of the intercept. The influence on the resulting balance can be determined by calculating the moment around the GHJ due to each band as a function of the flexion angle.

2.4.3. Elastic Bands Characterization

Two factors that influence the performance of the brace are the stiffness and lifetime of the elastic bands. An experimental test rig (Fig. 2.6) is developed to measure the force-length characteristics of the elastic bands over time during cyclic loading. From the data the stiffness can be computed. The system can also automatically detect failure of the elastic bands by analysis of sudden changes in the motor current. These data are used to compute the average lifetime. The setup includes LSB200 force sensors (Futek, USA) in series with elastic bands to measure the force during cyclic movements applied by an EC90 brushless rotary stage (Maxon Motor AG, Switzerland) connected to a rotating arm. The worst-case scenario involves cyclic stretching of the elastic bands between 150% and 350% of their length with a frequency of 1/3 Hz. These lengths equals a shoulder flexion angle between 0° and 90° for a 50th percentile male, see also Table 2.3. Four elastic bands are tested simultaneously of which two are connected to force sensors. Every 5 minutes force sensor data is collected during one complete cycle. Elastic bands of type 1 and 2 (see Table 2.2) are tested. The test setup was placed in an air-conditioned room (18 °C) to ensure equal test conditions.

1) *Stiffness*: From the force-length relation of the elastic bands we can determine the stiffness in the zero-free-length range. A decreased stiffness will reduce the maximum force that the bands can apply to the arm. The stiffness of the elastic bands is derived from the slope (k) of the linear regression model (Eq. 2.4).

2) *Lifetime*: If the elastic bands fail during use, the user will experience an undesired, sudden change in the magnitude of the force applied to the arm. By evaluating the lifetime during a worst-case scenario we can determine the average time required to replace the elastic bands.

2.4.4. Pilot Evaluation Methods

Two patients with GHS are included in a pilot evaluation study to assess the functionality and subjective experiences of the shoulder subluxation support. Ethical approval for this study was obtained from the local Medical Ethics Committee.

A physiatrist of the Roessingh, Center for Rehabilitation (Enschede, NL) selected the participants for this evaluation. The characteristics of the participants are listed in Table 2.4. Both subjects are clinically diagnosed with GHS of approximately 1 cm upon palpation, and suffer from GHS-related shoulder pain in rest and during movement. None of the participants had been prescribed a shoulder orthosis or other intervention prior to the study as none of the available commercially available orthoses were considered suitable for their condition and residual capabilities by their rehabilitation physician. Written informed consent was obtained from all participants before the study.

The pilot evaluation consisted of two sessions. During the first session (~30 min) several measurements of the patient's arm, shoulder and trunk were taken to customize the shoulder brace. The aim of the second session (~1 hour) was to gain insight in the functionality and comfort of the brace through quantitative measures, and qualitative observations. First the forces in the elastic bands were assessed. The subjects are instructed to tension the elastic bands to a level that feels comfortable, after which the lengths of the elastic bands were measured. The lengths are related to the applied forces according to Eq. 2.3. Then, the participants were asked to rate their average shoulder pain level during a normal day, and the minimum and maximum pain in the last 24 hours before the session on a scale from 0 to 10. Also, qualitative remarks about aspects such as restriction during arm movements due to the brace, stability of the GHJ and comfort of the design were obtained during a structured interview. Additionally the donning and doffing time were recorded. Finally, the System Usability Scale (SUS) was conducted to subjectively assess usability. The provided SUS indices of the new design are important indicators during the development process. Subjects are asked to score the agreement or disagreement with 10 statements on a 5-point Likert scale. The results are translated to a score between 0 and 100 [28]. Higher scores represent a better usability.

	Subject 1	Subject 2
Age	54	19
Sex	M	M
Condition	Dysplasia and secondary osteoarthritis with involvement of capsule and rotator cuff musculature	Hypermobility of rotator cuff caused by Ehlers-Danlos syndrome
Condition phase	Chronic	Chronic
Affected shoulder	R	R
Dominant side	R	L
Length (cm)	180	186
Weight (kg)	92	72

Table 2.4 – Subject characteristics

2.5. Results

2.5.1. Attachment Point Locations

Valid elastic band locations are identified that satisfy the conditions for static balance (Eq. 2.1 to Eq. 2.3) and don't violate the proposed constraints (Table 2.3).

For 90% of the adult population, the attachment points P_1 and P_2 are located on the dashed line of Fig. 2.4. For the 50th percentile male, the solution is indicated with markers (o) in Fig. 2.4. This solution allows the users to freely move their arm between angles $\theta f = 90°$ and

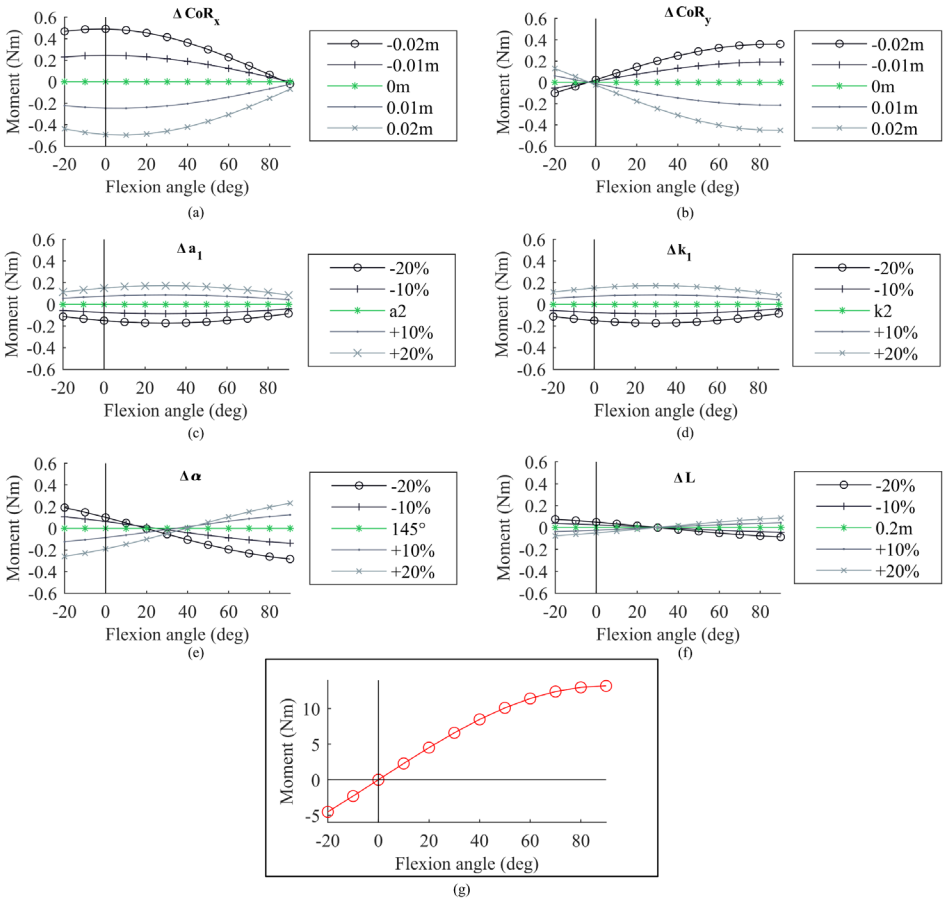

Figure 2.7 – Moments caused by the shoulder brace for a 50th percentile male when parameters of the shoulder brace are varied with respect to the optimal configuration. The parameters are graphically depicted in Fig. 2.4. In the optimal configuration the system is balanced. In this configuration, the moment caused by the shoulder brace is 0 Nm over the complete movement from 20° to 90° flexion. A negative value represents a moment that counteracts arm flexion. A) X-coordinate of CoR changed with 2 cm. B) Y-coordinate of CoR changed with 2 cm. C) Distance a1 changed 20% with respect to a2. D) Stiffness k1 changed 20% with respect to k2. E) Angle α changed 20% with respect to optimal configuration (145°). F) Length L changed 20% with respect to optimal configuration (0.2 m). G) Moment required by a 50th percentile male to lift his arm against gravity for different flexion angles. (Note: the scale of the y-axis has changed.)

θe = 20° without touching the shoulder bracket. Also, the spring attachment points stay close to the body within the specified limits.

2.5.2. Conditions for Balance

A detailed overview of the resulting moments due to shifts of model parameters can be found in Appendix 2.1. A deviation from the optimal configuration of the elastic band attachment points of the shoulder brace will affect the equations for balance (Eq. 2.1 to Eq. 2.3). For each model parameter change (see also Fig. 2.5), the effects on the balance of the system were investigated. In summary, the study showed that in neutral position, the alignment of the brace is most sensitive for shifts between the mechanism CoR and anatomical CoR in x-direction. For example, a 2 cm shift leads to an additional moment of 0.5 Nm (Fig 2.7A). Furthermore, a shift in y-direction of the CoR does not lead to an unbalance in neutral position (Fig. 2.7B). However, the moment increases for larger flexion angles. Also, a vertical displacement of the distal attachment points (Fig. 2.7F), which occurs during tensioning of the elastic bands, does not create large additional moments (<0.1 Nm).

2.5.3. Elastic Bands Characterization

1) *Lifetime*: For each elastic band tested, the number of cycles until failure is recorded. Elastic bands of type 1 have an average number of cycles until failure of $29 \times 10^3 \pm 8.9 \times 10^3$ (n = 20). Type 2 bands have an average number of cycles until failure of $9.5 \times 10^3 \pm 2.9 \times 10^3$ (n = 20). All elastic bands failed at the interface between pin and band. The average number of arm movements of healthy individuals reported in literature (above 40° with a duration between 1 and 5 s) is approximately between 100 and 120 movements per hour [15,19].When the number of cycles until failure are compared to the average number of arm movements, we can conclude that the elastic band of type I is able to withstand at least 30 days of usage in worst-case scenario (continuous stretching between 0° and 90° for 8 hours per day). For the type 2 elastic bands the average lifetime equals approximately 10 days of use in the extreme case.

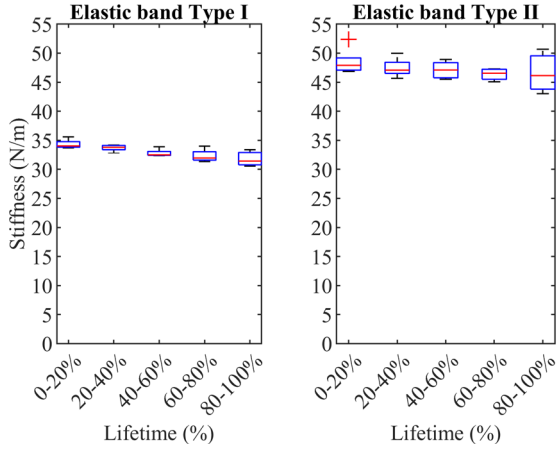

Fig. 2.8 – Boxplots showing the stiffness (N/m) of the measured elastic bands type I (left) and type II (right) over bins of Δ20% of their lifetime.

2) *Stiffness*: The stiffness of the elastic bands of type I and type II is determined using a linear regression fit. The average stiffness of the elastic bands is plotted as a function of the lifetime binned over intervals of 20% in Fig. 2.8. The average stiffness of the type I elastic bands drops from 34.3 N/m to 31.7 N/m. This equals a decrease of 7.8%. The average stiffness of the type II elastic bands drops from 48.5 N/m to 46.6 N/m. This equals a decrease of 3.9%. As a result, the maximum force that the elastic bands can generate will also decrease. The user can compensate for this decreased force by adding more elastic bands or stretch the bands to generate the same amount of supporting force.

2.5.4. Pilot evaluation

The results of the pilot evaluation are presented in Table 2.5.

1) *Applied force*: The tension in the elastic bands was measured and scaled to the arm weight of the subjects. The arm weight was estimated from the body mass [27]. Subject 1 applied a force of 32 N. This equals a percentage of 71% of his approximated arm weight. The tension in the elastic bands of subject 2 was 29 N. This equals 83% of his approximated arm weight.

2) *Glenohumeral stability*: The glenohumeral stability was subjectively assessed. Both patients reported a feeling of increased stability of the shoulder when wearing the orthosis. Subject 2 mentioned that he could lift objects more easily due to this increased stability.

3) *Restriction during movement*: The restriction of the arm due to the construction of the brace during movements was scored on a scale from 0 to 10 by the subjects, where 0 indicates no restriction and 10 is a high level of restriction. Subject 1 reported no hindrance (0/10) during voluntary arm movements. Subject 2 experienced very little hindrance (1/10) during voluntary arm movements. Also, both subjects were asked to rate the additional effort they had to provide during movement due to resistance by the brace caused by possible misalignment on a scale from 0 (no added resistance) to 10 (high level of resistance). Both subjects reported no added resistance (0/10) by the elastic bands during maximal arm flexion and abduction movements.

4) *Pain*: The least and worst shoulder pain experienced by subject 1 in the last 24 hours was respectively 0 and 6. He reported an average pain during a normal day of 4. Subject 2

	Subject 1	Subject 2
Force elastic bands (% of arm weight)	71	83
Type of elastic band used	Type II	Type II
Restriction due to construction of brace (0-10)	0	1
Restriction due to added resistance by elastic bands (0-10)	0	0
Pain score, min-max during last 24h (0-10)	0-6	2-6
Pain score, average of normal day (0-10)	4	5
Pain score without brace (0-10)	4	4
Pain score with brace (0-10)	1	4
SUS score (0-100)	97.5	92.5

Table 2.5 – Results of the pilot evaluation.

experienced a pain with a score between 2 and 6 in the last 24 hours. During a normal day his average pain score is 5. The instantaneous effect of the brace on the shoulder pain was assessed by scoring the pain without and with the shoulder brace. At the start of the second session, subject 1 experienced a pain of 4. With the brace his pain score reduced to 1. For subject 2 there was no difference in pain score without and with the orthosis. In both cases his pain score was 4.

5) *Comfort*: Regarding comfort of the device, the subjects reported high pressures on the shoulder arc. The arm cuff stayed in place when applying tension to the elastic band. No irritation of the skin occurred. Subject 1 noted that it was difficult to attach the posterior elastic band to the shoulder bracket. Subject 2 mentioned that the comfort during seating could be improved since the harness of the brace is running over the spine and touches the back rest of a chair. Currently, the orthosis has a weight of 650g.

6) *Usability*: The average donning time of both participants over three trials is 86s. The average doffing time measured across three trials is 22s. Both participants completed the SUS for the shoulder brace after the second session. The SUS score of subject 1 was 97.5 and the score of subject 2 was 92.5.

2.6. Discussion

Patients with GHS and GHS-related shoulder pain may benefit from a shoulder brace that provides a restoring force to realign the GHJ. Current solutions are limited in that they impede the retaining range of motion of the upper arm. For these patients, a new shoulder subluxation support is developed that does not have the disadvantages of the currently available braces. The orthosis is applicable to a wide target population, including, but not limited to stroke, rotator cuff injury and neuromuscular diseases. Also, the orthosis can be used in a clinical and home setting to facilitate training and activities of daily living.

The brace contains two statically balanced zero-free length springs that realign the shoulder joint while providing a restoring glenoid-directed force. To guarantee the static balance of the system, and thus allow unrestricted arm movement within the retaining range of motion of the user, the shoulder brace should be aligned such that the equations for static balance (Eq. 2.1 to Eq. 2.3) hold. Misalignment of the brace is defined as the offset of one or more elastic band attachment point locations from the desired position. Providing clear instructions for the initial fitting by the orthotist is important, because only inaccurate brace fitting can result in a misalignment of the elastic bands, leading to a supporting force that is not directed toward the center of rotation of the shoulder joint. When misalignment occurs, the user will experience either a resistive or assistive force when the arm is kept in a certain position. The orthotist should in this case realign the elastic bands to match the conditions for static balance.

For each error source contributing to the misalignment of the brace, the effect on the balance of the system is investigated. Simulation results revealed that shifts in x- or y-direction of the shoulder brace CoR with respect to the anatomical CoR have the most detrimental effects on

the balance. However, even in these cases, the added moment due to misalignment is low (<0.5 Nm).

In our simulation, we determined the influence of one parameter at the time on the unbalance of the system. In practice, misalignment of the brace can violate multiple parameters of the conditions for static balance simultaneously. Depending on the specific configuration of the brace, the change of multiple parameters can either reinforce or reduce the unbalance.

Also, we only considered arm movements in the sagittal plane (flexion/extension). A detailed analysis of the balance in the frontal plane during abduction is presented in Appendix 2.2. In the frontal plane the system acts as a gravity equilibrator, compensating the (partial) weight of the arm in abduction. Changing the location of the distal spring attachment points will change the magnitude of the abduction force provided by the mechanism.

The average lifetime of the elastic bands is determined during a worst-case test. The disposable elastic bands are very cheap and easily replaceable. Tests have confirmed that both types of elastic bands survive during a sufficient time before replacement of the bands is required. All bands failed at the attachment point. Improving this interface by reducing the friction between the attachment point and elastic band will probably extend the lifetime of the elastic bands.

In a pilot study with two participants several aspects of the shoulder orthosis were investigated. Both patients reported that the shoulder subluxation support provided a stabilizing force to the shoulder and, to a lesser extent, provided an immediate shoulder pain relief. The participants also addressed several issues regarding the comfort of the brace. Both subjects reported large reaction forces on the shoulder arc. The shoulder subluxation support reduces the stress by applying a force between the humerus and scapula. The magnitude of these reaction forces is directly related to the tension in the elastic bands. The comfort will likely be increased if the pressure distribution of the shoulder bracket is improved, for example, by using softer materials. Another improvement could be the reduction of weight. The results of the SUS suggest that the usability of the proposed system is promising. The device is likely to be accepted in daily activities for scores above 70. Truly superior products score better than 90 [29]. A comparison with other orthoses is not possible, as the SUS scores of these devices are not available.

The conclusions presented in this study are based on quantitative and qualitative remarks about glenohumeral stability, pain, comfort and usability during a pilot evaluation with only two patients. Still, the results provide valuable insights and suggestions for improvements. A clinical study will be performed to further investigate the functionality and usability of the system. The shoulder pain will be evaluated after (medium) prolonged orthosis usage to assess the added benefit of the device for pain reduction. In this future study, we will also investigate the GHJ alignment using an imaging modality such as ultrasound, in order to objectively establish the re-positioning of the humeral head in the glenoid by the brace. This method has an advantage over conventional radiographs since there is no radiation involved.

2.7. Conclusion

In this study, a new shoulder subluxation support is presented for patients with GHS and GHS-related shoulder pain. The brace uses two statically balanced zero-free-length springs that provide an external force to the arm in the direction of the glenoid in different arm postures. Compared to existing shoulder braces, our design has the potential to reduce GHS-related shoulder pain without impeding the range of motion of the user, even when the arm is moved away from the neutral position. Preliminary tests with two participants showed promising results.

Appendix 2.1

A deviation from the optimal configuration of the elastic band attachment points of the shoulder brace will affect the equations for balance which are given by Eq. 2.1 to Eq. 2.3. For each model parameter change, the effects on the balance of the system are investigated.

The results of this sensitivity analysis are depicted in Fig. 2.7. The horizontal line at 0 Nm represents the optimal configuration of the elastic band attachment points. The resulting moments can be visually compared to a reference moment Fig. 2.7G. This is the moment required to lift the arm against gravity for each flexion angle. These results are discussed in the paragraphs below.

Potential Energy

A shift in the center of rotation with respect to the anatomical center of rotation in both x- and y-direction was simulated. A shift in x-direction (Fig. 2.7A) disturbs the balance when the arm is in neutral position and decreases to approximately 0 Nm at a flexion angle of 90°. For the y-direction (Fig. 2.7B) the opposite occurs. A slight shift does not affect the resulting moment in neutral position. However, the moment added by the brace increases when the arm is flexed. For a shift of 2 cm a resulting moment of approximately 0.45 Nm occurs at a flexion angle of 90°.

The effect of changing length a_1 (with respect to a_2) on the resulting moment can be seen in Fig. 2.7C. From this graph we can see that a maximum moment of approximately 0.2 Nm occurs around 30° shoulder flexion for an increase in length of a_1 of 20%.

The stiffness of the anterior and posterior elastic bands are varied. In Fig. 2.7D the results are shown. A maximum moment of approximately 0.2 Nm is observed at 30° flexion.

Enclosed Angles

Changing angle α will affect Eq. 2.1, which is required for balance of the system. The results are shown in Fig. 2.7E. It can be seen that in neutral position the arm will experience a moment due to the misalignment of the brace. When the arm is flexed, the moment reduces to 0 Nm at about 30° after which it increases again to a maximum of about 0.3 Nm at 90° flexion.

Changing the vertical location (L) of attachment points D_1 and D_2 on the upper arm will alter angle β. The resulting moment (Fig. 2.7F) shows a similar trend as was seen when varying angle α. The maximum moment occurs at 90° flexion and is approximately 0.25 Nm.

Zero-Free-Length

The force-length characteristics of the elastic bands type I and type II are shown in Fig. 2.9 averaged over their lifetime.

For each data set, a linear regression fit was computed. A zero-free-length is achieved when the 95% confidence interval of the intercept includes the value 0. The dashed lines in Fig. 2.9 indicate the average length range in which the elastic bands show zero-free-length behavior.

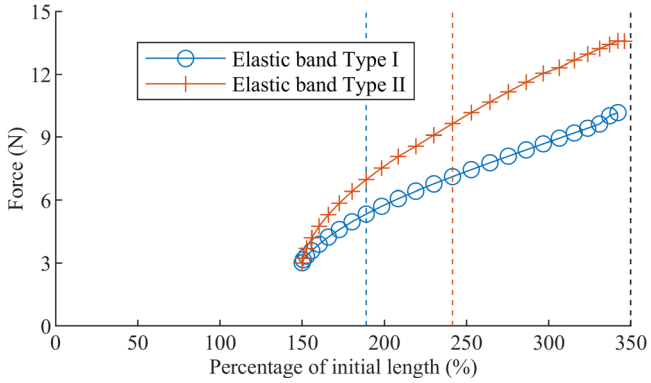

Fig. 2.9 – Force-length characteristics of elastic bands of type I and II averaged over their lifetime. The type I elastic band shows zero-free- length behavior between 180% and 350% of their initial length . The type II elastic band shows zero-free-length behavior between 230% and 350% of their initial length..

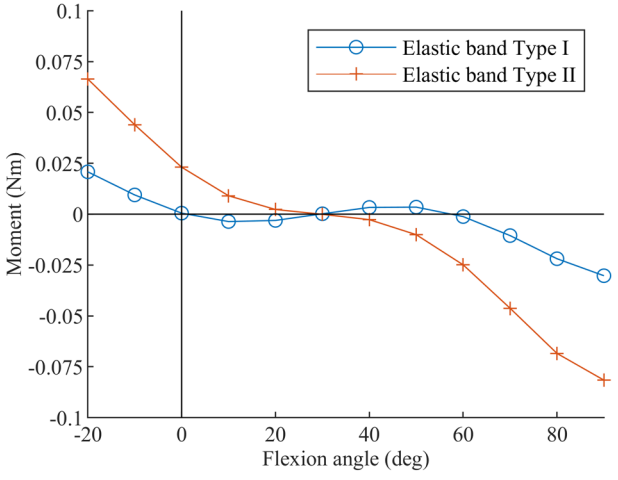

Fig. 2.10 – Moments caused by the non-zero-free-length characteristics of the elastic bands for a 50th percentile male.

For the type I elastic bands the zero-free-length behavior is observed between 180% and 350% of their initial length. The type II elastic bands show zero-free-length behavior between 230% and 350%. In the shoulder support, the elastic bands are used between 150% and 350%, which is outside their linear range. This will affect the balance of the system. The moment that is added by the elastic bands is plotted in Fig. 2.10 as a function of the flexion angle. For the type I elastic bands the maximum moment is approximately 0.03 Nm. For the type II elastic bands the maximum moment is approximately 0.08 Nm. Compared to the moment required to move the arm through the range of motion (see also Fig. 2.7G), this additional moment is negligible.

Appendix 2.2

In the manuscript, only the balance of the arm in the sagittal plane has been considered (Fig. 2.11A). The moments created by the anterior and posterior elastic bands are balanced, such that no net moment is introduced around the CoR of the shoulder joint. The locations of the attachment point A and P are shown in the frontal plane, see Fig. 2.11B.

In the frontal plane, the combination of the two elastic bands acts as a gravity equilibrator. Depending on the distance (a_A and a_P, Fig. 2.11B) of points A and P with respect to the CoR, each of the bands contribute to exactly compensating (part of) the weight of the arm. An elastic band that is attached above the CoR (e.g., point A in Fig. 2.11) will contribute to an abducting moment of the arm, whereas an elastic band that is attached below the CoR (e.g., point P in Fig. 2.11) will contribute to an adducting moment of the arm.

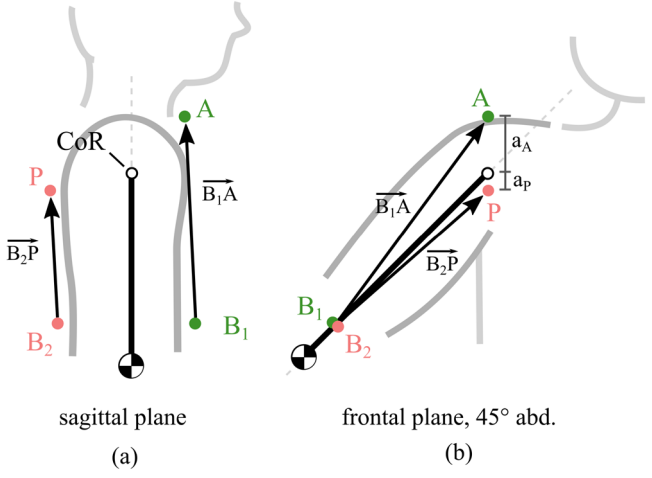

Fig. 2.11 - A) Sagittal view of the arm showing the CoR, the elastic band anterior (A) and posterior (P) attachment points (dots) and force vector (arrow). B) Frontal view with the arm in 45° abduction. In abduction, a net abducting moment is introduced as a result of both force vectors FA and FP.

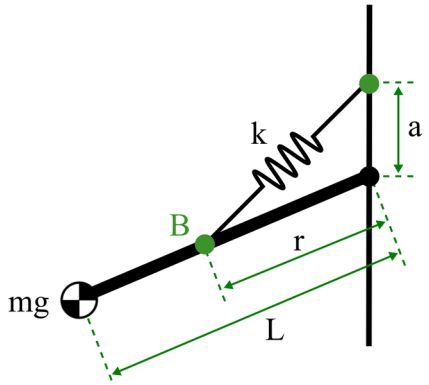

Fig. 2.12 – Schematic overview showing the basic components of the gravity equilibrator. Force mg acting on a distance L from the shoulder joint is balanced by a zero-free-length spring with stiffness k attached at distance a and r from the rotational center.

The condition for static balance of this gravity equilibrator in the frontal plane is [24]:

$$mgl = akr \tag{2.5}$$

Here mg is the force caused by the arm weight, acting on distance L from the CoR. The elastic bands with stiffness k are attached at a distance r from the CoR to the upper arm and a distance a to the trunk. See also Fig. 2.12 for a schematic overview. From the equation it can be seen that the amount of weight that is compensated (m) is, among others, determined by the position of the attachment points A and P.

Given the optimized position of attachment points A and P in the sagittal plane, the combination of elastic bands will compensate approximately 6% (220g) of the arm weight of a 50th percentile adult male throughout the entire range of motion in the frontal plane (abduction angle).

In general, having an assistive abducting moment can be beneficial, as patients with reduced muscle strength are aided (to a small extent) in abduction. Also, patients with continuous tension on the rotator cuff musculature due to glenohumeral subluxation may find assistance by the brace during abduction beneficial. If desired by the patient, the abducting moment can be increased by moving attachment point locations A and/or P up. However, this will deteriorate the balance of the arm in the sagittal plane during flexion. The abducting moment can also be increased by moving attachment points A and P laterally in the frontal plane. However, then the system is no longer a perfect gravity equilibrator, which means that the relative amount of weight compensation changes with the abduction angle. This is shown in Fig. 2.13. If A and P are shifted medially (‘o’, solid line), additional effort is required to overcome the adducting moment caused by the bands. But if A and P are shifted laterally (‘$*$’, solid line), the assisting moment helps the patient to abduct his arm.

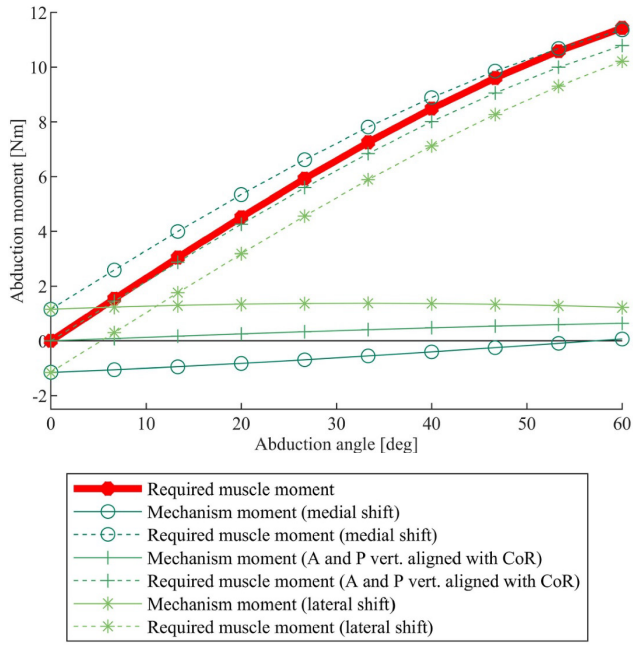

Fig. 2.13 – Abduction moment versus angle plots for three locations of the anterior (A) and posterior (P) elastic band attachment points. If points A and P are vertically aligned with the CoR in the frontal plane, the abduction moment caused by the elastic bands increases for larger abduction angles of the arm (+). Moving the attachment points in lateral (*) or medial (o) direction causes an offset of the abduction moment (solid lines). This moment now counteracts (in case of a lateral shift) or assists (in case of a medial shift) the patient's voluntary abduction moment, as can be seen by comparing the moment required to lift the arm (solid thick line) and the resulting moments when the elastic bands act on the arm (dashed lines).

References

[1] K. Moore and A. Dalley, “Shoulder anatomy,” in Clinically Oriented Anatomy, 4th ed. Philadelphia, PA, USA: LippincottWilliams andWilkins, 1999, pp. 788–795.

[2] D. Jenkins, “Shoulder and upper limb,” in Functional Anatomy of the Limbs and Back, 9th ed., Maryland Heights, MO, USA: Saunders Elsevier, 2009, pp. 86–89.

[3] T. Ikai et al., “Evaluation and treatment of shoulder subluxation in hemiplegia: Relationship between subluxation and pain,” Amer. J. Phys. Med., Rehabil., vol. 77, no. 5, pp. 421–426, 1998.

[4] L. Turner-Stokes and D. Jackson, “Shoulder pain after stroke: A review of the evidence base to inform the development of an integrated care pathway,” Clin. Rehabil., vol. 16, no. 3, pp. 276–298, 2002.

[5] L. T. Andersen, “Shoulder pain in hemiplegia,” Amer. J. Occupational Ther., vol. 39, no. 1, pp. 11–19, 1985.

[6] M. Nadler and M. M. H. H. Pauls, “Shoulder orthoses for the prevention and reduction of hemiplegic shoulder pain and subluxation: Systematic review,” Clin. Rehabil., vol. 31, no. 4, pp. 444–453, 2016.

[7] D. Stolzenberg, G. Siu, and E. Cruz, “Current and future interventions for glenohumeral subluxation in hemiplegia secondary to stroke,” Topics Stroke Rehabil., vol. 19, no. 5, pp. 444–456, 2012.

[8] L. Ada, A. Foongchomcheay, and C. G. Canning, “Supportive devices for preventing and treating subluxation of the shoulder after stroke,” Stroke, vol. 36, no. 8, pp. 1818–1819, 2005.

[9] K. Li, N. Murai, and S. Chi, “Clinical reasoning in the use of slings for patients with shoulder subluxation after stroke: A glimpse of the practice phenomenon in California, OTJR: Occupation, Participation Health, vol. 33, no. 4, pp. 228–235, 2013.

[10] S. Hesse et al., “A new orthosis for subluxed, flaccid shoulder after stroke facilitates gait symmetry: A preliminary study,” J. Rehabil. Med., vol. 45, no. 7, pp. 623–629, 2013.

[11] M. Hartwig, G. G. Gelbrich, and B. Griewing, “Functional orthosis in shoulder joint subluxation after ischaemic brain stroke to avoid posthemiplegic shoulder-hand syndrome: A randomized clinical trial,” Clin. Rehabil., vol. 26, no. 9, pp. 807–816, 2012.

[12] K. Dieruf et al., “Comparative effectiveness of the GivMohr sling in subjects with flaccid upper limbs on subluxation through radiologic analysis,” Archives Phys. Med. Rehabil., vol. 86, no. 12, pp. 2324–2329, 2005.

[13] A. van Bladel et al., “A randomized controlled trial on the immediate and long-term effects of arm slings on shoulder subluxation in stroke patients,” Eur. J. Phys. Rehabil. Med., vol. 53, no. 3, pp. 400–409, 2017.

[14] A. Morley et al., “Management of the subluxed low tone shoulder,” Physiotherapy, vol. 88, no. 4, pp. 208–216, 2002.

[15] B. Coley et al., “Arm position during daily activity,” Gait Posture, vol. 28, no. 4, pp. 581–587, 2008.

[16] K. Meijer et al., “Characteristics of daily arm activities in patients with COPD,” Eur. Respiratory J., vol. 43, no. 6, pp. 1631–1641, 2014.
[17] G. D. G. Langohr, “Comparing daily shoulder motion and frequency after anatomic and reverse shoulder arthroplasty,” J. Shoulder Elbow Surger., vol. 27, no. 2, pp. 325–332, 2018.
[18] R. Chapman et al., “Assessing shoulder biomechanics of healthy elderly individuals during activities of daily living using inertial measurement units: High maximum elevation is achievable but rarely used,” J. Biomech. Eng., vol. 141, no. 4, pp. 1–7, 2019.
[19] M. Acuna, T. Amasay, and A. R. Karduna, “The reliability of side to side measurements of upper extremity activity levels in healthy subjects,” BMC Musculoskeletal Disorders, vol. 11, no. 1, 2010, Art. no. 168.
[20] S. H. Collins, P. G. Adamczyk, and A. D. Kuo, “Dynamic arm swinging in human walking,” in Proc. Royal Soc. B: Biol. Sci., vol. 276, no. 1673, pp. 3679–3688, 2009.
[21] J. D. Ortega, L. A. Fehlman, and C. T. Farley, “Effects of aging and arm swing on the metabolic cost of stability in human walking,” J. Biomech., vol. 41, no. 16, pp. 3303–3308, 2008.
[22] M. Paci, L. Nannetti, and L. A. Rinaldi, “Glenohumeral subluxation in hemiplegia: An overview,” J. Rehabil. Res. Develop., vol. 42, no. 4, 2005, Art. no. 557.
[23] P. Mckee and A. Rivard, “Foundations of orthotic intervention,” in Rehabilitation of the Hand and Upper Extremity, 6th ed. Philadelphia, PA, USA: Elsevier, 2011, pp. 1565–1580.
[24] J. L. Herder, “Energy-free systems: Theory, Conception, and Design of Statically Balanced Spring Mechanisms,” Ph.D. dissertation, Fac. Mech., Maritime, Mater. Eng.,DelftUniv. Technol., Delft, The Netherlands, 2001.
[25] A. G. Dunning, “Slender spring systems,” Ph.D. dissertation, Dept. Precis. Microsystems Eng., Fac. Mech., Maritime Mater. Eng., Delft Univ. Technol., Delft, The Netherlands, 2016.
[26] C. D. Fryar, Q. Gu, and C. L. Ogden, “Anthropometric reference data for children and adults: United States, 2007-2010,” Vital Health Statistics, vol. 11, Oct. 2012, Art. no. 252.
[27] P. de Leva, “Adjustments to Zatsiorsky-Seluyanov’s segment inertia parameters,” J. Biomech., vol. 29, no. 9, pp. 1223–1230, Sep. 1996.
[28] J. Brooke, “SUS: A Quick and Dirty Usability Scale,” in Usability Evaluation in Industry. London, U.K.: Taylor & Francis, 1996, pp. 189–194.
[29] A. Bangor, P. T. Kortum, and J. T. Miller, “An empirical evaluation of the system usability scale,” Int. J. Human-Comput. Interact., vol. 24, no. 6, pp. 574–594, 2008.

3. Feasibility of reconstructing the glenohumeral center of rotation with a single camera setup

Abstract—Background: An accurate estimation of the glenohumeral joint center of rotation (CoR) is important during alignment of braces and exoskeletons, as a misalignment will introduce undesired forces on the human body. The aim of this research was to develop a new method to estimate the glenohumeral CoR and register the location to the body using a single camera and two printed markers. Methods: During shoulder anteflexion, the arm roughly describes an arc in the sagittal plane, with the glenohumeral joint in the center. Two binary square-fiducial ArUco markers were secured to the upper arm and the scapula, their position and orientation were obtained, and a sphere was fitted to the coordinates of the arm marker. The sphere center position was then registered on the skin. The accuracy was assessed with a test bench with a known rotational center. The repeatability was assessed in vivo with five healthy participants. Results: The mean absolute offset between the true CoR of the test bench and the fitted sphere centers across multiple trials was 2.7mm at a velocity of 30°/s, and 2.5mm at 60°/s. The root mean squared distance from the estimated sphere centers after each trial to the mean sphere center across all trials per participant was 5.1 mm on average for the novice examiner and 5.2mm for the expert examiner. Conclusions: The proposed method is able to accurately and precisely estimate the glenohumeral CoR.

Published as: Haarman, C. J. W., Hekman, E. E. G., Rietman, J. S. & van der Kooij, H. (2022). Feasibility of reconstructing the glenohumeral center of rotation with a single camera setup. Prosthetics and Orthotics International - *Online ahead of print*.

3.1. Background

The center of rotation (CoR) is the point around which an object rotates. Locating the CoR of a limb inside a joint is important when aligning braces and exoskeletons. A misalignment between the CoR of a brace or exoskeleton and the anatomical CoR creates undesired forces on the human body and will negatively interfere with the working principle of the brace or exoskeleton [1].

Recently, we developed a shoulder brace which provides support to patients with shoulder pain due to glenohumeral subluxation [2]. Springs apply a restoring force between the humerus and glenoid joint surface of the scapula, such that the joint is re-positioned while residual motion is not impeded. Correct positioning of the springs that create this upward force depends on a correct estimation of the glenohumeral joint CoR (GH-CoR) in the sagittal plane. Incorrect assumptions about the location of its rotational center will create external forces that impede arm movement.

Typically, brace alignment involves positioning a mechanical (2D) hinge relative to a plane of motion. So instead of representing the CoR as a three-dimensional coordinate, we only have to deal with the CoR as a two-dimensional coordinate. Brace alignment requires a reliable method to accurately locate the GH-CoR using low-cost equipment. Also, the estimated location should be easily registered on the patient's body to allow alignment of the brace to the estimated CoR. Besides, the method should be quickly performed to be accepted in the clinical practice.

3.1.1. Center of rotation estimation

During brace alignment, often bony landmarks are palpated to estimate the location of the rotation axis of a joint. Unfortunately, palpation of the GH-CoR is not possible as it is an internal anatomical landmark [3].

Functional identification methods estimate the CoR from the relative motion of adjacent body segments. Motion of one segment is recorded with respect to another segment [4]. A spherical or circle fit on the cluster of the measured marker positions will reveal the rotational center of the joint in 3D or 2D respectively. These methods are valid for the glenohumeral joint since it can be considered a spherical (or ball-and-socket) joint with a fixed rotational center [5].

Different techniques have been proposed to obtain the relative motion of moving body segments, including (miniaturized) magneto-inertial measurement units (MIMUs) [6-9], optical motion tracking with two or more synchronized cameras [4,10-12] (e.g. stereophotogrammetry [13]), electromagnetic tracking [3,14] or ultrasound [12]. Many of these methods involve the use of expensive equipment, or are time-consuming, which limits their availability and usability.

3.1.2. Square-based fiducial markers

Square-based fiducial markers are passive markers that are placed in the field of view of a camera. Knowing the markers are square, their pose with respect to the camera can be estimated [15]. If the markers are attached to body segments such as the upper arm or scapula,

the 3D position and orientation of these segments can be obtained. The setup may consist of only one cheap fixed-focus webcam. The markers itself are printed on paper.

Several types of square-based fiducial markers are reported in literature, such as ArUco [16-17] and AprilTag [18]. These markers consist of a black border and a unique inner (black and white) binary code for identification. Based on fiducial marker performance criteria such as false-negative rate (probability that a marker is present while not reported), and intermarker confusion rate (probability that a wrong marker id is reported) [19], ArUco markers were selected [20]. Previously, fiducial markers have been used for motion capture purposes [21-22]. To our best knowledge, these markers have never been used before to estimate the rotational center of the glenohumeral joint for brace alignment.

3.1.3. Registration

Registration of the estimated CoR position on the skin allows us to visually align the rotational centers of the brace and the glenohumeral joint.

3.1.4. Aim

The objective of this study is (1) to develop a procedure to estimate the GH-CoR using a single-camera setup and two square-based fiducial ArUco markers and to register the estimated location on the skin, and (2) to evaluate the proposed procedure by determining the repeatability and accuracy of the estimated values. Accuracy was assessed with a test bench with a known rotational center. Repeatability was assessed in vivo with healthy participants.

3.2. Methods

3.2.1. CoR estimation

Because the GH joint is a ball-and-socket joint, a marker attached to the arm describes an arc that approximates a sphere with respect to the GH-CoR. The projected center of this sphere on the sagittal plane is defined as the GH-CoR in the sagittal plane. The CoR estimation procedure described below provides an estimate of the GH-CoR.

Setup

The setup for the CoR estimation consisted of a generic, fixed focus webcam with a resolution of 1920x1080 pixels (C-400, Hama), a computer for data processing, a chair with back rest and two ArUco markers (Fig. 3.1). The webcam was mounted on a tripod, with its principal axis aligned perpendicular to the sagittal plane of the glenohumeral joint. One ArUco marker (Ma) was secured to the upper arm with a strap, and the other marker (Ms) was secured to the scapula with a custom L-shaped holder and double-sided adhesive. Both markers were printed on plain paper and their size was 32.5 x 32.5 mm.

It is important to tightly fasten both markers to their respective body segments, since relative motion between the marker and the body segment may introduce errors when estimating the CoR. The webcam was calibrated by obtaining several views of a calibration pattern with a known geometry to quantify distortions that were introduced by the lens. The calibration procedure only has to be performed once for each camera.

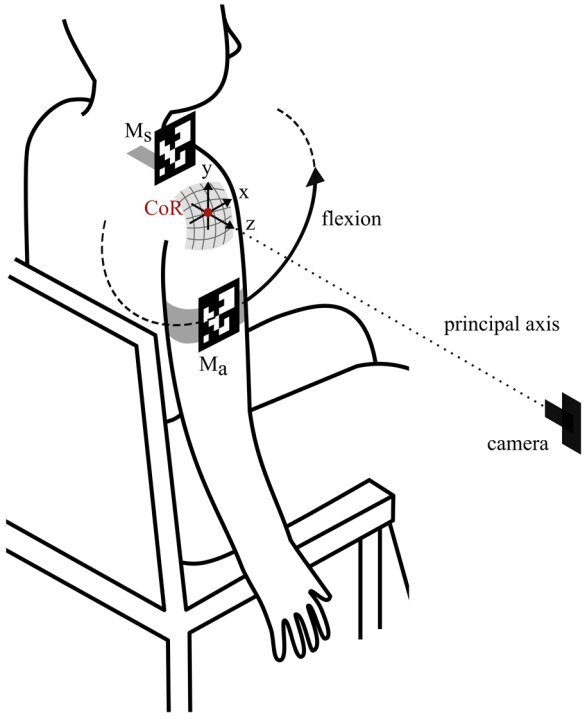

Fig. 3.1 – Schematic overview of the measurement setup showing a subject sitting on a chair with the two ArUco markers (Ma and Ms) and camera with its principal axis placed perpendicular to the sagittal plane, approximately in line with the z-axis of the CoR. When the subject is performing an anteflexion movement of the arm (movement in the sagittal plane), marker Ma that is attached to the upper arm describes an arc. Marker Ms is attached to the lateral portion of the scapula. From the relative movement of the marker Ma with respect to the marker Ms the CoR can be estimated through sphere fitting. An adhesive with grid pattern is placed on the humeral head region, and is used for registering the estimated CoR position to the skin.

Aruco markers

The pose of the two ArUco markers was detected with the open-source ArUco library [16-17,23]. To increase the accuracy of the marker pose estimation, the marker pose tracker algorithm with discriminative correlation filters was implemented [23]. This algorithm detects the initial position of each marker and tracks the marker's position in subsequent frames.

Procedure

The CoR estimation procedure consists of four main steps:

1. *Obtain arm marker coordinates from video*. Video recordings (frame rate = 25 frames per second) of arm flexion movements in the sagittal plane were processed with the ArUco marker pose tracking algorithm [23] to obtain the transformation matrices that express the translation and rotation from the local coordinate systems Ψ_S (scapula) and Ψ_A (arm) to the

(global) camera coordinate system Ψ_C, see also Fig. 3.2. H_S^C is the 4x4 homogeneous transformation matrix from Ψ_S to Ψ_C, and H_A^C from Ψ_A to Ψ_C.

2. *Transform arm marker coordinates from camera coordinate system to scapula marker coordinate system*. To account for possible trunk movements of the subject with respect to the camera during a measurement, the arm marker coordinates (H_A^C) were expressed in the scapula marker coordinate system Ψ_S. This transformation is provided by the 4x4 homogeneous matrix (H_A^S) which transforms data from Ψ_A to Ψ_S:

$$H_A^S = (H_S^C)^{-1} H_A^C \tag{3.1}$$

3. *Fit sphere to arm marker data*. The equation of a sphere is given by:

$$(p_x - s_x)^2 + \left(p_y - s_y\right)^2 + (p_z - s_z)^2 = R^2 \tag{3.2}$$

With (p_x, p_y, p_z) points on the sphere, (s_x, s_y, s_z) the center of the sphere and R its radius.

A sphere was fitted to the 3D arm marker coordinates (expressed in Ψ_S) using a least-squares method. Finding the least squares fit corresponds to minimizing the squared Euclidean (geometric) distances (d_i) between the arm marker coordinates ($p_{x,i}$, $p_{y,i}$, $p_{z,i}$) and the estimated sphere center (s_x, s_y, s_z):

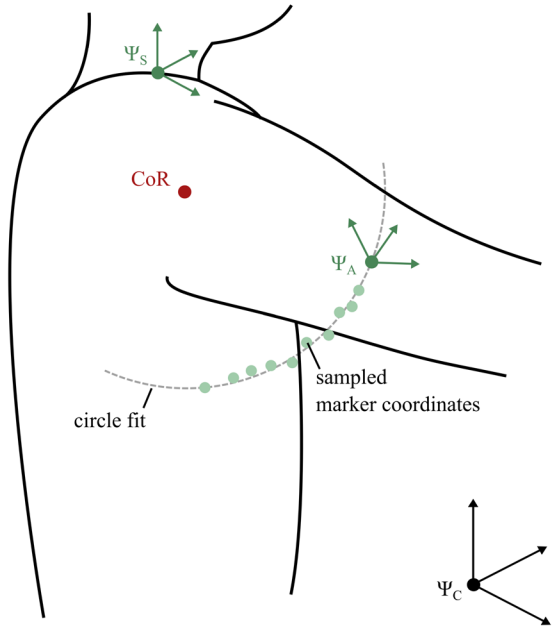

Fig. 3.2 – Schematic overview of the local marker coordinate systems (Ψ_S and Ψ_A) and global camera coordinate system (Ψ_C). Each video frame the arm marker coordinates are sampled. The CoR in the sagittal plane is defined as the projected center of a sphere that is fitted to the processed marker coordinates.

$$\text{Min}\,\mathcal{F} = \sum_{i=1}^{n} {d_i}^2 \tag{3.3}$$

with:

$$d_i = \sqrt{\left(p_{x,i} - s_x\right)^2 + \left(p_{y,i} - s_y\right)^2 + \left(p_{z,i} - s_z\right)^2} - R \tag{3.4}$$

4. *Project sphere center coordinates on to image plane*. Finally, the (3D) sphere center coordinates (s_x, s_y, s_z) which are expressed in reference frame Ψ_S, were projected onto the camera plane using OpenCV's *projectPoints* function [24]. The resulting sphere center location in the camera plane ($\bar{c}_x, \bar{c}_y$) allows for registration of the estimated sphere center to the body.

3.2.2. Registration

The estimated sphere center location should be registered on the upper arm to be able to align the brace to the shoulder center of rotation in the sagittal plane.

Setup

Before the measurement, an adhesive with a grid pattern (5 x 5 mm grid size) was placed on the lateral region of the shoulder (see Fig. 3.3A) to guide the registration of the estimated rotational center on to the body.

Procedure

The registration procedure consisted of three steps: (1) plot the projected sphere center (in pixels) on the captured image using Matlab 2019a (MathWorks, USA). (2) Measure the center position in the grid coordinate system (where (0,0) is the lower left corner of the grid). (3) Mark the location on the body. In Fig. 3.3B a close-up of the adhesive with grid pattern is shown, together with the estimated projected sphere centers across individual trials and its mean value.

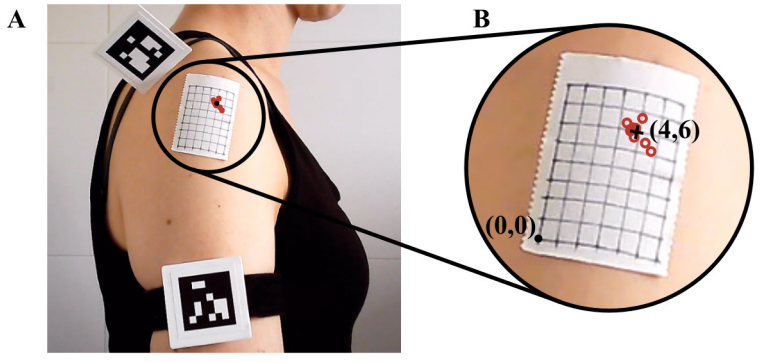

Fig. 3.3 – A) The projected sphere centers can be plotted on the captured video frame. The adhesive that was attached to the subject's skin serves as a reference during registration of the found center to the skin. B) Close-up of the grid pattern showing the estimated sphere centers across individual trials (o) and the mean sphere center (+) and its position in the grid coordinate system.

3.2.3. Experimental procedure

With two experiments both the accuracy and repeatability of the CoR estimation procedure were determined.

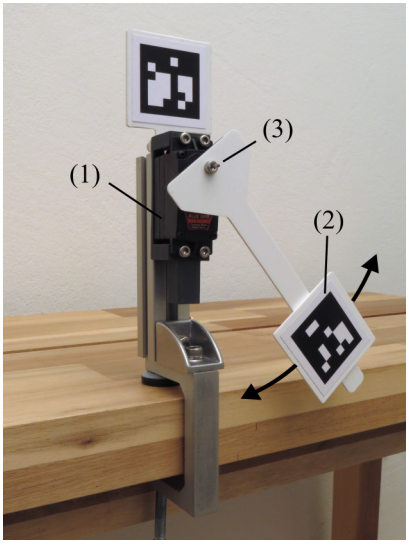

Fig. 3.4 – Setup that was used to determine the accuracy of the CoR estimation method. A servo (1) rotates the moving ArUco marker (2) at a fixed speed. Since the true rotational center (3) is known, the offset of the estimated sphere center with respect to the actual center can be determined.

Accuracy

Accuracy is defined as the mean difference between the estimated rotational center and the true rotational center across multiple trials. A test bench with a known rotational center was used to determine the accuracy of the CoR estimation procedure (Fig. 3.4). The test bench consisted of a fixed and moving segment to which two ArUco markers (size = 32.5 mm) are attached. The camera was placed 50 cm from the test bench, and was horizontally aligned with the rotational center of the test bench. The distance from the moving marker to the rotational center was 10 cm. The rotation of the moving segment was controlled with a servo motor and custom software. Measurements were performed at two velocities: 30 and 60°/s. Each trial, the segment was moved 5 times between 0 and 60° anteflexion.

In total, 10 trials were recorded and the data was processed with Matlab 2019a (Mathworks, USA). The estimated center of rotation $(\bar{c}_x, \bar{c}_y)$ was obtained for every trial by performing the steps described in the CoR estimation procedure. The true center of rotation (c_x, c_y) was obtained by manually registering the actual location on the image. The mean absolute offset (d_{off}) between the estimated and true rotational center across *n* trials was calculated according to:

$$d_{off} = \frac{1}{n}\sum_{i=1}^{n}\sqrt{\left(\bar{c}_{x,i} - c_x\right)^2 + \left(\bar{c}_{y,i} - c_y\right)^2} \tag{3.5}$$

The mean offset was reported, and a two-sample t-test was performed to determine whether the offset distance between the true and estimated rotational center significantly changed ($p < 0.05$) for different velocities (30°/s and 60°/s).

Repeatability

Repeatability is defined as the degree to which repeated measurements would lead to similar results under similar circumstances and was evaluated with five non-impaired subjects with a median age of 35 (range 32-63). The subjects had no history of shoulder-related complaints and were able to follow simple instructions. Ethical approval for this study was obtained from the Ethics Committee of the University of Twente (ref. number 2021.74). All participants gave their written informed consent prior to the start of the study. The subjects were seated on a chair with back rest, and faced such that their sagittal body plane was perpendicular to the camera. The subjects were instructed to lift their right arm, with fully extended elbow, in the sagittal plane without excessively moving their trunk. One movement consisted of moving from a neutral position to 60° anteflexion and back. One trial consisted of 5 consecutive movements, with a constant velocity of approximately 30°/s that was guided by a metronome. Prior to each measurement session, an adhesive with a grid pattern (5 mm spacing) was attached to the subject's skin at the humeral head region for registration purposes. The distance from the shoulder to the camera was 60 cm. The camera was positioned at an approximate equal height with the shoulder joint.

Subjects were instructed to move their arm between 0 and 60° anteflexion. Although participants were able to lift their arm higher, a maximum angle of 60° anteflexion was chosen to restrict the motion from occurring in other joints of the shoulder complex than the glenohumeral joint as much as possible. During the first 60° the movement primarily occurs at the glenohumeral joint, with only a small contribution from the scapulothoracic joint.

A strap with marker Ma was attached to the upper arm, approximately 15 cm from the glenohumeral axis of rotation. Marker Ms was attached to the flat portion of the acromion (lateral portion of the scapula, above the spinal process) using a 3D-printed part and double-sided adhesive tape. This reduced skin movement artifacts as much as possible, as the acromion is said to have the least amount of skin movement artifact compared to other locations on the scapula [24].

Each trial was repeated 20 times. This includes putting on both markers, and positioning the subject in front of the camera. During the first 10 trials the subjects placed the markers on their body themselves. This condition resembled a novice examiner. During the last 10 trials, the researcher placed the markers on the subject. This condition resembled an experienced examiner.

Video recordings were made during all measurements and the data was processed according to the CoR estimation and registration procedure described above. The repeatability of the method was assessed by calculating the root mean squared distance (RMS) from the estimated projected sphere centers ($\bar{c}_{x,i}, \bar{c}_{y,i}$) after each trial to the mean sphere center across all n trials $(\bar{x}, \bar{y})$ per subject:

$$RMS = \sqrt{\frac{1}{n}\sum_i \left(\left(\bar{c}_{x,i} - \bar{x}\right)^2 + \left(\bar{c}_{y,i} - \bar{y}\right)^2 \right)} \quad (3.6)$$

A paired t-test was performed to detect significant differences in RMS ($p < 0.05$) between the two examiners.

3.3. Results

3.3.1. Accuracy

The mean absolute offset (d_{off}) between the true center of rotation of the test bench and the fitted sphere centers across multiple trials was 2.7 mm (SD 0.72) when moving at a velocity of 30°/s. The mean absolute offset was 2.5 mm (SD 1.0) at 60°/s. A two-sample t-test revealed no significant difference between the two velocities.

3.3.2. Repeatability

The repeatability was assessed by evaluating how close individual measurements are to each other. For two participants only 19 trials were available for analysis, instead of 20. Once, because the video was not properly recorded, and once because the arm marker was rotated such that it was not detected by the marker pose tracker algorithm. For the other three subjects 20 trials were available: 10 conducted by the novice examiner, and 10 by the expert examiner. A pair-wise comparison per subject revealed a mean distance of 6.6 mm (range 2.4 – 10.8 mm) between the novice and expert examiner estimations.

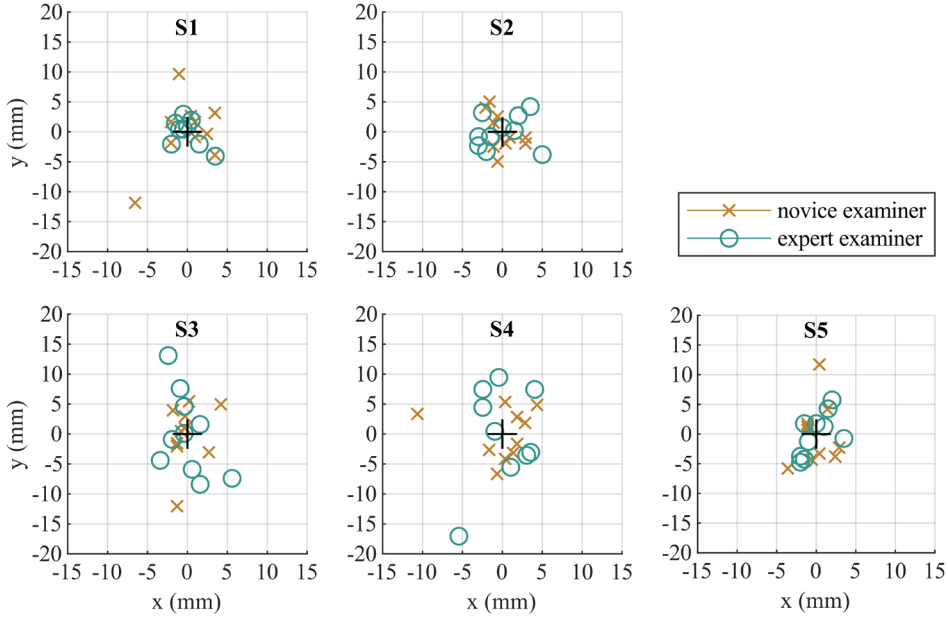

Fig. 3.5 – Mean-centered projected sphere center estimates for each of the five subjects (S1-S5) displayed on a 5 mm spaced grid. Trials where the novice examiner performed the measurements are marked with (x) and where the expert examiner performed the measurements are marked with (o).

In Fig. 3.5 the estimated projected sphere center positions for each individual trial are shown per subject. To allow for a visual comparison of the data between the two conditions ('novice' and 'expert') the sphere center positions were mean-centered on the grid.

The mean RMS value across all subjects was 5.1 mm (range 3.4 – 6.0 mm) for the novice examiner, and 5.2 mm (range 2.7 – 8.5 mm) for the expert examiner. A paired-sample t-test was performed. The difference between examiners was not statistically significant ($p = 0.96$). The 95% confidence interval of the difference was (-3.2, 3.0 mm).

3.4. Discussion

In this study we have shown that our proposed method can accurately estimate the rotational center of the glenohumeral joint. Accurate knowledge may improve the quality of the brace alignment. Not only because proper fitting will increase the performance of the brace, but also since undesired external forces may cause the brace to loosen over time. The accuracy and repeatability of our method is comparable with state-of-the-art methods, such as presented by Crabolu et al. [8] (accuracy mechanical test bench <3 mm), and Lempereur et al. [5] (in-vivo repeatability <4.11 to 8.25 mm). Compared to other methods our setup only comprises a cheap webcam (around €40) that can be used for many measurement sessions and the total assessment (including preparation time) takes less than three minutes to complete, which will further improve uptake in the clinical practice. In addition we have created a simple technique to register the found sphere center location to the body.

Relative movements between the marker and the bony segment to which it was attached may potentially have negatively impacted the quality of the sphere fitting process. All trials have therefore been visually inspected for any large deviations from the marker coordinates to the fitted sphere. In general, the data seemed to match the fitted sphere outline well. Incidental skin marker artifacts may have occurred, but their influence on the CoR estimation was considered be minor, as the sphere fits were always based on the averaged data of one full trial (5 movements). Still, skin marker artifacts could have contributed to the variation among subjects, especially if they have a high body fat percentage. Difficulties in maintaining a constant arm speed throughout the measurement may have caused an uneven spreading of sampled marker coordinates within the movement range for several trials. This may affect the performance of the marker tracking algorithm. Also, excessive rotation of the upper arm during flexion-extension movements may have decreased the algorithm performance.

3.5. Conclusion

In this study we proposed a method to estimate the GH-CoR and register this location on the body for brace alignment. The accuracy of the method ranged from 2.5 to 2.7 mm under the assumption of no skin artifacts. The repeatability ranged from 5.1 to 5.2 mm for the novice and expert examiner. From these results we can conclude that our method is able to accurately estimate the GH-CoR with a high degree of repeatability. We observed no significant

differences between the measurements that were conducted by novice or expert examiners which means that the proposed method is robust for inter-rater differences.

In the current study, healthy participants performed anteflexion movements from a neutral position to 60° anteflexion and back. Patients may not be able to perform these complete movements due to pain or other limitations. For these patients, we will explore the influence of a smaller movement arc (e.g. 30° anteflexion) on the quality of the estimation in a future research. However, it should be noted that patients with a very limited range of motion may not benefit from a dynamic orthosis that requires alignment with the shoulder joint.

In the current work we only applied the method to the glenohumeral joint. In future research we will explore the possibilities of transferring the method to other joints such as the hip, knee or elbow.

References

[1] Schiele A and van der Helm FCT. Kinematic design to improve ergonomics in human machine interaction. IEEE Transactions on Neural Systems and Rehabilitation Engineering. 2006; 14(4): 456–469.

[2] Haarman CJW, Hekman EEG, Haalboom MFH et al. A new shoulder orthosis to dynamically support glenohumeral subluxation. IEEE Transactions on Biomedical Engineering. 2021; 68(4): 1142–1153.

[3] Meskers CG, van der Helm FCT, Rozendaal LA et al. In vivo estimation of the glenohumeral joint rotation center from scapular bony landmarks by linear regression. Journal of Biomechanics. 1997; 31(1): 93–96.

[4] Lempereur M, Leboeuf F, Brochard S et al. In vivo estimation of the glenohumeral joint centre by functional methods: accuracy and repeatability assessment. Journal of Biomechanics. 2010; 43: 370–374.

[5] Veeger HE. The position of the rotation center of the glenohumeral joint. Journal of Biomechanics. 2000; 33(12): 1711–1715.

[6] Crabolu M, Pani D, Raffo L et al. In vivo estimation of the shoulder joint center of rotation using magneto inertial sensors: MRI based accuracy and repeatability assessment. BioMedical Engineering OnLine. 2017; 16: 37.

[7] Crabolu M, Pani D and Cereatti A. Evaluation of the accuracy in the determination of the center of rotation by magneto-inertial sensors. 2016 IEEE Sensors Applications Symposium (SAS); 2016: 1–5.

[8] Crabolu M, Pani D, Raffo L et al. Estimation of the center of rotation using wearable magneto-inertial sensors. Journal of Biomechanics. 2016; 49(16): 3928–3933.

[9] McGinnis RS and Perkins NC. Inertial sensor based method for identifying spherical joint center of rotation. Journal of Biomechanics. 2013; 46(14): 2546–2549.

[10] Amabile C, Bull AMJ and Kedgley AE. The centre of rotation of the shoulder complex and the effect of normalisation. Journal of Biomechanics; 2016; 49(9): 1938–1943.

[11] Monnet T, Atchonouglo K and Vall C. Location of the shoulder joint centre and identification of the body segment parameters. Proceedings in Applied Mathematics & Mechanics. 2007; 7: 3050005–3050006.

[12] Monahan K. Functional identification of shoulder joint centers. [Thesis]. Delaware, USA: University of Delaware; 2009.

[13] Cappozzo A, Della Croce U, Leardini A et al. Human movement analysis using stereophotogrammetry. Part 1: Theoretical background. Gait and Posture. 2005; 21(2): 186– 196.

[14] Stokdijk M, Nagels J and Rozing PM. The glenohumeral joint rotation centre in vivo. Journal of Biomechanics. 2000; 33(12): 1629–1636.

[15] Fiala M. ARTag, a fiducial marker system using digital techniques. 2005 IEEE Computer Society Conference on Computer Vision and Pattern Recognition (CVPR'05). 2005; 2: 590–596.

[16] Garrido-Jurado S, Muñoz-Salinas R, Madrid-Cuevas FJ et al. Generation of fiducial marker dictionaries using Mixed Integer Linear Programming. Pattern Recognition. 2016; 51: 481– 491.
[17] Romero-Ramirez FJ, Muñoz-Salinas R and Medina-Carnicer R. Speeded up detection of squared fiducial markers. Image and Vision Computing. 2018; 76: 38–47.
[18] Olson E. AprilTag: A robust and flexible visual fiducial system. 2011 IEEE International Conference on Robotics and Automation. 2011; 3400–3407.
[19] Fiala M. Designing highly reliable fiducial markers. IEEE Transactions on Pattern Analysis and Machine Intelligence. 2010; 32(7): 1317–1324.
[20] Garrido-Jurado S, Muñoz-Salinas R, Madrid-Cuevas FJ et al. Automatic generation and detection of highly reliable fiducial markers under occlusion. Pattern Recognition. 2014; 47(6): 2280–2292.
[21] Nagymate G and Kiss RM. Affordable gait analysis using augmented reality markers. PLoS ONE. 2019; 14(2): e0212319.
[22] Sementille AC, Lourenço LE, Brega JRF et al. A motion capture system using passive markers. Proceedings of the 2004 ACM SIGGRAPH international conference on Virtual Reality continuum and its applications in industry (VRCAI '04). 2004; 440–447.
[23] Romero-Ramirez FJ, Munñoz-Salinas R and Medina-Carnicer R. Tracking fiducial markers with discriminative correlation filters. Image and Vision Computing. 2021; 107: 104094.
[24] Bradski G. The OpenCV Library. Dr Dobb's Journal of Software Tools. 2000; 25: 120–125.
[25] Matsui K, Shimada K and Andrew PD. Deviation of skin marker from bone target during movement of the scapula. Journal of Orthopaedic Science. 2006; 11(2): 180–184.

4. Accurate estimation of upper limb orthosis wear time using miniature temperature loggers

Abstract—Objective: To propose and validate a new method for estimating upper limb orthosis wear time using miniature temperature loggers attached to locations on the upper body. Design: Observational study. Subjects: Fifteen healthy participants. Methods: Four temperature loggers were attached to the arm and chest with straps. Participants were asked to remove and re-attach the straps at specified time-points. The labelled temperature data obtained were used to train a decision tree classification algorithm to estimate wear time. The final performance (mean error and 95% confidence interval) of the trained classifier and the wear time estimation were assessed with a hold-out data-set. Results: The trained algorithm can correctly classify unseen temperature data with a mean classification error between 1.1% and 3.1% for the arm, and between 1.8% and 4.0% for the chest, depending on the sampling time of the temperature logger. This resulted in mean wear time errors between 0.5% and 8.3% for the arm, and 0.13% and 13.0% for the chest. Conclusion: The proposed method based on a classifier can accurately estimate upper limb orthosis wear time. This method could enable healthcare professionals to gain insight into the wear time of any upper limb orthosis.

Published as: Haarman, C. J. W., Hekman, E. E. G., Rietman, J. S., & van der Kooij, H. (2022). Accurate Estimation of Upper Limb Orthosis Wear Time Using Miniature Temperature Loggers. Journal of Rehabilitation Medicine, 54(SE-Articles), jrm00277

4.1. Introduction

Upper limb orthoses are frequently prescribed to support patients with impairment of the shoulder, arm and hands. However, an orthosis can be effective only if it is used by patients. Little is known about treatment adherence with wearing upper limb orthoses. Physicians or therapists assume that the patient adheres to their prescribed treatment, but the actual wear time may deviate strongly from the prescribed time. The rate of non-use may be as high as one-third of all devices provided [1]. To evaluate the efficacy of a treatment that involves an orthosis, a reliable estimation of the wear time is required.

Subjective methods, such as diaries or questionnaires, are low-cost and easy to implement, but are vulnerable to reporting bias (e.g. social desirability or recall errors) [2-3]. These subjective methods lack accuracy, as most patients tend to overestimate the degree of actual wear time [4]. Objective methods, such as measuring force [5–7], acceleration [8] or temperature [2, 4, 7, 9–11], have been proposed to overcome these problems.

Of these proposed methods, temperature seems to be most suitable for measuring orthosis wear time, because of the small size of the sensors, low cost, ease of implementation in existing orthoses, and ability to take measurements over a prolonged period (up to a few months) without human intervention. Currently, no algorithms have been developed to estimate upper limb orthosis wear time using temperature sensors. Previous efforts to estimate wear time have focused mainly on orthopaedic footwear [2, 9] and spinal correction braces [4, 7]. In these applications, orthoses are typically worn for long, consecutive periods (from a few hours up to 23 h/day). The device is thus donned and doffed only once or twice per day. In contrast, upper limb orthoses are generally donned and doffed more frequently; for example when performing rehabilitation exercises at home (e.g. 3 times a day for 20 min), or when performing specific daily activities. Algorithms developed previously rely on absolute temperature thresholds [4, 7], or peak detection algorithms to discriminate between on and off states [9]. Reported accuracies in these studies range from 86% to 99%, but these results may not be valid if the sensors are applied to other body parts, are donned and doffed more frequently, or if the sensors are not worn directly on the skin.

The aim of this study is to propose and validate a new method to estimate orthotic device wear time using temperature sensors attached to locations on the upper body. The method should accurately estimate wear time during frequent donning and doffing, and while not wearing the sensors directly on the skin. A decision tree classification algorithm was trained using labelled temperature data obtained from healthy participants, and its performance assessed using unseen test data. Instead of using only a single temperature sensor, the study investigated whether a dual sensor configuration (1 sensor directed away from the body and the other directed towards the body) improved the performance of the wear time estimation algorithm. A further aim was to investigate the effect of sampling time on the performance of the algorithm.

4.2. Methods

4.2.1. Temperature sensor data loggers

Thermochron® iButtons® (Maxim Integrated, San Jose, CA, USA) are miniature data loggers that measure and store temperature (Fig. 4.1A). The sensors are 17 mm in diameter and 6 mm high, and thus are a suitable size for integration into an orthotic device. The DS1922L Thermochron® can store up to 8,192 values with a resolution of 0.5°C. Its sampling time can be programmed from 1 s up to 273 h. With a sampling time of 1 min, the device can store up to approximately 5.5 days of consecutive temperature readings. When the sampling time of the sensor is increased, longer measurements can be performed before data has to be retrieved. Table 4.1 shows the maximum periods of unsupervised data collection for different sampling times. Under normal operating conditions (1-min logging interval, and a temperature of 30°C), the DS1922L battery lasts for at least 1 year.

The temperature loggers are secured to the body with 2 elastic straps. One strap is positioned around the chest and the other around the forearm (Fig. 4.1B). Temperature sensors are attached to each strap by means of a custom 3D-printed case (Fig. 4.1C). One sensor is positioned facing towards the body (S_{IN}), such that it touches the participant's clothing. The other sensor is positioned facing away from the body (S_{OUT}). In order to provide a comfortable interface, the length of the straps is adjusted for each participant.

4.2.2. Smartphone app

To simulate donning and doffing of an orthosis, the participant was asked to remove and re-attach the temperature sensors at specified time-points. For this, a custom Android smartphone application was developed, which cues the participant and registers whether the action has been completed. Based on the timestamps logged by the smartphone app, a label was assigned to each temperature data-point that contains its true state. The app notified

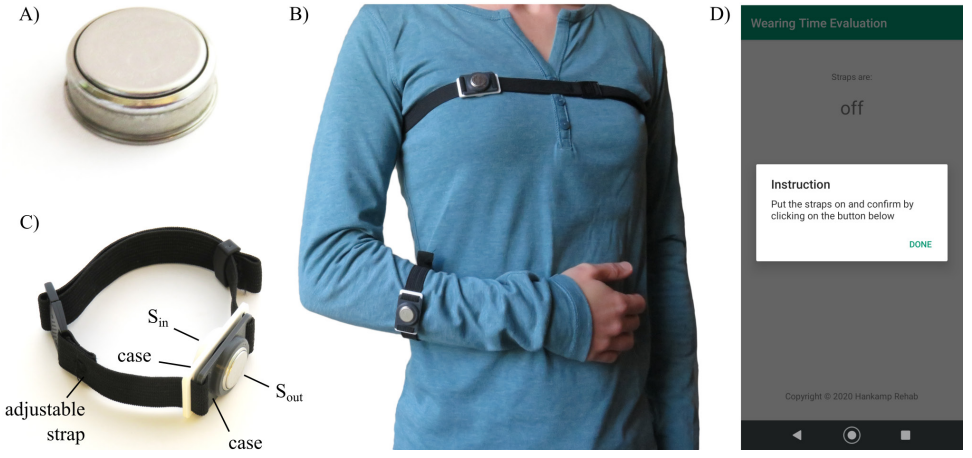

Fig. 4.1 – A) DS1922L Thermochron® iButton®. B) Close-up of the adjustable strap with 2 sensors mounted in a 3D-printed case; 1 sensor facing towards the body (Sin), and the other sensor facing away from the body (Sout). C) Placement of the straps on the forearm and chest. D) Screenshot of smartphone app.

Sampling time	Maximum measurement duration
1 min	5.5 days
5 min	28.4 days (~4 weeks)
10 min	56.9 days (~8 weeks)
15 min	85.3 days (~12 weeks)

Table 4.1: Maximum duration of one measurement when different temperature logger sampling times are programmed

participants with an audio signal when it was time to don or doff the straps. Fig. 4.1D shows a screenshot of the instruction a participant receives after a notification. To record sufficient transitions between use and non-use states (to represent frequent donning and doffing of the orthosis), the intervals between 2 notifications were randomly programmed between 15 and 60 min. The smartphone time was synchronized with the sensor time prior to each measurement.

4.2.3. Measurement protocol

From each participant approximately 24h of measurement data were collected, consisting of 8h of active sensor donning and doffing and 16h of non-use. Both straps (with sensors attached to them) were worn on top of the participant's clothing. During the period in which they actively don and doff the sensors (8h), participants were instructed to carry out their normal daily routines. Prior to the measurements, participants were instructed to pay attention to the correct sensor orientation (the same sensor should always face towards the body). They were also instructed to immediately confirm their action in the smartphone app after sensor donning or doffing, to minimize the difference between the time of the actual change and the time logged by the smartphone. Participants were allowed to doff the sensors temporarily (e.g. during a clothes change). Unexpected doffing periods that lasted more than 30 s had to be noted. After each measurement session, temperature data from the sensors and timestamp data from the smartphone app were transferred to a computer for further processing and analysis.

4.2.4. Participants

A total of 15 healthy subjects (7 males and 8 females), with a median age of 35 years (range 24–67 years) participated in the study. Inclusion criteria included the ability to follow simple instructions. The study was approved by the ethics committee of the University of Twente (reference number 2020.39). Written informed consent was obtained from all subjects before the study.

4.2.5. Data processing

Each temperature sample was assigned a label 0 (‘*off*’) or 1 (‘*on*’) according to the timestamps logged by the smartphone app when the sensors were donned and doffed. Seventy percent of the measurement data was randomly assigned to a training set and 30% to a test set. Stratification was applied to maintain an equal distribution of the classes within these 2 sets.

Feature	Abbreviation	Equation
Sensor temperature	T_{IN}	
	T_{OUT}	
Temperature difference between current and previous data point	$dT_{IN}dt$	$T_{IN}(i) - T_{IN}(i-1)$
Temperature between 2 sensors	ΔT	$T_{IN}(i) - T_{OUT}(i)$

Table 4.2 – Features that were extracted from the measurement data.

Sensor configuration	Selected features
Single	$T_{IN} + dT_{IN}dt$
Dual	$T_{IN} + dT_{IN}dt + \Delta T$

Table 4.3 – Selected features for the single and dual sensor configuration.

In this study, the data were captured with a sampling time of 1 min. The obtained data-sets were down-sampled by a factor, n, leaving only every nth sample in the data-set. Thus, multiple data-sets with different sampling times were obtained from the original measurement data to allow for an in-depth evaluation of the algorithm performance at different sampling times. The chosen down-sampling factors (n) are: 1, 5, 10 and 15, corresponding to sampling times (t_S) of: 1, 5, 10 and 15 min.

Depending on the configuration used, different features can be calculated and the selected features were used during data processing. The study investigated whether a dual sensor configuration can better estimate wear time compared with a single sensor configuration. In a single sensor configuration, temperature readings from only 1 sensor, directed towards the body (T_{IN}), are available. A derived feature is the temperature difference of this sensor from its previous reading ($dT_{IN}dt$). In a dual sensor configuration, temperature readings from a sensor directed away from the body (T_{OUT}) are also available. Thus, the temperature difference between the 2 sensors (ΔT) can also be computed. Table 4.2 summarizes the features that were calculated from the measurement data. Table 4.3 lists the selected features that were used for data processing in the single and dual sensor configuration.

4.2.6. Binary classification

In total, 16 different data-sets were constructed based on the collected measurement data (Fig. 4.2). A decision tree classifier was trained to map temperature data (input) to corresponding device states (output) based on example input-output pairs. This can be considered a binary classification problem, as there are only 2 classes to be discriminated for each sample in the data-set: use ('*on*') or non-use ('*off*'). A well-trained model correctly predicts these classes ('*on*' and '*off*') for each data point obtained during a certain measurement period. Any inconsistency between the predicted state (predicted by the trained model) and the true state (recorded by the smartphone app) will decrease the accuracy with which the class can be correctly determined.

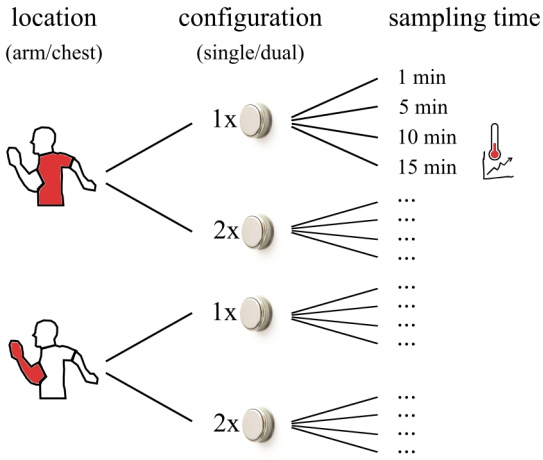

Fig. 4.2 – Construction of different 16 data-sets based on collected measurement data. For all participants 16 data-sets are created, differentiating between location (arm or chest), sensor configuration (single or dual) and sampling time (1, 5, 10 and 15 min).

4.2.7. Classifier training and performance evaluation

The classification error rate (e_{CLASS}), or misclassification rate, is defined as the number of incorrect predictions, divided by the total number of predictions. Fig. 4.3 shows an overview of the classifier training and performance evaluation procedure. Stratified K-fold cross-validation was used to evaluate and optimize the performance (error rate) of the classification algorithm. For this, the training data was split into k subsets (folds). In each fold the class ratios were maintained. For every iteration a different fold was held out as a validation set. The mean classification error rate was then determined over all iterations and the model parameters resulting in the best mean performance were selected.

For each data-set (different sampling times and body location), and for the 2 feature subsets (representing a single or dual sensor configuration), the classification error rates and the 95% confidence intervals (95% CI) of the trained model were determined using the held-out test set, containing 30% of the original data. The 95% CIs were calculated using the following equation:

$$CI = 1.96 * \sqrt{\frac{e_{class} * (1 - e_{class})}{n}} \tag{4.1}$$

where e_{CLASS} is the classification error rate.

4.2.8. Wear time estimation (interval data-set)

The cumulative wear time (T_{WEAR}) is the total time that the orthotic device is worn during a certain measurement period, and is calculated by multiplying the total number of data points labelled "on" by the sampling time. The estimated cumulative wear time (T_{EST}) is calculated by multiplying the total number of data points with the classification label "on" by the sampling time.

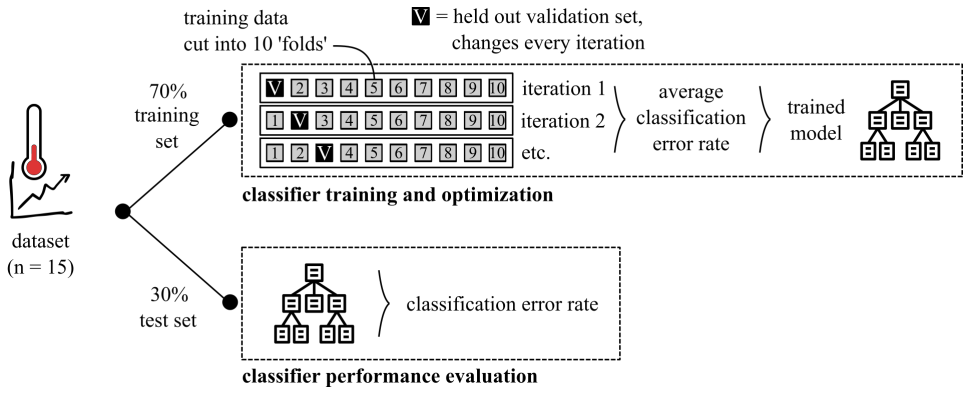

Fig. 4.3 – Graphical overview the classifier training and optimization, and performance evaluation procedure. For each of the 16 data-sets (e.g. single sensor mounted to the chest, and a 5-min sampling time) the temperature data of all 15 participants were used to construct a data-set. Seventy percent of the data were used to train the classifier and the other 30% were used to evaluate the classifier performance of the trained model.

The wear time error is then defined as the ratio between the estimated and true wear times. The wear time error can be positive (overestimation of the wear time) or negative (underestimation of the wear time). For each data-set mean the wear time errors including their 95% CIs were estimated by bootstrapping the test set (sample size=80%, iterations=1000). Boot-strapping is a sampling method to estimate a quantity of a population [12]. For this, the test set is randomly sampled many times with replacement.

Each bootstrap sample represents 1 realization of a test set. The resulting mean wear time errors were then calculated, and the 95% CIs were obtained that bound the estimated skill of the trained model. Differences between mean wear time errors of the single and dual sensor configuration are statistically significant ($p < 0.05$) if the degree of overlap of the 95% CIs is < 50% of the mean margin of error (MOE). The MOE is defined as half the CI width [13].

4.2.9. Wear time estimation (continuous use data-set)

The performance of the trained model to estimate the wear time was also evaluated when sensors were not frequently donned and doffed, but worn for a single long, consecutive period per day. For this purpose, 5 additional data-sets were obtained from healthy participants who only donned and doffed the sensors once (at the beginning and end of an 8h period of use) during a 24h measurement session. Temperature and timestamp data from these measurements were processed and provided as test sets to the trained classifier. The wear time error was calculated in a similar manner as for the original test set.

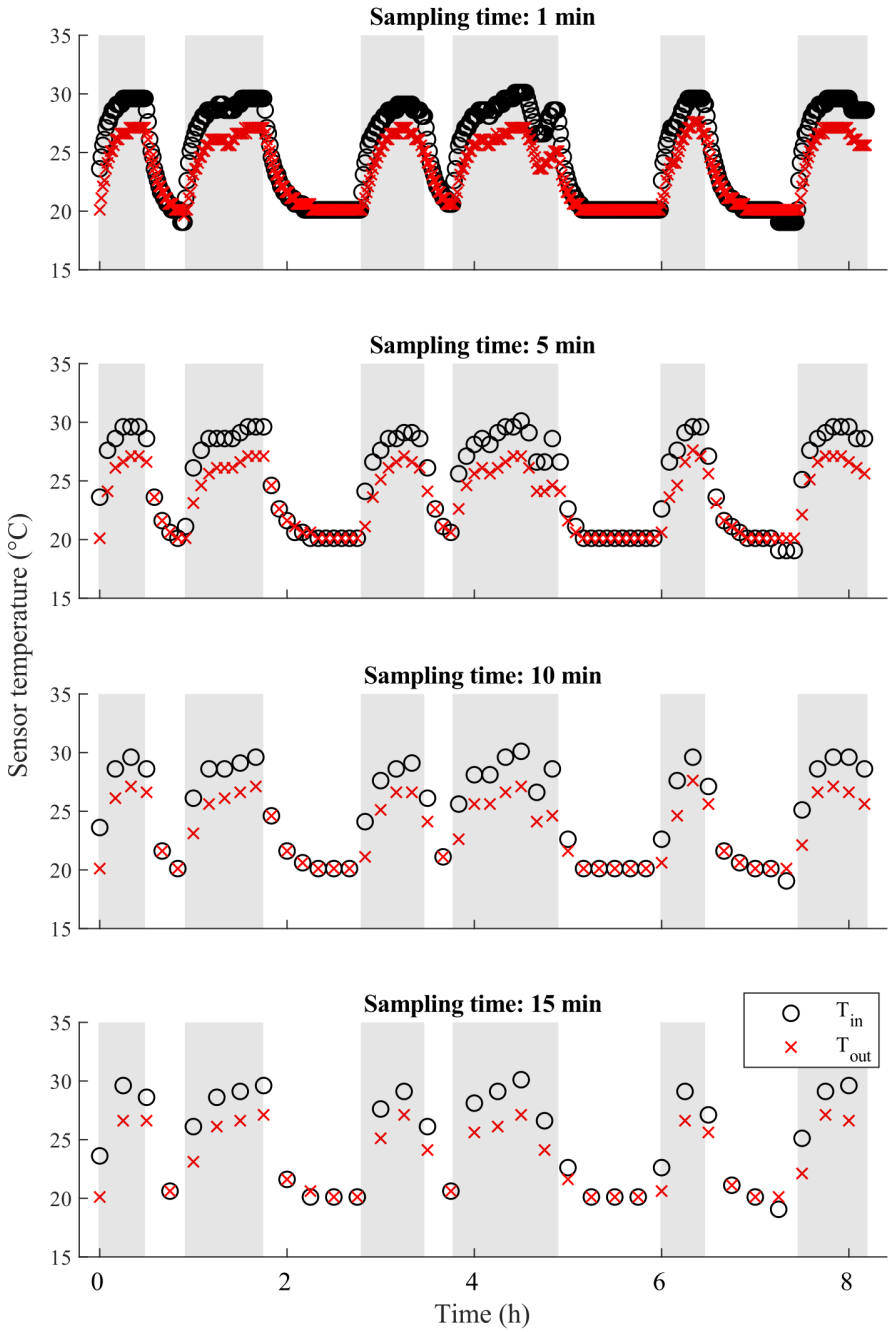

Fig. 4.4 – Typical temperature data from the inward (o) and outward (x) directed sensors on the arm, for different sampling intervals. The top figure shows the original temperature data, the other figures show the down-sampled measurement data (5, 10 and 15 min). The shaded areas indicate the intervals that the sensors were marked "on" in the smartphone app.

4.3. Results

4.3.1. Data-sets

In total, 22,427 data samples were collected from 15 participants. Unbalanced data-sets (unequal distribution of classes '*on*' and '*off*') were obtained due to the nature of the data collection (8h of repeated donning and doffing, during a 24h measurement period). Two participants reported intervals with inconsistent sensor orientation during their measurement. In 1 occasion the participant noticed that the donning action was not confirmed in the app. The corresponding samples were removed from their data-set to maintain internal consistency, leaving 22,224 data points for classification. Fig. 4.4 shows a plot of the 8h measurement time-period with periods of repeated donning and doffing for a typical participant. This figure shows data from both temperature sensors T_{IN} (o) and T_{OUT} (x), which were mounted on the forearm, for increasing sampling times (top to bottom). The *grey areas* indicate the intervals that the sensors were marked '*on*' in the smartphone app. As can be seen from the data, after donning, the temperature increases slowly until the temperature of the contact surface is reached, while after doffing, the temperature slowly returns to the ambient temperature. It can also be seen from the graphs that the temperature T_{IN} was higher than the temperature T_{OUT} throughout the entire measurement period, which lasted over 8h.

4.3.2. Classifier performance

The classifier performance was evaluated by cross-validating the training set and determining the mean of the calculated classifier errors. In Fig. 4.5 the classification errors (%) are presented for the arm (left) and chest (right), and for the single (o) and dual (x) sensor configuration and different sampling times. Error bars indicate the 95% CIs of the classification error. Overall, the mean classification error increased for increasing sampling times. Classification errors of the chest sensor(s) were, in all cases, higher than the errors of the arm sensor(s). Fig. 4.5 shows that the lowest classification errors (1.4% and 1.1%) were seen when the sensor(s) were mounted to the arm and sampled every 1 min. The highest classification errors (4.0% and 3.0%) were made when the sensor(s) were mounted to the chest and sampled every 15 min. For all data-sets, the classification errors in the dual sensor configuration were lower than in the single sensor configuration. In addition, the classifier performance on unseen data (test set containing 30% of held-out data) was also reported (x) in Fig. 4.5.

4.3.3. Wear time estimation (interval data-set)

Besides the classifier performance, the wear time estimation performance was also obtained by comparing the estimated wear times of the test set with the true wear times. In Fig. 4.6 (*top*) the mean wear time errors (%) and their 95% CIs are shown for each data-set.

For the arm, the mean wear time errors were –2.3%, –0.5%, –0.1% and 4.9%, respectively, for a 1, 5, 10 and 15 min sampling time. For the chest, these mean errors were 1.5%, –0.4%, –1.9% and –11.5% for a 1, 5, 10 and 15 min sampling time, respectively. The 95% CIs increased with increasing sampling times, meaning that the range of plausible values for the true wear time error increased. The mean wear time errors between the single (o) and dual

(x) sensor configuration were not significantly different, as their 95% CIs overlap sufficiently (13).

4.3.4. Wear time estimation (continuous use data-set)

To evaluate the performance of the trained classification model for alternative use cases, an alternative test set was presented to the trained model. The test set consists of data from 5 participants who wore the sensors for 8h consecutively, and then doffed the sensors. In total, 24h of data were collected from each participant. For this test set the mean wear time errors were obtained after bootstrapping, based on the trained classification algorithm. Fig. 4.6 (*bottom*) shows these wear time errors. It can be seen that the algorithm in all cases overestimates the actual wear times (positive error). Also, the mean errors were larger than for the 15–60 min use intervals test set.

The mean wear time errors were 4.3%, 3.8%, 8.5% and 15.3%, respectively, for 1, 5, 10 and 15 min sampling times. For the chest, these mean errors were 5.4%, 5.7%, 5.2% and 11.6%, respectively, for 1, 5, 10 and 15 min sampling times. The 95% CIs, however, were smaller than for the other test set, which indicates a smaller range of plausible values of the true error. The differences between the mean wear time errors between the single (o) and dual (x) sensor configuration were statistically significant in 4 out of 8 data-sets (see Fig. 4.6, *bottom*).

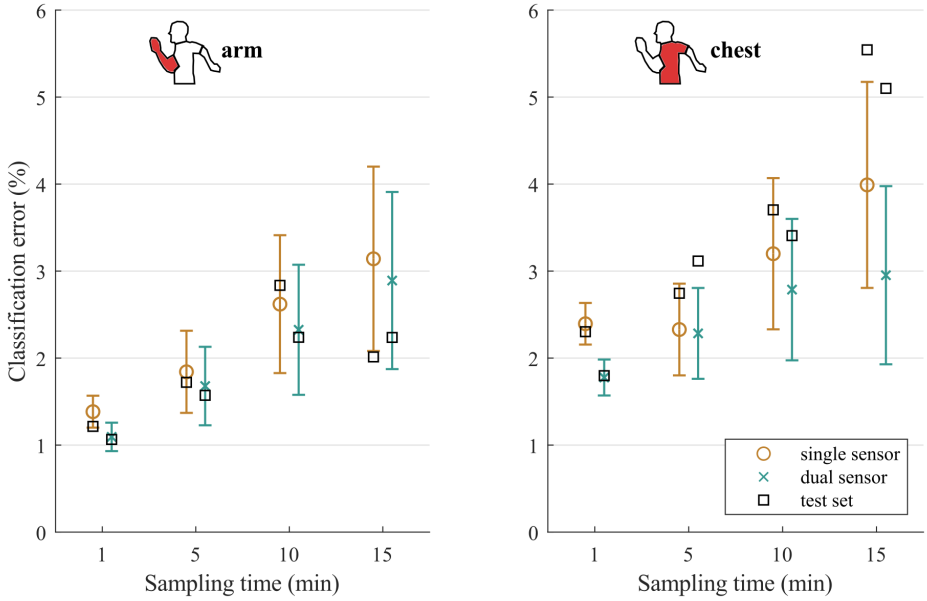

Fig. 4.5 – Mean classification errors for the arm (left) and chest (right) obtained after cross-validating the training set. Results are shown for the single (o) and dual (x) sensor configuration as well as for different sampling times. The error bars represent the 95% confidence intervals (95% CIs). Classification errors resulting from the test set are indicated with (□).

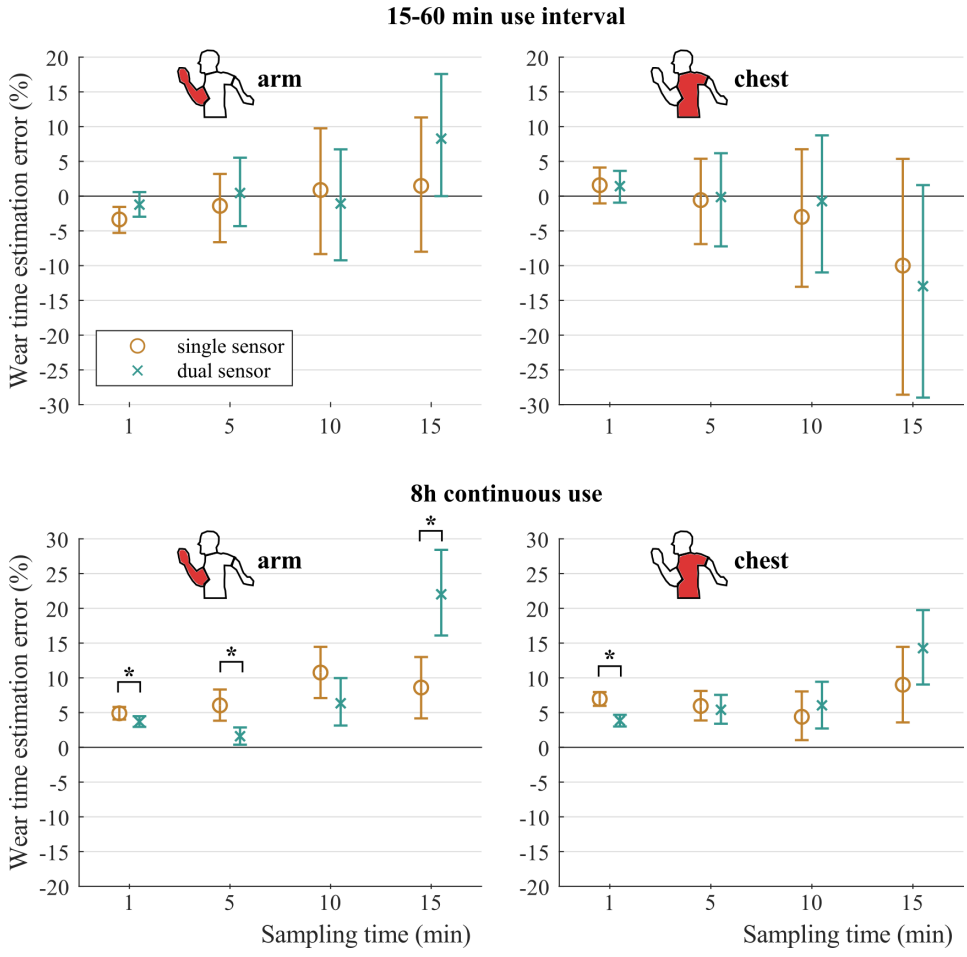

Fig. 4.6 – Test set performance for the single (o) and dual (x) sensor configuration. The mean wear time errors were calculated from sensors that were worn during 15–60-min use intervals (top) and 8h of consecutive use (bottom), on the arm (left) or chest (right). Error bars represent the 95% CIs of the wear time error, obtained after bootstrapping the test set. Significant differences between the single and dual sensor configuration are indicated with (*).

4.4. Discussion

Obtaining information about upper limb orthotic device wear time can improve treatment outcomes. This study proposed a new method, based on a trained decision tree classification algorithm, to estimate the wear time, using miniature temperature loggers attached to the arm and chest, and evaluated its performance. Data were captured during periods of frequent donning and doffing of the sensors, and while wearing the sensors on top of the clothing, mounted on the arm and chest. The study showed that the trained algorithm can correctly classify unseen temperature data with a mean classification error of between 1.1% and 3.1% for the arm, and between 1.8% and 4.0% for the chest. This results in mean wear time errors

of between 0.5% and 8.3% for the arm, and between 0.13% and 13.0% for the chest. The wide availability and low cost (approximately 30 USD) of the selected miniature temperature logger makes it an affordable solution for healthcare professionals to gain insight into the wear time of any prescribed (commercial) upper limb orthosis.

This study investigated whether the wear time can be better predicted when 2 sensors (dual sensor configuration) are used, compared with one sensor (single sensor configuration). For the 15–60 min interval use case, the algorithm performed equally well for the single and dual sensor configuration. For the 8h continuous use case, the dual sensor configuration performed significantly better for the arm (1 and 5 min sampling times) and chest (1 min sampling time), and worse for the arm (15 min sampling time) compared with the single sensor configuration. In the other conditions, the algorithm performed equally well for the single and dual sensor configuration. The added value of using 2 sensors is thus dependent on the use case, sampling time and body location. In general, we can conclude that, in most conditions, there is no practical benefit of using 2 sensors, as this will only increase the volume and cost of the solution, while not resulting in a significantly better wear time estimation.

Compared with subjective alternatives, such as diaries or questionnaires where patients tend to overestimate their wear time by as much as 200% [14], the proposed method is a preferable choice. A direct comparison between the results of this study and other studies using objective methods based on temperature sensors is difficult, as the use cases differ to a great extent. However, some general remarks can be made, as follows.

Firstly, we have shown that we can accurately estimate wear times without the need for direct contact between the sensor and the skin. This enables a wide application of our method, as many upper limb orthoses, such as arm slings, are often worn on top of clothing instead of directly on the skin. The temperature sensor can therefore be easily applied to many types of (commercial) upper limb orthoses. In other studies, the sensor was embedded in the thermoplastic of an orthosis or insole of a shoe, limiting the potential use for different orthoses.

Secondly, we have shown that our algorithm is able to accurately estimate wear time, even during periods of frequent donning and doffing. Temperature sensors need time to warm up when donned or cool down when doffed. These periods of transition may be difficult to detect otherwise, but our algorithm was able to capture these effects, as indicated by the reported classification errors. In other studies, results during frequent donning and doffing are not available as their use case was different (prolonged, continuous use).

Thirdly, the performance of our algorithm was evaluated with unseen test data, leading to unbiased results that show the actual classification and wear time estimation errors. Other studies trained and evaluated their model on the same data-set, leading to overestimated algorithm accuracies.

Depending on the use case, the wear time prescription generally includes a range of several hours, e.g. 2 times a day for half an hour, to 20–23 h/day consecutively. As an example, a wear time error of 5% results in an absolute error of 12 min when the orthosis is worn for 4h

during a 24h period. The choice for an acceptable level of wear time estimation accuracy is up to the physician or therapist, but, in general, knowledge of wear time to within 90% accuracy is sufficient. For short sampling intervals, reported wear time estimation errors in this work are well within this requirement.

Our method allows monitoring of the patient's adherence for a prolonged period (up to a few months), without supervision, return to the clinic, or recharging of the device, depending on the chosen sampling time. This will further increase the chance of successful implementation in the current clinical practice. For longer sampling times, the amount of data that can be stored on the sensor increases, but the estimated wear time error and estimation error range (indicated by the 95% CIs) also increase. The therapist or physician using this technology should be aware of these implications for the margin of error when choosing a sampling time.

The timestamps logged by the smartphone app were used to label the measurement data ('*on*' or '*off*'). Participants were instructed to respond in a timely manner to the notification and immediately confirm their action ('*don*' or '*doff*') once done. Theoretically, there could have been a difference between the actual and reported timestamps, which could have negatively affected the classifier performance. However, only 1 participant reported a discrepancy between 1 donning action and subsequent confirmation in the app during 1 interval. Therefore, it was assumed that any discrepancy between the actual and reported timestamps was negligible.

The data for this study were collected in December and January in the Netherlands. As no data were recorded on warm days, the model was not specifically trained for conditions with a high ambient temperature. However, a large variation was still present in the recorded data-sets, to allow for a proper training of the classification model. During the measurements, the ambient temperature outside was in the range 5–10°C. Therefore, participants often wore a coat on top of their clothing when they went outside. Indoors, the ambient temperature was limited, and was approximately in the range 18–21°C. All participants wore long sleeves, but the thickness of their clothing varied, enabling us to train the model for a wide variety of clothing types. We believe that the data presented here represent a worst-case, as (thick) clothing in between the sensors and skin make it more difficult to correctly estimate the wear time. Future studies should address the effect of a higher number of parameters (high ambient temperature, sensors worn directly on skin) on the classifier performance and wear time estimation. By adding these data to the data-set, the classification and subsequent wear time estimation may be improved.

References

[1] Scherer M, Galvin J. Matching people with technology. Rehabil Manag 1994; 7: 128–130.

[2] Ehrmann D, Spengler M, Jahn M, Niebuhr D, Haak T, Kulzer B, et al. Adherence Over time: the course of adherence to customized diabetic insoles as objectively assessed by a temperature sensor. J Diabetes Sci Technol 2018; 12: 695–700.

[3] Helfenstein A, Lankes M, Ohlert K, Varoga D, Hahne HJ, Ulrich, HW, et al. The objective determination of compliance in treatment of adolescent idiopathic scoliosis with spinal orthoses. Spine 2006; 31: 339–344.

[4] Benish BM, Smith KJ, Schwartz MH. Validation of a miniature thermochron for monitoring thoracolumbosacral orthosis wear time. Spine 2012; 37: 309–315.

[5] Havey R, Gavin T, Patwardhan A, Pawelczak S, Ibrahim K, Andersson GB, et al. A reliable and accurate method for measuring orthosis wearing time. Spine 2002; 27: 211–214.

[6] Lou E, Hill D, Hedden D, Mahood J, Moreau M, Raso J. An objective measurement of brace usage for the treatment of adolescent idiopathic scoliosis. Med Eng Phys 2011; 33: 290–294.

[7] Hunter LN, Mitell SW, Mendoza MM, McDonald CM, Molitor F, Mulcahey MJ, et al. The validity of compliance monitors to assess wearing time of thoracic-lumbar-sacral orthoses in children with spinal cord injury. Spine 2008; 33: 1554–1561.

[8] Chadwell A, Kenney L, Granat M, Thies S, Head JS, Galpin A. Visualisation of upper limb activity using spirals: a new approach to the assessment of daily prosthesis usage. Prosthet Orthot Int 2018; 42: 37–44.

[9] Lutjeboer T, Van Netten JJ, Postema K, Hijmans JM. Validity and feasibility of a temperature sensor for measuring use and non-use of orthopaedic footwear. J Rehab Med 2018; 50: 920–926.

[10] Schwarze M, Horoba L, Block J, Putz C, Alimusaj M, Wolf SI, et al. Wearing time of ankle-foot orthoses with modular shank supply in cerebral palsy: a descriptive analysis in a clinically prospective approach. Rehabil Res Pract 2019; 2019.

[11] Takemitsu M, Bowen JR, Rahman T, Glutting JJ, Scott CB. Compliance monitoring of brace treatment for patients with idiopathic scoliosis. Spine 2004; 29: 2070–2074.

[12] Efron B. Bootstrap methods: another look at the jackknife. Ann Statistics 1979; 7: 1–26.

[13] Cumming G, Finch S. Inference by eye: confidence intervals and how to read pictures of data. Am Psychol 2005; 60: 170-180.

[14] Nicholson GP, Ferguson-Pell MW, Smith K, Edgar M, Morley T. The objective measurement of spinal orthosis use for the treatment of adolescent idiopathic scoliosis. Spine 2003; 28: 2243–2250.

5. Evaluating the clinical effects of a dynamic shoulder orthosis

Abstract—Shoulder orthoses reduce the gravitational pull on the shoulder by providing an upward force to the arm, which can decrease shoulder pain caused by stress on the glenohumeral structures. In this interventional study, the clinical effects of a recently developed dynamic shoulder orthosis were assessed in 10 patients with chronic shoulder pain. The shoulder orthosis provides an upward force to the arm with two elastic bands. These bands are arranged to statically balance the arm, such that the supportive force is always directed towards the glenohumeral joint and shoulder movements are not impeded. The study population was provided with a dynamic shoulder orthosis for two weeks. In the week before the orthosis fitting, the participants had no intervention. The primary outcome measures were the mean shoulder pain scores before and during the intervention, and the distance between the humeral head and the acromion without and with orthosis. Ultrasound evaluation showed that the shoulder orthosis resulted in a reduction of the distance between the acromion and humeral head at different levels of arm support. Also, it was demonstrated that the mean shoulder pain scores (range 0-10) decreased from 3.6 to 3 (in rest), and from 5.3 to 4.2 (during activities) after two weeks of orthosis use. In general, patients were satisfied with the weight, safety, ease in adjusting and effectiveness of the orthosis. The results of this study show that the orthosis has the potential to reduce shoulder complaints in patients with chronic shoulder pain.

Haarman, C. J. W., Hekman, E. E. G., van der Kooij, H., & Rietman, J. S. Evaluating the clinical effects of a dynamic shoulder orthosis. (*under review*)

5.1. Introduction

The shoulder joint permits a large range of motion (ROM), at the expense of its stability. Decreased muscle tone or a lesion of the rotator cuff muscles may cause glenohumeral subluxation (GHS) which is defined as a, inferior, partial dislocation of the humeral head from the glenoid [1]. Reported incidences of GHS vary from 17 up to 67% in CVA [2]. Other causes of GHS include shoulder trauma and operative procedures [3], neuromuscular disorders such as cerebral palsy and brachial plexus injury [4], and brachial neuritis (also called neuralgic amyotrophy) [5].

The passive stabilizing structures such as the capsule and ligaments become more dominant as a result of the reduced tone in one or more shoulder muscles. A continuous, passive stretch of these structures due to the weight of the arm can provoke pain, even if no GHS is present [6].

Patients suffering from chronic shoulder pain are frequently prescribed a shoulder orthosis (also called brace or support) to reduce the gravitational pull on the shoulder by providing an upward force to the arm [7]. Studies assessing the effects of shoulder orthoses on shoulder pain only show low to modest improvements in pain measures [8-10]. Also, many available shoulder orthoses have a disadvantage in that they limit the remaining range of motion of the arm to stabilize the glenohumeral joint [11].

In previous research a dynamic shoulder orthosis was developed to reduce the stress on the passive structures surrounding the glenohumeral joint by applying an upward force to the arm with two elastic bands that are attached between an upper arm cuff and a shoulder bracket [12]. The unique feature of this device is that the elastic bands are arranged to statically balance the arm, such that the supportive force is always directed towards the center of rotation of the glenohumeral joint. Therefore, this force will not the impede the remaining range of motion of the arm, as no additional moment around the shoulder joint in the sagittal plane is introduced. A prototype was designed and tested with two patients to subjectively assess the immediate effects of the orthosis on shoulder pain, glenohumeral stability and the range of motion. This pilot clinical evaluation showed promising results.

In this study, we redesigned the dynamic shoulder orthosis to increase the robustness, usability and level of comfort of the device without altering the working principle of the orthosis. Also, the weight was reduced from 605g to 247g. The prototype that was used in this study can be seen in Fig. 5.1. The shoulder orthosis includes elastic bands suspended at the anterior and posterior side of the shoulder that provide an external, upward force to the arm. The magnitude of the supportive force can be altered by tensioning the elastic bands. Proximally, these bands are connected to a rigid wireframe construction supported on the shoulder. Straps around the waist and the chest hold this construction in place. Two main differences between the previous and current version of the orthosis are: (1) A thin, metal wire-frame was used at the lateral side of the body, instead of a large aluminum construction. (2) The silicone arm cuff of the previous prototype relied on friction which is associated with warmth and perspiration and contributes to discomfort [13]. In the current prototype we

Fig. 5.1 – A) Prototype of the dynamic shoulder orthosis. 1) elastic bands. 2) rigid construction. 3) forearm cuff. 4) tensioning mechanism. 5) strap around contralateral side of the chest. B) Close-up of the arm cuff and tensioning mechanism with flexed elbow. 6) Forearm cuff with soft Velcro straps. 6) Ring aligned with elbow joint center of rotation. 8) Upper arm part to guide the force from the elastic bands (1) to the forearm cuff.

therefore used an arm cuff made of fabric that locks itself around the forearm due to its conical shape.

The aim of this interventional study was to assess the clinical benefit of the dynamic shoulder orthosis in a population of patients with chronic shoulder pain that is probably caused by stress on the glenohumeral structures. The study population was provided with a dynamic shoulder orthosis for the duration of two weeks. In the week before the orthosis fitting, the participants had no intervention. The primary outcome measures were the mean shoulder pain scores before and during the intervention, and the distance between the humeral head and the acromion without and with orthosis. The secondary outcome measures included the pain-free active range of motion, shoulder function and arm activity before and during the intervention, the orthosis wear time, and user satisfaction with the orthosis.

5.2. Methods and materials

5.2.1. Participants

Patients with chronic shoulder pain that was probably caused by stress on the glenohuermal structures were recruited from the Roessingh, Center for Rehabiliation (Enschede, the Netherlands) and Radboud University Medical Center (Nijmegen, the Netherlands). Exclusion criteria were defined as an inability to sit upright in a chair without supporting the arm for at least 15 minutes consecutively, an irritated skin in the application area of the orthosis, recent shoulder or arm surgery (<6 months before participation in the study) or inability to understand and follow simple verbal instructions.

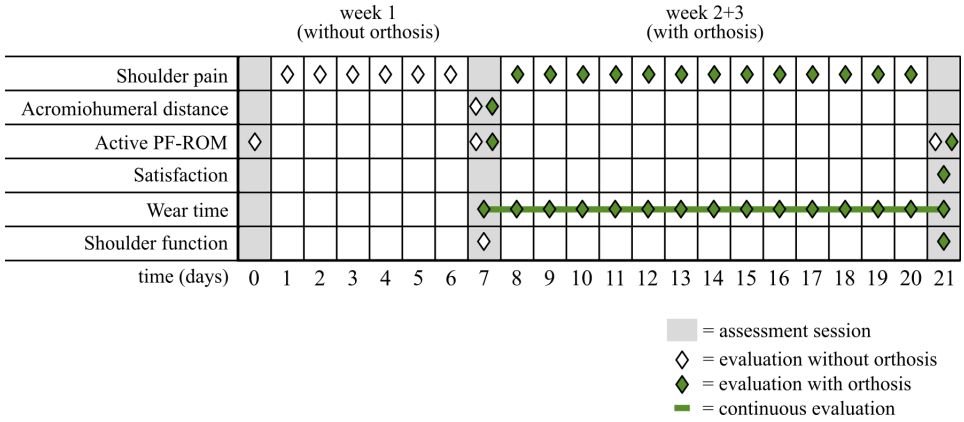

Fig. 5.2 – Schedule depicting the tests that are conducted throughout the a period of three weeks. Each row represents a different test. On day 0, 7 and 21 the assessments were conducted.

Ethical approval for the study was granted by the Committee on Research involving Human Subjects, region Arnhem-Nijmegen (number NL74819.091.20). Written informed consent was obtained from all subjects before the start of the study.

The patients' age, weight, height, dominant arm and affected shoulder, diagnosis, and time since the onset of their shoulder complaints were recorded prior to the start of the study.

5.2.2. Study outline

The study consisted of three assessment and two monitoring sessions per participant, see Fig. 5.2 for a detailed overview of the study outline. The participants carried out their normal daily routine at home for a period of three weeks (one week without orthosis, and two weeks with orthosis). The first week provided a baseline to which the second and third week (with orthosis) were compared.

During the initial assessment (day 0), the pain-free range of motion (PF-ROM) during shoulder anteflexion and abduction movements were measured, and general patient characteristics were noted. Also, the initial orthosis fitting was performed to obtain body measures that are required for the customization of the orthosis.

During the intermediate assessment (day 7), several questionnaires were conducted regarding arm activity and shoulder pain, and the PF-ROM was measured. Additionally, the acromiohumeral distance (AHD), i.e. the distance between the acromion and humerus, was measured. Both the PF-ROM and AHD measurements were carried out without and with orthosis, and at three levels of supportive force (40%, 80% and 120% of the arm weight) to assess the immediate effects of the orthosis. At the beginning of this session, final adjustments were made to the shoulder orthosis.

During the final assessment session (day 21) the same tests were performed as on day 7. Additionally, a questionnaire regarding user satisfaction (D-QUEST) and a short interview

were conducted, the latter containing custom questions about the type of activities the participants performed with the orthosis.

5.2.3. Shoulder pain

The shoulder pain was measured with a 10-cm visual analogue scale (VAS) [14-15]. All subjects reported their daily average shoulder pain over the last 24 hours in rest and during activities for a period of three weeks (1 week before and 2 weeks during the intervention). Subjects were asked to mark their response on the scale, where the ends of the scale represent extreme limits of the pain, orientated from left (no pain at all) to right (worst pain imaginable).

5.2.4. Acromiohumeral distance

The AHD was assessed with diagnostic ultrasound without and with the shoulder orthosis to measure the immediate effect of the orthosis on the AHD. The change in AHD caused by shoulder supports are most often assessed using radiography [16]. However, exposure to radiation and high costs limit the clinical application of this technique [17]. Diagnostic ultrasound does not involve exposure to radiation and was therefore adopted in this research. The AHD was defined as the shortest distance from humeral head to the tip of the acromion [18], see Fig. 5.3.

The ultrasound examination was performed with a ACUSON s1000 system (Siemens, Germany) and 5-14 MHz (14L5) linear array transducer. A custom preset was defined to optimize image quality. The transducer was placed over the lateral border of the acromion. This placement does not interfere with the position of the orthosis on the body.

First, the AHD of the (unsupported) affected and unaffected shoulder were measured to be able to compare both shoulders. Then, the orthosis was fitted to the patient and the AHD of the affected shoulder was measured again, this time with the orthosis. To investigate the influence of the magnitude of the supportive force on the AHD, three supportive force conditions were defined. The tension of the elastic bands was set to support 40%, 80% and

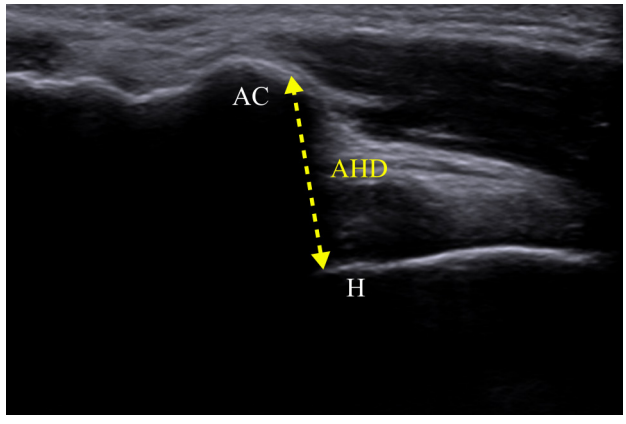

Fig. 5.3 – Example of acromiohumeral distance measurement with the arm in a neutral position. Indicated are the acromion (AC), humerus (H) and acromiohumeral distance (AHD).

120% of the arm weight. The arm weight was estimated from the total body weight, according to the values presented by de Leva [19].

Subjects were examined while seated upright in a chair (hips and knees in 90° flexion). They were instructed to keep their arm in a neutral position (without internal or external rotation), and elbow in 0° flexion, while keeping their trunk still. No additional loading was placed on the shoulder other than the own weight of the arm. Each condition was repeated three times.

The ultrasound device was operated by a researcher who received training from an expert with over 20 years of experience in ultrasound examination. After the training session on healthy volunteers, the researcher was familiar with the device and the measurement protocol. The operator was also the rater of the ultrasound images. The rater was blinded to the supporting condition (unsupported, or 40%, 80% and 120% of arm weight supported). The captured ultrasound images were then transferred to a computer for further analysis. The AHD was measured from the ultrasound images with Matlab 2019a (Mathworks, USA) using a custom script. The recorded ultrasound images were presented in a random order to the rater. Each image was presented three times to the rater, from which the mean AHD could be measured. Additionally, two-sample t- tests were performed to investigate whether the mean AHD significantly changed between conditions ($p < 0.05$).

5.2.5. Active PF-ROM

A decreased shoulder range of motion can adversely affect a person's ability to perform tasks and independent functioning in daily life. Many shoulder supports hold the arm internally rotated and adducted at the shoulder, encouraging disuse which in turn may lead to muscle shortening and/or changes in muscle tone [20]. Our device permits a large range of motion. Application of the shoulder orthosis should at least preserve, and preferably increase, the remaining shoulder ROM. Techniques for measuring the end points of the shoulder ROM measurement include the maximum active shoulder ROM, the ROM until passive resistance is first felt, or the ROM until the point of pain [21]. As pain is often a movement-limiting factor for patients with shoulder pain, in this study we adopted the definition of the active ROM until the point of pain, or pain-free ROM (PF-ROM), for the examination of the shoulder range of motion [21-22].

The PF-ROM measurements were performed without the orthosis and with the elastic bands tensioned to 40%, 80% and 120% of the total arm weight, for both anteflexion and abduction movements. The PF-ROM measurement without orthosis was conducted at the beginning of the session. In case the participants indicated fatigue of their shoulder muscles after measurements with orthosis, the measurement without orthosis was repeated at the end of the session and both results were inspected for large differences. The measurements at 40%, 80% and 120% arm weight support were conducted in randomized order.

Subjects were seated on a chair with back rest in upright position, with their hip and knees in 90° flexion. They were instructed to fully extend their elbow and keep their wrist in a neutral position. The thumb was leading in the sagittal plane. The goniometer app Clinometer (Plaincode, Munich, Germany) was used to measure the active PF-ROM. This smartphone app is validated for shoulder anteflexion and abduction movements [23]. For anteflexion

movements, the smartphone screen was aligned with the longitudinal axis of the humerus, perpendicular to the sagittal plane. Subjects were instructed to move their arm in the sagittal plane while keeping their trunk still until they reached the threshold of pain or the end of their active ROM. At this point, the inclination angle of the goniometer app was read from the smartphone. The same procedure was repeated for abduction movements, only the movement now occurred in the frontal plane, and the smartphone screen was oriented perpendicular to the frontal plane. Both anteflexion and abduction angle measurements were repeated three times for each condition and the mean PF-ROM was calculated. With these data two-sample t-tests were performed to investigate whether the mean PF-ROM for anteflexion and abduction movements significantly changed between conditions ($p < 0.05$).

5.2.6. User satisfaction with device

The Quebec User Evaluation of Satisfaction with assistive Technology 2.0 (QUEST2.0) [24] is the only validated questionnaire available in Dutch to evaluate the satisfaction regarding assistive devices [25]. This questionnaire was conducted at the end of the intervention to assess the user's satisfaction with the provided shoulder orthosis. All eight items of this questionnaire that were related to the assistive device were rated by the subject on a scale from 1 (not satisfied at all) to 5 (very satisfied). Additionally, all subjects were asked about how they used the orthosis, and about the type of activities they performed the most while wearing the orthosis.

5.2.7. Orthosis wear time

To gain insight in the usage of orthotics and prosthetics in daily life, often questionnaires or logbooks are used to measure the time that the devices are worn by patients [26]. These results might be biased since they rely solely on the accuracy of reporting [27]. Therefore, we recently proposed a new method to objectively estimate orthosis wear times using miniature temperature loggers and a trained classification algorithm [28]. A temperature logger was attached to the chest strap of the shoulder orthosis and the temperature was automatically logged every 5 minutes during the two weeks of unsupervised orthosis use. After this period, the sensor was retrieved from the orthosis and the temperature data were transferred to the computer for further processing with the algorithm. The algorithm provides an estimated device state ('*on*' or '*off*') for every temperature sample. The number of 'on' states were multiplied with the sample time (5 minutes) to obtain the estimated wear time. From the data the total wear time, and mean wear time per day were calculated.

5.2.8. Shoulder function

Objective assessment of shoulder function is possible in a clinical setting. However, a patient's capacity to perform specific clinical tests (e.g. maximum active ROM) may not reflect their motor performance in daily life [29]. Instead, we proposed to assess the patient's perceived performance of their affected shoulder in daily life with an without the shoulder orthosis using the Motor Activity Log (MAL) [30-31] and the Simple Shoulder Test (SST) [32]. For the MAL, the participants were asked to rate the Quality of Movement (QOM) and Amount of Use (AOU) of their affected arm during several functional daily tasks. All 26 items were rated on an ordinal scale from 0 (*affected arm was never used*) to 5 (*ability to use the affected arm was as good as before the shoulder complaints*) on the QOM subscale, and

ID	Gender	Age (y)	Weight (kg)	Diagnosis	Length (m)	Dominant arm	Affected shoulder	Time since complaints (y)
S1	F	23	68	Plexus trauma	1.69	Left	Right	8
S2	F	50	98	NA	1.70	Right	Right	6
S3	F	52	75	NA	1.70	Right	Right	23
S4	F	46	64	NA	1.63	Right	Left	8
S5	F	55	58	NA	1.71	Right	Left	23
S6	F	59	110	NA	1.76	Right	Right	6
S7	F	35	75	NA	1.77	Right	Left	5
S8	M	60	84	CVA	1.86	Right	Left	<1
S9	F	43	90	Iatrogenic nerve injury	1.78	Right	Left	6
S10	F	19	70	Erb's palsy	1.71	Right	Left	19

Table 5.1 – Subject characteristics. ID: subject ID; F: female; M: male; NA: Neuralgic amyotrophy; CVA: cerebrovascular accident.

from 0 (*affected arm was never used*) to 5 (*affected arm was always used during the activity*) on the AOU subscale. The SST consists of 12 items to assess the functional limitations of the affected shoulder. Each item was scored as either 0 (*no*) or 1 (*yes*). The summed scores were divided by 12 and multiplied by 100 to obtain the total score (range 0-100 points). A higher score represents less functional limitations of the affected shoulder.

By conducting the MAL, SST twice (after the first week, and after three weeks), we were able to investigate the influence of the shoulder orthosis on the perceived shoulder performance. The mean AOU and QOM subscale scores of the MAL, and the total score of the SST were reported for all participants without and with the orthosis.

5.3. Results

Ten participants (1 male, 9 female) with a median age of 48 years (range 19 - 60) were recruited from Roessingh, Centre for Rehabiltiation and Radboud University Medical Center. A short summary of their characteristics is provided in Table 5.1.

5.3.1. Shoulder pain

The mean VAS scores in rest (Fig. 5.4, top), and during activities (Fig. 5.4, bottom) were calculated from the daily VAS scores without orthosis (the week before the intervention) and the daily VAS scores with orthosis (during the two-week intervention period) for each subject. Days without reported VAS scores (due to incomplete subject logs), or without active use of the shoulder orthosis were not taken into account during the calculation. The mean shoulder pain in rest, represented by the VAS score, across all subjects was 3.6 (range 0.3 to 7.5) without orthosis, and 3.0 (range 0.1 to 7.7) with orthosis. The mean shoulder pain during activities across all subjects was 5.3 (range 2.5 to 8.4) without orthosis, and 4.3 (range 1.8 to 8.0) with orthosis. To see whether the use of the shoulder orthosis led to a decrease in

shoulder pain, the difference (ΔVAS) between the mean VAS scores without and with shoulder orthosis was also determined in rest (Fig. 5.4, top right) and during activities (Fig. 5.4, bottom right). For 8 out of 10 subjects, the mean shoulder pain in rest decreased when the subjects wore the shoulder orthosis, while for 9 out of 10 subjects, the mean shoulder pain during activities decreased. The mean difference in VAS score across all subjects was -1.0 in rest and -0.6 during activities.

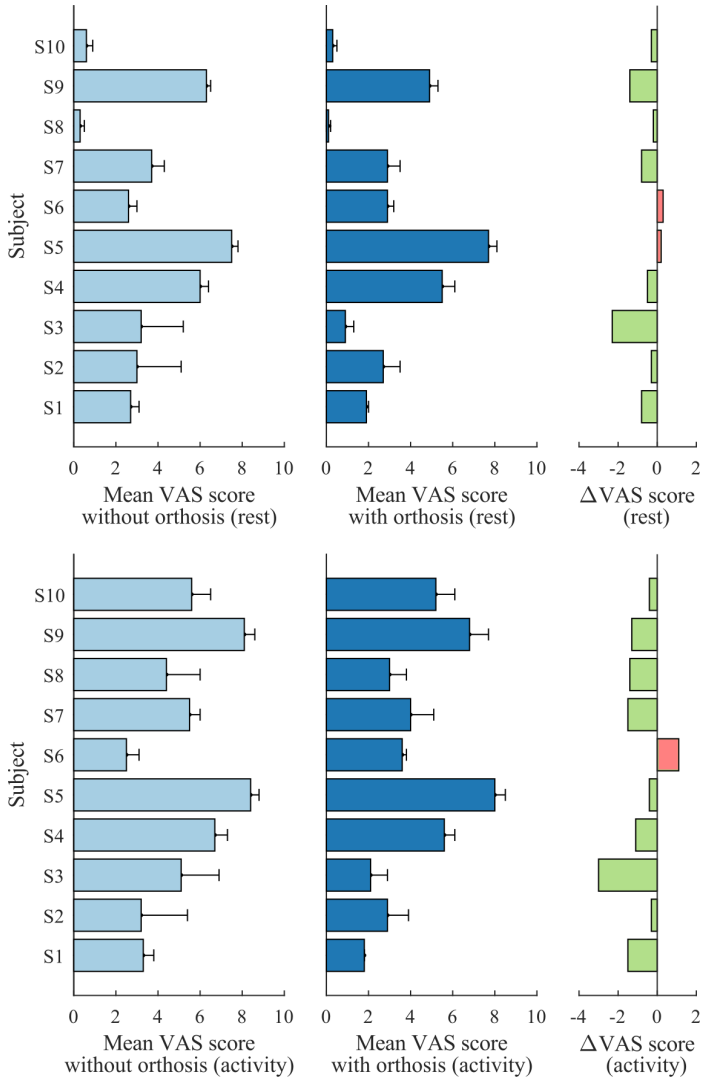

Fig. 5.4 – The VAS scores in rest (top) and during activities (bottom). Left: mean VAS without shoulder orthosis; Middle: mean VAS after wearing the shoulder orthosis. Right: differences in VAS scores without and with orthosis. A decrease in VAS score (negative Δ) corresponds to reduced shoulder pain. Error bars represent the standard deviation of the mean.

5.3.2. Acromiohumeral distance

The mean AHD was determined for the following conditions: non-affected (N), unsupported affected (UA), and affected shoulder with 40% (A40), 80% (A80) or 120% (A120) of the arm weight supported. The results are shown in Table 5.2. For two subjects (S1, S2) no recordings were available from the non-affected side and the 120% support condition as these conditions were added to the measurement protocol after the first two participants. For subject S5, the data were not correctly stored for the non-affected shoulder. The mean AHD of the non-affected shoulder across all subjects was 13.0 mm (range 10.2 to 15.5 mm). The mean AHD of the affected, unsupported shoulder across all subjects was 11.9 mm (range 9.7 to 14.5 mm). The difference in mean AHD between the non-affected and affected unsupported shoulder was not statistically significant ($p = 0.11$).

The differences in mean AHD between the affected, unsupported condition and the conditions at 40% ($p = 0.003$) respectively 80% ($p = 0.011$) and 120% ($p = 0.015$) arm weight support were all statistically significant. For the three supported conditions, the mean AHD was smaller than for the unsupported condition.

The results show that the shoulder orthosis was able to significantly reduce the AHD between the affected unsupported and supported force conditions (Δ(UA-A40), Δ(UA-A80), Δ(UA-A120)), even though for none of the patients a glenohumeral subluxation could be established. A comparison between the different supported force conditions revealed no statistically significant differences.

ID	N (mm)		UA (mm)		A40 (mm)		A80 (mm)		A120 (mm)		Δ(N-UA) (mm)	Δ(UA-A40) (mm)	Δ(UA-A80) (mm)	Δ(UA-A120) (mm)
	mean	std	mean	std	mean	std	mean	std	mean	std				
S1	-	-	9.7	0.3	8.5	0.2	9.2	0.3	-	-	-	1.2	0.5	-
S2	-	-	11.3	1.1	11.6	0.7	10.5	1.0	-	-	-	-0.3	0.8	-
S3	13.0	0.6	13.5	0.3	11.5	0.6	12.0	0.8	11.4	0.3	-0.5	2.0	1.5	2.1
S4	10.2	0.2	10.0	0.4	9.8	0.3	9.6	0.4	9.9	0.5	0.2	0.2	0.4	0.1
S5	-	-	13.7	0.2	11.5	0.2	11.3	0.2	11.4	0.7	-	2.2	2.4	2.3
S6	12.2	0.4	12.0	0.4	10.6	0.3	12.0	0.3	12.1	0.3	0.2	1.4	0.0	-0.1
S7	15.0	0.8	14.5	1.0	11.4	0.8	10.7	0.5	9.9	1.3	0.5	3.1	3.8	3.0
S8	13.4	0.8	12.8	0.9	9.4	0.6	9.5	0.4	9.0	0.5	0.6	3.4	3.3	3.8
S9	15.5	0.4	12.2	0.6	10.1	1.3	9.4	1.3	9.6	1.0	3.3	1.4	2.8	2.3
S10	11.9	0.3	9.2	0.3	8.9	0.3	9.7	0.5	8.9	0.4	2.7	0.3	-0.5	0.3

Table 5.2 – Acromiohumeral distance measured with ultrasound for different conditions. ID: subject ID, N: non-affected shoulder; UA: unsupported affected shoulder; A40: affected shoulder with 40% arm weight support; A80: affected shoulder with 80% arm weight support; A120: affected shoulder with 120% arm weight support and 120%. std: standard deviation.

	Initial		Intermediate								Final							
ID	UA (°)		UA (°)		A40 (°)		A80 (°)		A120 (°)		UA (°)		A40 (°)		A80 (°)		A120 (°)	
	mean	std	mean	std	mean	std	mean	std	mean	std	mean	std	mean	std	mean	std	mean	std
S1	76	2.0	71	3.2	76	6.9	82	3.9	-	-	-	-	-	-	-	-	-	-
S2	70	4.6	70	3.7	82	2.6	83	3.9	-	-	86	2.6	87	2.0	87	1.2	-	-
S3	69	15.7	50	4.0	37	2.4	53	0.7	42	8.3	57	8.9	49	11.4	61	4.7	47	10.8
S4	82	4.1	68	2.4	72	4.8	70	2.4	65	1.8	66	1.0	72	1.6	67	2.4	63	3.1
S5	74	2.3	59	0.7	67	3.6	77	4.4	74	2.1	75	0.6	69	0.6	68	0.5	56	1.0
S6	98	8.2	81	4.0	76	4.4	77	2.6	66	3.5	-	-	56	4.9	69	1.7	53	1.4
S7	84	1.6	80	3.9	74	2.8	67	3.4	70	3.0	72	3.9	75	3.0	69	3.2	69	1.9
S8	-	-	-	-	-	-	-	-	-	-	-	-	-	-	-	-	-	-
S9	12	1.1	11	1.4	13	0.6	14	1.8	9	1.3	25	1.8	24	1.7	16	2.7	12	1.2
S10	79	4.7	83	6.8	67	2.9	75	1.8	65	1.1	69	1.6	69	0.5	76	2.1	72	2.5

Table 5.3 – Anteflexion PF-ROM of the unsupported shoulder, and with 40%, 80% and 120% of the arm weight supported by the shoulder orthosis, measured during the initial, intermediate and final assessment.. Initial: initial assessment; Intermediate: intermediate assessment; Final: final assessment; ID: subject ID; UA: unsupported affected shoulder; A40: affected shoulder with 40% arm weight support; A80: affected shoulder with 80% arm weight support; A120: affected shoulder with 120% arm weight support and 120%. std: standard deviation.

	Initial		Intermediate								Final							
ID	UA (°)		UA (°)		A40 (°)		A80 (°)		A120 (°)		UA (°)		A40 (°)		A80 (°)		A120 (°)	
	mean	std	mean	std	mean	std	mean	std	mean	std	mean	std	mean	std	mean	std	mean	std
S1	68	7.0	76	4.1	77	0.8	84	1.4	-	-	-	-	-	-	-	-	-	-
S2	75	2.1	75	4.1	75	0.8	79	1.6	-	-	85	1.2	89	1.2	85	0.6	-	-
S3	30	9.6	32	5.8	24	3.6	44	7.3	40	7.8	33	8.3	31	6.5	37	6.5	36	3.5
S4	73	4.6	62	2.2	60	2.1	59	1.9	60	2.6	59	2.5	57	0.8	56	1.1	59	1.8
S5	66	0.6	55	5.2	51	1.3	64	1.8	66	2.0	68	3.5	66	1.7	62	3.2	55	2.0
S6	66	2.6	56	3.4	51	2.6	62	1.2	51	3.1	-	-	46	6.3	51	0.7	49	1.8
S7	67	3.5	55	1.7	47	1.3	49	2.9	53	0.6	44	10.4	43	3.8	47	1.2	46	1.5
S8	-	-	-	-	-	-	-	-	-	-	-	-	-	-	-	-	-	-
S9	16	0.4	14	1.5	20	0.8	21	1.1	25	1.4	12	1.2	15	1.5	13	0.0	17	0.6
S10	64	2.6	46	2.8	62	1.2	61	4.0	55	2.6	59	5.8	58	1.3	63	3.6	62	0.7

Table 5.4 – Abduction PF-ROM of the unsupported shoulder, and with 40%, 80% and 120% of the arm weight supported by the shoulder orthosis, measured during the initial, intermediate and final assessment. Initial: initial assessment; Intermediate: intermediate assessment; Final: final assessment; ID: subject ID; UA: unsupported affected shoulder; A40: affected shoulder with 40% arm weight support; A80: affected shoulder with 80% arm weight support; A120: affected shoulder with 120% arm weight support and 120%. std: standard deviation.

5.3.3. Active PF-ROM

For the active PF-ROM we assessed the pain-free shoulder anteflexion and abduction ROM of the affected unsupported shoulder, and with 40%, 80% and 120% of the arm weight supported during the initial, intermediate and final assessment, see also Tables 5.3 and 5.4. For two participants (S1, S2) no measurements were available for the 120% arm weight

condition as this condition was added to the protocol after the first two participants were measured. For S1, the final assessment was not completed as the subject was unable to travel to the measurement location. For S8 no PF-ROM measurements were carried out as he was not able to actively lift his arm against gravity.

The results suggest that the shoulder orthosis had no instantaneous effect on the active PF-ROM for both anteflexion and abduction movements, as no significant differences were found between the mean PF-ROM of the unsupported and supported affected shoulder at 40%, 80 % and 120 % arm weight support.

The results also suggest that using the orthosis for two weeks had no effect on the active PF-ROM, as no statistically significant differences were found between the intermediate and final assessment.

5.3.4. User satisfaction

Overall, the 10 subjects reported a high level of satisfaction with the assistive device (mean 4.1, range 3.3-4.9). See also Fig. 5.5 for the D-QUEST subscores per subject. Subjects were most satisfied with the weight (247g) of the device (4.5), the safety (4.3), the ease in adjusting (4.2) and the effectiveness (4.2). Of all aspects, comfort was rated lowest (3.4). The

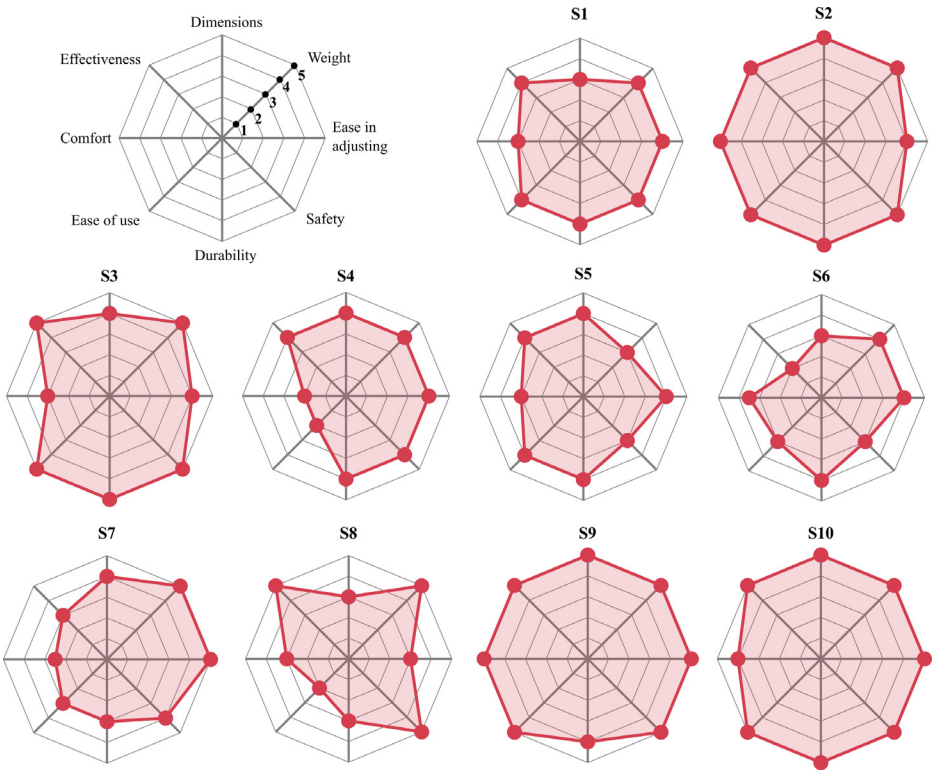

Fig. 5.5 – Results of the D-QUEST questionnaire, showing the satisfaction with the shoulder orthosis for the aspects 'dimensions', 'weight', 'ease in adjusting', safety', 'durability', 'ease of use', 'comfort' and 'effectiveness' per subject. The further away from the center, the higher the score (1-5).

downward force pressing on the shoulder arc, required to lift the arm, was mentioned by several subjects as a factor that decreased the comfort of the orthosis.

Subjects reported that they used the orthosis both at home and outdoor. Most subjects wore the orthosis over their clothing. A wide range of activities that were performed with the orthosis. Among frequently reported activities are walking (6x), cooking (4x) and gardening (3x). Two participants (S4 and S10) reported that they used the orthosis during their work. Apart from these participants, only S1 was employed. For the majority of the participants, the level of comfortable arm weight compensation ranged between 40% and 80%, depending on the type of activity that was performed.

5.3.5. Orthosis wear time

For 9 subjects, the temperature data were processed with the estimation algorithm. For one subject (S10) the self-reported wear times were used during the analysis as the temperature data could not be retrieved from the data logger. The orthosis wear time was highly variable between subjects. In total, the measurement period consisted of 15 days (including the day of the intermediate and final assessment). See Fig. 5.6 for an overview of the days that the subjects used the shoulder orthosis, including the total and average wear time per day. On average, subjects used the orthosis 9.5 days (range 3-14 days) for 155 minutes per day (range 63-397 min./day). In general, subjects who were more satisfied with the orthosis, used the orthosis more. S1 used the orthosis the least (270 min. across 3 days) due to a lack of comfort, and stopped wearing the orthosis after one week. S6 was not satisfied with the effectiveness, ease of use and the dimensions. This was also reflected as she used the brace only during 8 days, with an average wear time of 63 min./day. S7 reported a low effectiveness and comfort level. From the wear time results it can be seen that her orthosis usage dropped significantly after one week. S8 used the orthosis the most (4760 min. across 12 days). While this subject

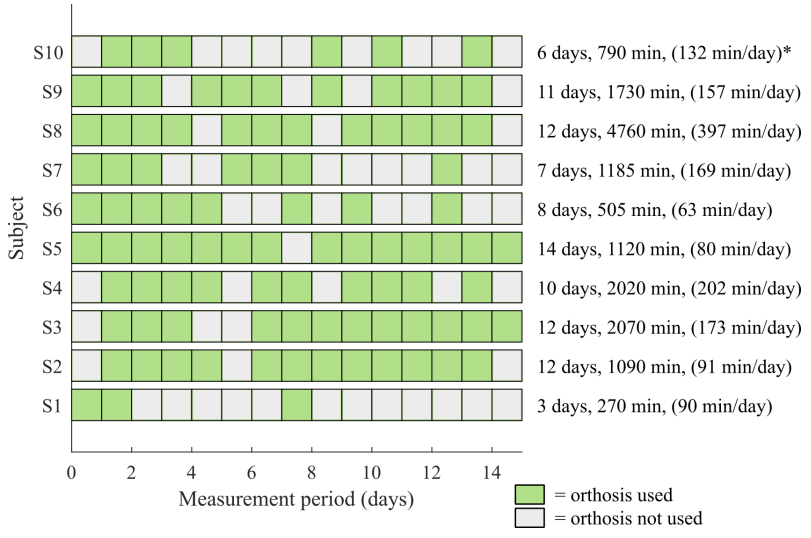

*Fig. 5.6 – Overview of the days when each subject used or did not use the orthosis during the measurement period, including the total estimated wear time from the miniature temperature loggers and the average wear time per day that the orthosis was used. * indicates self-reported wear times.*

indicated that he could not don the orthosis without help, he reported a high effectiveness score.

5.3.6. Shoulder function

The MAL and SST scores are presented in Table 5.5. The mean amount of use (AOM) and quality of movement (QOM) of the affected arm across all participants improved from 3.3 to 3.6 (AOM), and from 3.0 to 3.3 (QOM) for the situation without and with orthosis. These changes, although minor, suggests that wearing the shoulder orthosis can improve the perceived functional performance of the affected arm. For none of the subjects the SST scored decreased for the situation without and with orthosis. For five subjects, the SST score remained the same, while for the other five subjects the score improved. The mean improvement on the SST questionnaire across all participants was 7.5 points.

5.4. Discussion

In this study we evaluated the immediate effects of a dynamic shoulder orthosis in a group of 10 patients with chronic shoulder pain, and the effects after two weeks of medium-prolonged use. It was demonstrated that the mean shoulder pain scores decreased in from 3.6 to 3 (in rest), and from 5.3 to 4.2 (during activities) after two weeks of orthosis use. Also, ultrasound evaluation showed that the shoulder orthosis was able to reduce the distance between the acromion and humeral head at different levels of arm support. The pain-free range of motion of the affected shoulder was not compromised while wearing the shoulder orthosis. Additionally, the perceived shoulder function also improved slightly. In general, patients were satisfied with the weight (4.5 out of 5), safety (4.3 out of 5), ease in adjusting (4.2 out of 5) and effectiveness (4.2 out of 5) of the orthosis.

	AOU (0-5)		ΔAOU	QOM (0-5)		ΔQOM	SST (0-100)		ΔSST
	without	with		without	with		without	with	
S1	3.3	3.3	0.0	3.6	3.5	-0.1	67	67	0
S2	5.0	5.0	0.0	4.3	4.4	0.1	67	67	0
S3	1.8	2.0	0.2	2.2	2.2	0.0	17	33	17
S4	2.4	2.9	0.5	2.9	3.0	0.1	8	8	0
S5	2.5	2.3	-0.2			0.0	8	25	17
S6	4.8	4.1	-0.8	3.9	3.6	-0.3	30	30	0
S7	4.6	4.4	-0.2	3.3	3.7	0.4	42	42	0
S8	5.0	5.0	0.0	2.0	2.0	0.0	8	17	8
S9	2.3	4.7	2.3	2.0	4.7	2.7	0	8	8
S10	1.7	2.4	0.7	2.3	2.8	0.5	58	83	25

Table 5.5 – MAL subscale scores, and SST scores of each participant during a typical week without shoulder orthosis and after two weeks of orthosis use. Δ indicates the difference in test scores without and with orthosis. ID: subject ID; AOU: amount of use subscale score; QOM: quality of movement subscale score. SST: simple shoulder test scores.

In our study pain scores improved for 8 of 10 participants (80%) in rest, and for 9 of 10 participants (90%) during activities. Across three studies found in literature, 57% of the patients reported improved pain scores after wearing a shoulder orthosis for several weeks [8,9,16,33]. However, as none of these studies used the VAS as a measure of shoulder pain, a direct comparison of pain scores was not possible. The improvements were either described as better (10 of 40 patients) or definitely better (8 of 40 patients) by Hesse et al. [9], and in the study by Hartwig et al. sensory pain scores were provided as a subset of the shoulder hand syndrome score, ranging from 0 (no pain) to 5 (spontaneous pain). Here the mean pain scores improved from 1.8 ± 1.1 to 0.4 ± 0.6 (n=20) [8].

Limitations of this study included a lack of participants with objectively established glenohumeral subluxations, large individual differences in baseline shoulder pain and range of motion, limited sample size, and the relatively short duration and uncontrolled nature of the intervention period.

Nadler et al. reported pooled data about the reduction of vertical subluxation caused by three main orthosis design types [16]. However, these data are difficult to compare to our results due to a different methodology (radiography vs. ultrasound) and target population (stroke vs neuralgic amyotrophy, and degree of subluxation). We hypothesized that continuous stress on the glenohumeral joint contributes significantly to shoulder pain instead of GHS, and therefore did not include an (objectively) established GHS as inclusion criterion. It turned out that none of the participants in our study suffered from glenohumeral subluxation.

In this research we assumed that the non-affected shoulder was healthy as none of the patients indicated shoulder issues in their non-affected shoulder. In theory the non-affected shoulder could also have been 'slightly' affected which may have affected the analysis. However, the acromiohumeral distances were well in the range of healthy controls [34], making this an unlikely scenario. The subacromial distance of the affected, unsupported shoulder was not significantly different from the non-affected shoulder in our population. Therefore, the amount of decrease in AHD was also expected to be less than would have been the case if the shoulder was subluxated, as the possible reduction in subacromial distance is dependent on the level of subluxation. This could explain the fact that supporting the arm more (with 80% or even 120% of the arm weight) would not further decrease the acromiohumeral distance. Even so, we did see a slight reduction in subacromial distance due to application of the shoulder orthosis. This means that the upward force created by the elastic bands caused the arm to move slightly towards the glenoid.

Previous studies were only able to relate a change in shoulder pain to a change of the vertical displacement of the glenohumeral joint, due to the type of orthosis used [8-10]. These shoulder orthoses are position-controlled, not allowing researchers to precisely control the applied force during the investigation. Therefore, they were not able to easily discriminate between different levels of shoulder off-loading. Our dynamic shoulder orthosis is force-controlled, meaning that the amount of upward force provided by the device is always equal, irrespective of the arm position. To our knowledge the current study is the first to investigate the difference between stress reduction and physical repositioning of the humeral head on the subacromial distance.

Our study confirms that wearing the shoulder orthosis reduces the shoulder pain, in spite of the lack of participants with glenohumeral subluxation. This supports the claim that shoulder pain reduction may be more dependent on a stress reduction of the structures surrounding the shoulder joint than an actual translation of the humeral head towards the glenoid. To confirm this hypothesis, future research should include a more diverse patient population in terms of baseline characteristics (diagnosis, degree of subluxation, etc.).

Most participants reported an unpleasant feeling in the glenohumeral joint region when large arm weight compensation forces (>80%) were applied by the orthosis during the intermediate and final assessment. The discomfort could have been caused by impingement of the muscle between the acromion and humeral head as the arm was pushed towards the glenoid more.

The results of the SST questionnaire suggest that the shoulder orthosis is able to improve shoulder function for some subjects after two weeks of use. This was mainly attributed to an increased comfort level of the arm at rest for 4 out of 5 subjects with improved SST scores.

Rather than looking at statistically significant differences, clinical benefit of the shoulder orthosis is determined by comparing the study results to the minimally important differences (MIDs). MIDs represent the minimal change in outcome that are important to the patient [35]. Typical MIDs are 0.5-3.0 for the VAS [36-39], 0.5 for the MAL [31], and 17 for the SST [40]. The improvements in shoulder pain (VAS) were not only statistically significant, but the results were also in the range of the MID. For the MAL and SST, the MIDs were not achieved. This might be caused by the relatively short use period (two weeks). Therefore, we suggest to extend the orthosis use period to a few months in a future study.

The VAS is an instrument that is frequently used to assess pain intensity. In clinical practice the amount of pain relief, assessed by VAS, is often considered as a measure of the efficacy of treatment. In this study we saw that the arm activity correlated with the reported the VAS score. Periods of high arm activity were reflected in the daily VAS scores. As we did not want to intervene in the subjects' daily activities, this could have affected the results. However, as many people schedule their activities on a regular basis, we accounted for this effect, since the measurement periods included both working days and weekends. In a future study we will extend the period of orthosis use to further reduce these effects.

References

[1] Paci M, Nannetti L and Rinaldi LA. Glenohumeral subluxation in hemiplegia: An overview. The Journal of Rehabilitation Research and Development 2005; 42(4): 557.

[2] Zorowitz RD, Idank D, Ikai T et al. Shoulder subluxation after stroke: A comparison of four supports. Archives of Physical Medicine and Rehabilitation 1995; 76(8): 763–771.

[3] Pritchett JW. Inferior subluxation of the humeral head after trauma or surgery. Journal of Shoulder and Elbow Surgery 1997; 6(4): 356–359.

[4] Vitoonpong T and Chang K. Shoulder subluxation. StatPearls Publishing [Internet] 2022; URL https://www.ncbi.nlm.nih.gov/books/NBK507847/.

[5] Al Khalili Y, Jain S, Lam J et al. Brachial Neuritis. StatPearls Publishing [Internet] 2022; URL https://www.ncbi.nlm.nih.gov/books/NBK499842/.

[6] Turner-Stokes L and Jackson D. Shoulder pain after stroke: a review of the evidence base to inform the development of an integrated care pathway. Clinical rehabilitation 2002; 16(3): 276–298.

[7] Li K, Murai N and Chi S. Clinical reasoning in the use of slings for patients with shoulder subluxation after stroke: a glimpse of the practice phenomenon in california. OTJR: Occupation, Participation and Health 2013; 33(4): 228–235.

[8] Hartwig M, Gelbrich GG and Griewing B. Functional orthosis in shoulder joint subluxation after ischaemic brain stroke to avoid post-hemiplegic shoulder-hand syndrome: a randomized clinical trial. Clinical rehabilitation 2012; 26(9): 807–816.

[9] Hesse S, Herrmann C, Bardeleben A et al. A new orthosis for subluxed, flaccid shoulder after stroke facilitates gait symmetry: A preliminary study. Journal of Rehabilitation Medicine 2013; 45(7): 623–629.

[10] van Bladel A, Lambrecht G, Oostra KM et al. A randomized controlled trial on the immediate and long-term effects of arm slings on shoulder subluxation in stroke patients. European Journal of Physical and Rehabilitation Medicine 2017; 53(3): 400–409.

[11] Boldt E, Burg M, Jackson L et al. Comparison of the Proprioceptive and Motion Reduction Effects of Shoulder Braces in Individuals With and Without Anterior Shoulder Dislocations: A Pilot Study. Retrieved from Sophia, the St Catherine University repository website: https://sophiastkateedu/dpt papers/13 2012.

[12] Haarman CJW, Hekman EEG, Haalboom MFH et al. A New Shoulder Orthosis to Dynamically Support Glenohumeral Subluxation. IEEE Transactions on Biomedical Engineering 2021; 68(4): 1142–1153.

[13] Verloop WR, Haarman CJ, van Vliet RO et al. A newly designed shoulder orthosis for patients with glenohumeral subluxation: a clinical evaluation study. Prosthetics & Orthotics International 2021; 45(4): 322–327.

[14] McCormack HM, Horne DJ and Sheather S. Clinical applications of visual analogue scales: a critical review. Psychological medicine 1988; 18(4): 1007–1019.

[15] Hawker GA, Mian S, Kendzerska T et al. Measures of adult pain: Visual Analog Scale for Pain (VAS Pain), Numeric Rating Scale for Pain (NRS Pain), McGill Pain Questionnaire (MPQ), Short-Form McGill Pain Questionnaire (SF-MPQ), Chronic Pain

Grade Scale (CPGS), Short Form-36 Bodily Pain Scale (SF. Arthritis Care & Research 2011; 63(S11): S240–S252.
[16] Nadler M and Pauls MMH. Shoulder orthoses for the prevention and reduction of hemiplegic shoulder pain and subluxation: Systematic review. Clinical Rehabilitation 2016; 31(4): 444–453.
[17] Park GY, Kim JM, Sohn SI et al. Ultrasonographic measurement of shoulder subluxation in patients with post-stroke hemiplegia. Journal of Rehabilitation Medicine 2007; 39(7): 526–530.
[18] Azzoni R, Cabitza P and Parrini M. Sonographic evaluation of subacromial space. Ultrasonics 2004; 42(1-9): 683–687.
[19] de Leva P. Adjustments to Zatsiorsky-Seluyanov's segment inertia parameters. Journal of Biomechanics 1996; 29(9): 1223–1230.
[20] Hanger HC, Whitewood P, Brown G et al. A randomized controlled trial of strapping to prevent post-stroke shoulder pain. Clinical Rehabilitation 2000; 14(4): 370–380.
[21] Andrews AW and Bohannon RW. Decreased shoulder range of motion on paretic side after stroke. Physical Therapy 1989; 69(9): 768–772.
[22] Shakeri H, Keshavarz R, Arab AM et al. Clinical effectiveness of kinesiological taping on pain and pain-free shoulder range of motion in patients with shoulder impingement syndrome: a randomized, double blinded, placebo-controlled trial. International journal of sports physical therapy 2013; 8(6): 800–10.
[23] Shin SH, Ro DH, Lee OS et al. Within-day reliability of shoulder range of motion measurement with a smartphone. Manual Therapy 2012; 17(4): 298–304.
[24] Demers L, Monette M, Lapierre Y et al. Reliability, validity, and applicability of the Quebec User Evaluation of Satisfaction with assistive Technology (QUEST 2.0) for adults with multiple sclerosis. Disability and rehabilitation 2002; 24(1-3): 21–30.
[25] Wessels RD and De Witte LP. Reliability and validity of the Dutch version of QUEST 2.0 with users of various types of assistive devices. Disability and rehabilitation 2003; 25(6): 267–272.
[26] Lou E, Hill D, Hedden D et al. An objective measurement of brace usage for the treatment of adolescent idiopathic scoliosis. Medical Engineering and Physics 2011; 33(3): 290–294.
[27] Chadwell A, Kenney L, Granat M et al. Visualisation of upper limb activity using spirals: A new approach to the assessment of daily prosthesis usage. Prosthetics and Orthotics International 2018; 42(1): 37–44.
[28] Haarman CJW, Hekman EEG, Rietman JS et al. Accurate Estimation of Upper Limb Orthosis Wear Time Using Miniature Temperature Loggers. Journal of Rehabilitation Medicine 2022; 54(SE - Articles): jrm00277.
[29] Young NL, Williams JI, Yoshida KK et al. The context of measuring disability: Does it matter whether capability or performance is measured? Journal of Clinical Epidemiology 1996; 49(10): 1097–1101.
[30] Uswatte G, Taub E, Morris D et al. The Motor Activity Log-28: assessing daily use of the hemiparetic arm after stroke. Neurology 2006; 67(7): 1189–1194.

[31] Van Der Lee JH, Beckerman H, Knol DL et al. Clinimetric properties of the motor activity log for the assessment of arm use in hemiparetic patients. Stroke 2004; 35(6): 1410–1414.
[32] van Kampen DA, van Beers LW, Scholtes VA et al. Validation of the Dutch version of the Simple Shoulder Test. Journal of Shoulder and Elbow Surgery 2012; 21(6): 808–814.
[33] Hurd MM, Farrell KH and Waylonis GW. Shoulder sling for hemiplegia: friend or foe? Archives of physical medicine and rehabilitation 1974; 55(11): 519–522.
[34] Mackenzie TA, Bdaiwi AH, Herrington L et al. Inter-rater Reliability of Real-Time Ultrasound to Measure Acromiohumeral Distance. PM&R 2016; 8(7): 629–634.
[35] Jaeschke R, Singer J and Guyatt GH. Measurement of health status. Ascertaining the minimal clinically important difference. Controlled clinical trials 1989; 10(4): 407–415.
[36] Tashjian RZ, Deloach J, Porucznik CA et al. Minimal clinically important differences (MCID) and patient acceptable symptomatic state (PASS) for visual analog scales (VAS) measuring pain in patients treated for rotator cuff disease. Journal of Shoulder and Elbow Surgery 2009; 18(6): 927–932.
[37] Christie A, Dagfinrud H, Garratt AM et al. Identification of shoulder-specific patient acceptable symptom state in patients with rheumatic diseases undergoing shoulder surgery. Journal of Hand Therapy 2011; 24(1): 53–61.
[38] Simovitch R, Flurin PH, Wright T et al. Quantifying success after total shoulder arthroplasty: the minimal clinically important difference. Journal of Shoulder and Elbow Surgery 2018; 27(2): 298–305.
[39] Tashjian RZ, Hung M, Keener JD et al. Determining the minimal clinically important difference for the American Shoulder and Elbow Surgeons score, Simple Shoulder Test, and visual analog scale (VAS) measuring pain after shoulder arthroplasty. Journal of Shoulder and Elbow Surgery 2017; 26(1): 144–148.
[40] Tashjian RZ, Deloach J, Green A et al. Minimal clinically important differences in ASES and simple shoulder test scores after nonoperative treatment of rotator cuff disease. Journal of Bone and Joint Surgery - Series A 2010; 92(2): 296–303.

Part II
the Hand

6. Mechanical design and feasibility of a hand exoskeleton to support finger extension of severely affected stroke patients

Abstract—In this paper we presented the mechanical design and evaluation of a low-profile and lightweight assistive hand exoskeleton that supports the finger extension of stroke patients during daily activities without applying axial forces to the finger. The hand exoskeleton consists of a flexible structure that is secured to the index finger of the user while the thumb is fixed in an opposed position. Pulling on a cable will extend the flexed index finger joint such that objects can be grasped. The device can achieve a grasp size of at least 7 cm. Technical tests confirmed that the exoskeleton was able to counteract the passive flexion moments corresponding to the index finger of a severely affected stroke patient (with an MCP joint stiffness of k = 0.63Nm/rad), requiring a maximum cable activation force of 58.8N. A feasibility study with stroke patients (n=4) revealed that the exoskeleton caused a mean increase of 46◦ in the range of motion of the index finger MCP joint. The patients (n=2) who performed the Box & Block Test were able to grasp and transfer maximally 6 blocks in 60 sec. with exoskeleton, compared to 0 blocks without exoskeleton. Our results showed that the developed exoskeleton has the potential to partially restore hand function of stroke patients with impaired finger extension capabilities.

Haarman, C. J. W., Hekman, E. E. G., Rietman, J. S. & van der Kooij, H., Mechanical design and feasibility of a hand exoskeleton to support finger extension of severely affected stroke patients. (*under review*)

6.1. Introduction

Stroke is one of the leading causes of permanent disability among adults. In 2017, 1.12 million incident strokes occurred in Europe [1]. Many stroke patients experience hand motor impairments such as decreased grip strength and finger extension impairment. Approximately 65% of the stroke patients do not involve their impaired hand during daily activities 6 months post-stroke [2]. Factors contributing to a loss of hand function after stroke may include extensor muscle weakness, increased flexor muscle tone, spasticity and contracture [3-4]. These symptoms typically causes the hand to be clenched, which affects the patient's ability to perform (bimanual) activities of daily living (ADL).

Assistive hand exoskeletons can support the impaired hand of stroke patients with reduced finger extension capabilities to improve the execution of bimanual tasks. Three common approaches are found in literature that are specifically aimed at extending the finger during daily activities using portable hand exoskeletons. (Exoskeletons focusing primarily on grasping assistance are not regarded in this overview.) Cable-driven finger extension exoskeletons use cables that are routed on the dorsal side of the finger through a glove [5-8]. Donning glove-based designs is considered challenging and is typically not possible without assistance [9]. Also, inherent to their design, these devices exert high, undesired, axial forces to the fingers during extension. Pneumatic systems can also extend impaired fingers [10], [11]. As no rigid structure is present to guide the extension torques to the finger, misalignment may lead to secondary injuries or discomfort [12]. Additionally, bulky and heavy actuators are required to provide the large extension torques necessary to extend the fingers of stroke patients, which limit the portability of these devices [12]. Spring-operated finger extension devices include the SaeboFlex [13] and SaeboGlove (Saebo Inc., USA). These devices rely on the stiffness of normal extension springs or rubber bands to extend the fingers. In order to grasp objects, patients require high voluntary flexion torques to overcome the (high) spring stiffness. If patients cannot provide sufficient flexion torques, then the functional benefit of these spring-operated extension devices during ADL is limited.

In this paper we present the mechanical design and evaluation of a novel, lightweight assistive hand exoskeleton that supports the finger extension of stroke patients. The hand exoskeleton consists of a flexible structure that is connected to the index finger of the user in a two-step donning process. The thumb is fixed in an opposed position. By pulling on a cable the finger is extended to provide enough hand opening to allow for object grasping, without applying axial forces to the finger. The required actuation forces to operate the extension mechanism were measured while being attached to a mechanical finger simulating a high finger joint stiffness. The orthosis-patient interaction was evaluated with four stroke patients in terms of kinematics and required cable forces. Also a performance-based test (Box & Block test) was conducted to investigate the difference in task execution between the supported and non-supported condition.

6.2. Requirements

In this research a novel hand exoskeleton was developed with a small form-factor and low weight, that supports the finger extension of stroke patients during ADL without applying axial forces to the finger. The main requirements for this assistive device are summarized in Table 6.1. An elaborate description can be found below.

Requirement	Description
Maximum grasp size	Between 5 and 7 cm
Compensated MCP finger joint stiffness	≥ 0.63 Nm/rad (when initiating movement from a resting angle of 40°)
Degrees of freedom	Enable precision and power grip
Wrist	Stabilized in functional position
Weight	<200g (hand-mounted part)
Size	<8 mm above dorsal surface of hand
Usability	Independent donning and doffing
Axial forces	No axial forces applied to fingers
Adaptability	Fit adult hand sizes

Table 6.1 – Summary of requirements for hand exoskeleton to support extension of the fingers during ADL.

Grasp size: Patients with a high finger joint stiffness will initiate their hand movement from a flexed position. Achieving a sufficient hand opening is crucial for enabling activities of daily living (ADL). Feix et al. found that a grasp size of 7 cm or less was sufficient for their observed (healthy) population to grasp 90% of the objects in a data set [14]. In 83% of the cases, the required grasp size was less than 5 cm. To accommodate grasping of a sufficiently large range of objects, it should therefore be possible to achieve a grasp size of at least 5 cm, and preferably 7 cm with the device. To achieve a hand opening of more than 5 cm with an average-sized finger, index finger flexion angles of approximately 10° (MCP) and 20° (PIP) are required. Here, a fixed thumb CMC abduction angle of 30° is assumed.

Finger joint stiffness: Antagonistic flexor and extensor muscles control the rotation of the metacarpophalangeal (MCP), proximal interphalangeal (PIP) and distal interphalangeal (DIP) joints of the finger (Fig. 6.1A). Mechanical resistance to rotation, or rotational stiffness (k), is expressed as the ratio of the change in moment (ΔM) to the change in joint rotation angle (Δθ):

$$k = \frac{\Delta M}{\Delta \theta} \tag{6.1}$$

Depending on the severity of their impairments, the finger joint stiffness may vary considerably among stroke patients. The Modified Ashworth Scale (MAS) is a clinical score commonly used to grade the degree of resistance against passive rotation of a joint on a scale from 0 (no resistance) to 4 (joint rigid in flexion or extension) [15]. MCP finger joint stiffness values associated with stroke range from approximately k=0.09-0.14 Nm/rad in mildly affected patients (MAS=1+), to k=0.52-0.54 Nm/rad in moderately affected patients (MAS=2), and up to k=0.63 Nm/rad in severely affected patients (MAS=3) [16], [17]. The associated MCP joint resting angle was 42° flexion for the most severe patient. For healthy

controls, the measured finger joint stiffness values were significantly lower (between 0.03-0.05 Nm/rad) [16]. With this exoskeleton we aim to extend the fingers of mildly to severely affected patients. Therefore, the hand exoskeleton should be able to extend fingers with an MCP joint stiffness up to 0.63 Nm/rad.

Degrees of freedom: The device should allow for the interaction with different types of objects to be useful in daily life. Both the precision and power grip are commonly used grasp modes during object manipulation [18]. For the precision grip, the object is clamped between the fingers and the opposing thumbF. For the power grip, the object is clamped between the fingers and the palm of the hand, whereas the counter pressure is applied by the thumb [18]. The precision grip requires only one degree of freedom (DOF), whereas the power grip requires two DOFs [19]. In both grips, the thumb should be opposed to the fingers [20]. Also, it is acceptable to couple the movements of the index and middle finger [20]. The device should allow for some passive finger abduction/adduction of the MCP joint to accommodate slightly deformed hands and be comfortable during use. For patients with impaired wrist stabilization, the wrist should be stabilized in a functional (neutral) position.

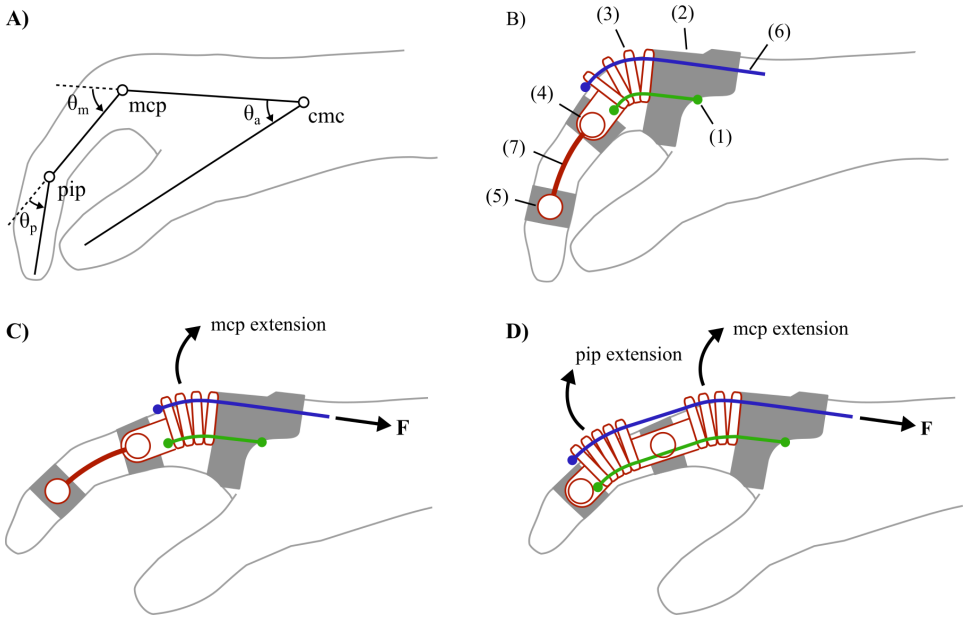

Fig. 6.1 – A) Side view of the hand with the index finger in a flexed (closed) position, showing the metacarpophalangeal (MCP) proximal interphalangeal (PIP) joints of the index finger, rotated by angles θm respectively θp. The thumb is rotated around the carpometacarpal (CMC) joint by an abduction angle θa. B) The finger extension mechanism applied to the MCP joint of the index finger consists of the following elements: (1) flexure that allows for MCP joint rotation while preventing axial forces being applied to the finger, (2) hand bracket, (3) spacer segments, (4) middle segment, (5) distal segment, (6) cable, (7) metal rod which length is customized during fitting such that the connectors are located halfway the proximal and middle segments of the index finger. C) Pulling on the cable with force (F) will extend the MCP joint of the index finger. The PIP joint angle is fixed. D) The finger extension concept extended to the PIP joint. Pulling on the cable results in a combined extension of the PIP and MCP joint.

Weight: The hand-mounted part of the exoskeleton should weigh less than 200g to be acceptable for use during daily activities [20].

Size: The height of the mechanism from the dorsal finger surface should be limited to not hinder hand function. We consider 8 mm (e.g. one-half the thickness of the finger) to be an acceptable mechanism height for ADL purposes.

Usability: The exoskeleton should allow for independent donning and doffing [20]. Control of the device should be easy and intuitive.

Adaptability: The device should be adaptable to fit various adult hand sizes [12].

6.3. Design

6.3.1. Finger extension mechanism

In Fig. 6.1B the key components of the finger extension mechanism are identified. The finger extension mechanism straightens a flexure that is mounted next to the index finger by pulling on a cable. The flexure allows for joint rotation, while preventing axial forces being applied to the finger. The rotational axis of the mechanism is aligned with the rotational axis of the MCP joint. The proximal end of the flexure is secured to a hand bracket. The distal end of the flexure is secured to the middle segment. This middle segment is connected to a female connector, which in its turn is attached to the proximal phalanx of the index finger. Spacer segments allow for bending of the flexure, but keep the cable at a fixed distance from the flexure. Pulling on the cable results in straightening of the flexure, and thus an extension of the MCP joint. The metal rod and distal segment prevent flexion of the PIP joint. The distal segment is attached to a female connector that is secured to the middle phalanx of the index finger. The length of the metal rod can be customized during fitting to align the connectors to the proximal and middle phalanxes of the index finger. For simplicity, only the extension of the MCP joint is considered in Fig. 6.1B and 6.1C. However, the mechanism can be easily extended to the PIP joint as seen in Fig. 6.1D. The DIP joint is left unsupported as to not impede fingertip sensation of the user. Hyperextension of the finger joints is prevented as the segments cannot be extended further than neutral position (0° flexion).

6.3.2. Wrist and thumb support

A Bowden cable configuration, including a PTFE liner and 1x7 nylon-coated stainless steel wire (0.5 mm diameter, 18.2 kg tensile strength) removes the need for having the actuation source mounted close to the finger. This reduces the weight of the hand-mounted part. A static wrist splint (LP Support, USA), mounted on the ventral side of the arm provides an anchoring point for the Bowden cable, and keeps the wrist in a neutral position. The thumb is fixed in an opposed position using a magnetic connector and metal rod, such that the flexed index finger touches the tip of the thumb.

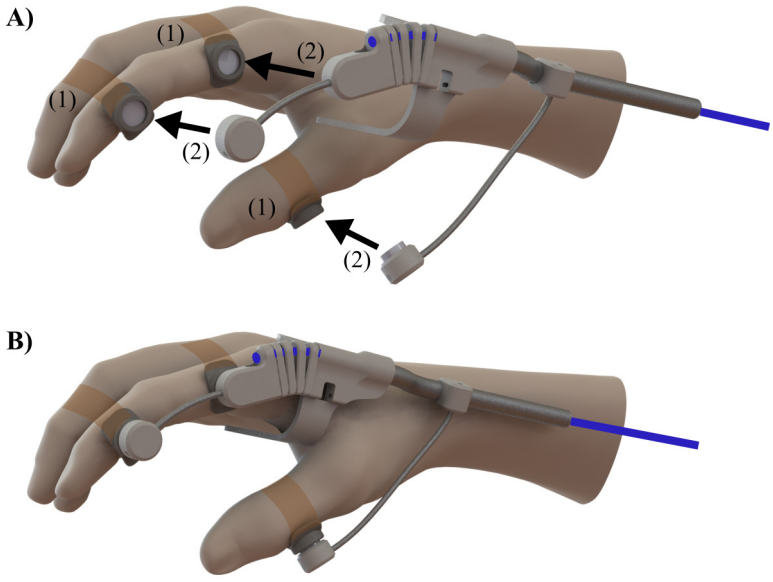

Fig. 6.2 – A) The donning process of the hand exoskeleton. (1) The female connectors are first secured to the finger and thumb with medical adhesive tape. (2) Then the middle and distal segments (containing magnets) are attached to the female connectors from the medial side. B) The hand exoskeleton when fully donned.

6.3.3. Donning procedure

Patients with hand motor impairment often have difficulties with correctly positioning their hands and fingers to facilitate exoskeleton donning. To ease the process of donning (Fig. 6.2A), this procedure is split into two steps: 1) The female finger connectors are secured to the index finger (proximal and middle phalanx) and thumb (proximal phalanx) with medical adhesive tape. If a simultaneous movement of the index finger and middle finger is desired, the adhesive tape can be wrapped around the combined index and middle finger. 2) The device is attached to the fingers by positioning the mechanism onto the female connectors from the medial side. The neodymium magnets (8x5mm, N45 grade) that are glued to the mechanism and will attach to the metal plate of the female connector, providing a sturdy connection. The female connectors are secured halfway the proximal and middle phalanxes, such that their position matches the position of the magnets. Fig. 6.2B shows the device when fully donned.

6.4. Technical characterization

6.4.1. Grasp size

The grasp size was evaluated by mounting the exoskeleton to an average-sized hand of a healthy subject.

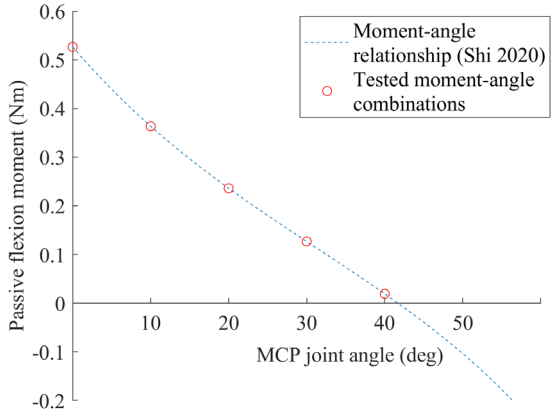

Fig. 6.3 – Moment-angle plot of stroke patient with high finger joint stiffness (dashed line), derived from [16]. The performance of the extension mechanism was tested by measuring the cable actuation forces at the marked locations (o).

6.4.2. Cable force

To characterize the performance of the finger extension mechanism, the cable activation forces were measured to extend a mechanical finger at different MCP joint angles while simulating a high joint stiffness. The cable activation force is defined as the lowest cable force that counteracts the passive flexion moment. The moment-angle relationship of a finger with a high MCP joint stiffness (k=0.63 Nm/rad) was derived from Shi et al. [16], see also Fig. 6.3 (dashed line). These data were used as a reference to set the passive flexion moment of the mechanical finger between 0° and 40° (resting angle) MCP flexion, see Fig. 6.3 (o markers).

Experimental setup: The measurement device (Fig. 6.4) consisted of a mechanical finger with a single degree of freedom (MCP joint). A support containing a load cell is bolted onto the base, such that when the finger is flexed, the tip rests perpendicularly against the load cell. By changing the position of the support, different flexion angles of the mechanical finger can be set, according to Fig. 6.3. The appropriate passive flexion moment at each flexion angle, also according to Fig. 6.3 were generated by tensioning a helical spring such that the force measured below the tip of the mechanical finger by the load cell (KD24s, ME Messsysteme, Germany) times the moment arm (90 mm) equals the passive flexion moment from Fig. 6.3 at that specific joint angle. The extension mechanism was mounted onto this mechanical finger to counteract the passive flexion moment. The extension mechanism was operated by pulling on the cable that was guided through a Bowden-cable arrangement to a handle. The cable force was measured with a force sensor (Futek, USA) mounted between the cable and the handle.

Methods: The extension mechanism was extended by slowly pulling on the cable with a constant rate and releasing the tension on the cable with a similar constant rate. This was

done at 0, 10, 20, 30 and 40° MCP flexion. The activation force is defined as the lowest cable force that causes the force measured below the tip of the mechanical finger to be <0.1N. This is an indirect measure that the passive flexion moment is compensated. Each moment-angle combination was measured 3 times and the mean and standard deviation of the cable force were determined.

6.5. Evaluation of patient interaction

The exoskeleton-patient interaction was evaluated with four stroke patients that have limited finger extension capabilities. Other inclusion criteria included a normal passive finger range of motion, patients should be capable of following verbal instructions and should be 18 years or older. Ethical approval for this study was obtained from the Ethics Committee of the University of Twente (ref. number 2022.129). Ethical approval from a medical ethical committee was not required, as the Medical Research Involving Human Subjects Act was not applicable. All participants gave their informed consent prior to the study onset. The goal of this evaluation was to investigate the performance of the exoskeleton when mounted to the hand of a patient.

At the start of the measurement, the mean grip strength of the impaired hand across three measurements was recorded with a hand-held dynamometer (Jamar). Also, the MAS score was determined for each subject.

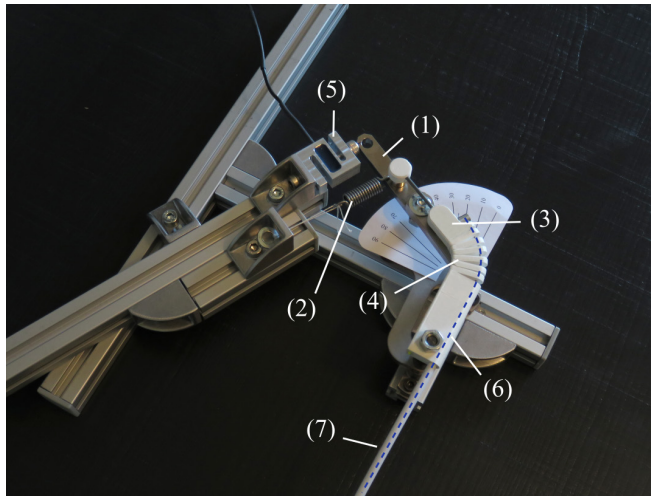

Fig. 6.4 – Setup consisting of a mechanical finger (1) to measure the cable actuation force required to counteract the flexion moment provided by the tensioned spring (2) with the extension mechanism (3) for different MCP joint angles. The extension mechanism is aligned with the MCP joint (4). The passive flexion force is measured by the load cell (5). The cable (6, in blue) is guided by the Bowden cable (7) to the actuation handle (not depicted). The Bowden cable was not bent during the measurement.

6.5.1. Range of motion

We measured the active range of motion (ROM) of the index finger while the subject was seated on a chair, with his elbow flexed to 90 degrees and wrist supinated. A webcam

(640x480px, 20 frames/second) was placed perpendicular to the sagittal plane of the hand, aligned with the flexion-extension axis of the MCP joint, at a distance of approximately 20 cm.

Without exoskeleton: To measure the active range of motion without exoskeleton, the subject voluntarily extend his index finger from the resting position to a maximum extended position, while the finger movements were recorded with the camera. Lines were drawn manually onto stills of the captured video with a custom Matlab script (Matlab 2021b, Mathworks, USA), to estimate the index finger MCP and PIP joint angles in rest and in during maximum finger extension.

With exoskeleton: The extension mechanism was mounted to the affected hand of the subject, to support extension of the index finger MCP joint. The subject was then asked to operate the extension mechanism by pulling on the cable with his unaffected hand to extend the index finger from a resting position to a maximum comfortable extended position and back to the resting position, at a slow, constant speed. These movements were repeated three times. Then, the same procedure was performed, but now with the extension mechanism connected to the combined index and middle finger. During each trial, video recordings of the finger movements were made from which the kinematics were determined, similar as was done for measurements without exoskeleton. Additionally, the cable forces required to extend the finger(s) were recorded with a force sensor (Futek, USA) that was mounted between the operating handle and the cable. See also Fig. 6.5 for an overview of the test setup.

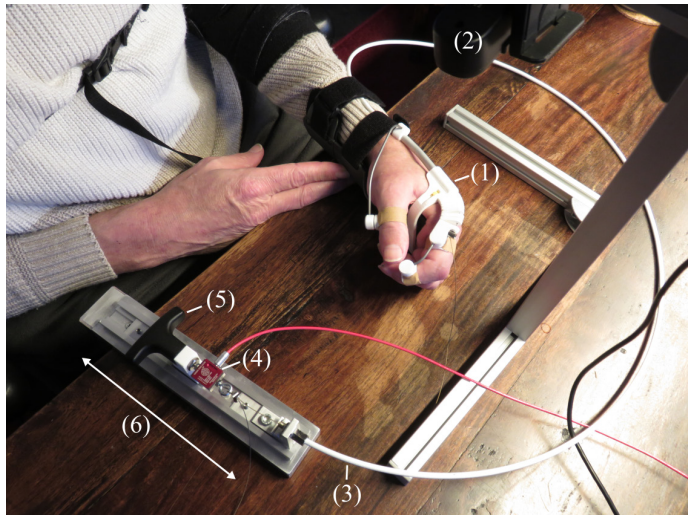

Fig. 6.5 – Test setup used during evaluation of the kinematics and cable forces with the hand exoskeleton supporting the extension movement of the index finger. (1) Hand exoskeleton; (2)Webcam; (3) Bowden cable; (4) Force sensor; (5) Actuation handle; (6) Slider.

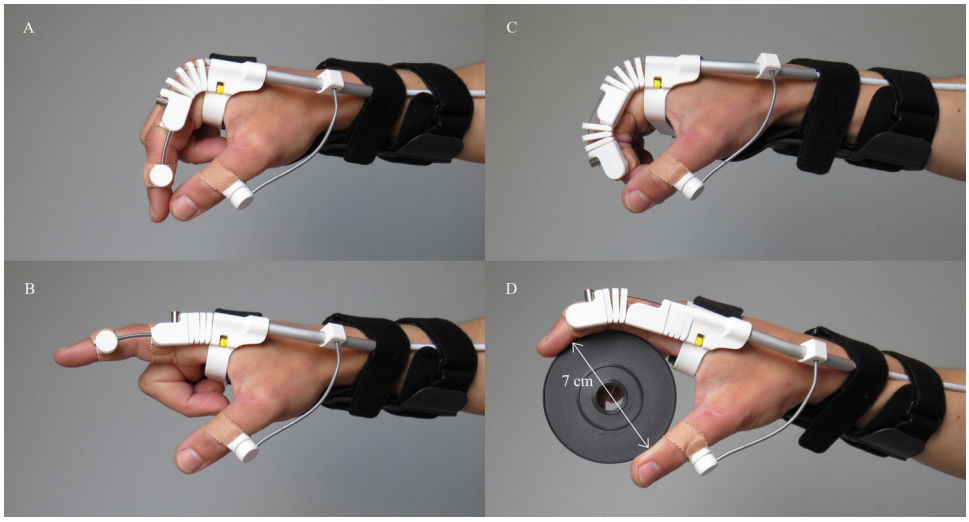

Fig. 6.6 – A) Prototype of the hand exoskeleton mounted to the hand of a healthy user, with the MCP joint in maximum flexion. B) Prototype of the hand exoskeleton, with MCP joint in maximum extension. C) Prototype of the hand exoskeleton with an active DOF at the MCP and PIP joint in maximum flexion. D) Grasping an object with a diameter of 7 cm is possible with the device.

6.5.2. Box & Block Test

The Box & Block Test is a functional test to measure gross manual dexterity [21]. The test consists of a rectangular box with two compartments that are separated by a partition and contains 150 colored wooden blocks (2.5cm in size) that should be grasped and transferred. Subjects were instructed to move as many blocks as possible in 60 seconds from one compartment to the other, (1) with their unsupported affected hand, and (2) with their affected hand supported by the exoskeleton that was operated by their unaffected hand. For each tested condition the number of transferred blocks in 60 seconds were counted.

6.6. Results

The developed hand exoskeleton is shown in Fig. 6.6 during maximum MCP joint flexion (A) and maximum MCP joint extension (B). The PIP joint is fixed. Instead of actuating only MCP joint extension, Fig. 6.6C shows the mechanism when controlling both MCP and PIP joint extension. In Fig. 6.6D, we show that an object with a diameter of 7 cm can be grasped with the device. The hand-mounted part of the hand exoskeleton weighs 87g, including a size S wrist splint (43g), or 105g including a size M wrist splint (61g). The form-factor of the device is small as the hand exoskeleton extends only 6 mm above the dorsal surface of the hand. The height of the cable above the flexure determines the extension moment that is created by the mechanism for a given cable force. In the prototype the height was fixed at 12.5 mm. To operate the mechanism in this configuration from a fully closed ($\theta_{MCP} = 90°$) to a fully extended ($\theta_{MCP} = 0°$) position, a cable excursion of 20 mm is required. The design is also modular: by removing or adding flexible segments, the device can be easily adjusted to

MCP joint angle (°)	Passive flexion moment (Nm)	Cable activation force (mean ± std) (N)
0	0.53	58.8 ± 1.24
10	0.36	38.5 ± 0.78
20	0.24	24.2 ± 0.44
30	0.13	12.0 ± 0.40
40	0.02	2.5 ± 0.13

Table 6.2 - Mean cable activation forces for each tested moment-angle combination while simulating a paretic finger with a high finger joint stiffness. Std: standard deviation.

ID	Gender	Age (y)	Weight (kg)	Dominant hand	Affected hand	Time since complaints (y)	Grip strength impaired hand (kg)	MAS score (0-4)
S1	M	61	80	Right	Left	1	0	3
S2	M	27	66	Right	Right	15	9.5	3
S3	M	76	85	Right	Left	5	4.2	3
S4	F	19	60	Right	Right	4	10.5	2+

Table 6.3 - Subject characteristics. ID: subject ID; F: female; M: male;

different hand dimensions. Because the flexure can bend anywhere along the line of flexible segments, no perfect alignment with the MCP (or PIP) joint is required.

6.6.1. Cable force

The mean cable activation forces were determined for each of the MCP moment-angle combinations marked in Fig. 6.3. The results are shown in Table 6.2. As an example, the measured cable and fingertip forces measured during three extension movements are shown in Fig. 6.7 while a passive moment of 0.53 Nm was set with the spring at 0° MCP flexion.

6.6.2. Evaluation of patient interaction

The characteristics of the four stroke patients who participated in this evaluation study are listed in Table 6.3. S1 had no voluntary muscle activation of the flexor and extensor muscles. For S3 we used no thumb support as his thumb was already in an opposed positioned. S2 and S4 struggled to relax their finger flexors which led to highly variable muscle tone. For S4, we therefore decided to stabilize the DIP joint with an additional metal rod secured to the index finger with adhesive tape, as excessive flexion caused the DIP to render the index finger dysfunctional. For S2 we decided to attach the distal portion of the extension mechanism to the distal segment of the index finger. Due to the excessive tone of the thumb flexor muscles, we required a stiffer thumb rod for this participant to keep his thumb in an opposed position.

6.6.3. Range of motion

The MCP and PIP joint angles of the index finger in resting and maximum extended position are listed in Table 6.4. For three subjects (S1, S2 and S4) no active joint extension was measured. For S3, the MCP range of motion was 12°, and the PIP range of motion was 14°.

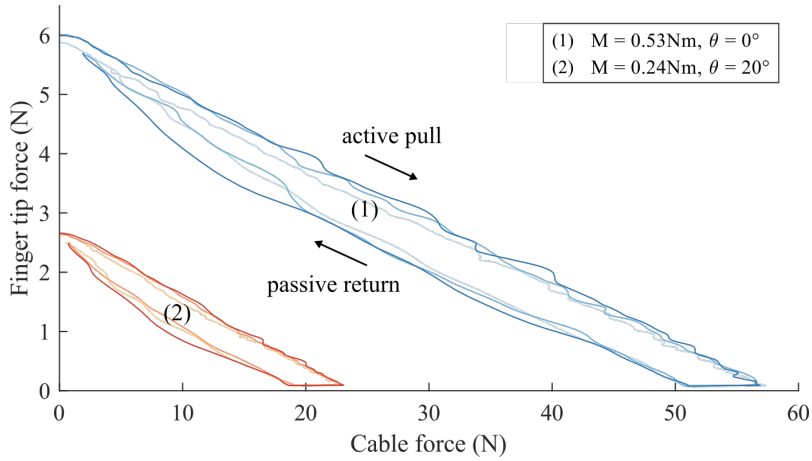

Fig. 6.7 – Cable forces and forces measured at the tip of the mechanical finger, while counteracting a passive flexion moment of 0.53 Nm at 0° MCP flexion (1) and while counteracting a passive flexion moment of 0.24 Nm at 20° MCP flexion (2).

In Table 6.5 the MCP joint resting angles and maximum extension angles are listed when the subject extended his finger with the extension mechanism to a maximum position by pulling on the actuation handle. The required cable forces to extend the finger to achieve this position are also listed in this table. Subjects with the highest MAS scores, required the highest cable forces to extend their index finger. Also, higher forces were required to extend the index and middle finger simultaneously, than to extend the index finger alone.

ID	$\theta_{MCP,R}$ (°)	$\theta_{PIP,R}$ (°)	$\theta_{MCP,E}$ (°)	$\theta_{PIP,E}$ (°)
S1	55	75	(55)[1]	(75)[1]
S2	53	32	(53)[1]	(32)[1]
S3	59	35	47	21
S4	74	96	(74)[1]	(96)[1]

Table 6.4 – Index finger resting and maximum active extension angles. [1]: no active joint extension was measured; ID: subject ID; θmcp,r: index finger MCP joint resting angle; θpip,r: index finger PIP joint resting angle; θmcp,e: index finger MCP joint maximum active extension angle; θpip,e: index finger PIP joint maximum active extension angle.

ID	Digit	$\theta_{MCP,R}$ (°) (mean ± std)	$\theta_{MCP,E}$ (°) (mean ± std)	F_c (N) (mean ± std)
S1	II	31 ± 1	5 ± 1	37.8 ± 4.3
	II + III	37 ± 55	3 ± 1	39.7 ± 4.3
S2	II	45 ± 8	9 ± 1	34.4 ± 4.0
	II + III	54[1]	7[1]	56.0[1]
S3	II	52 ± 8	40 ± 3	40.9 ± 4.5
	II + III	42 ± 7	23 ± 3	62.5 ± 9.4
S4	II	32 ± 0	1 ± 0	20.4 ± 2.0
	II + III	27 ± 1	5 ± 2	35.1 ± 3.5

Table 6.5 - Mean MCP joint angle (θmcp,e) and cable force (Fc) at maximum extension with the hand exoskeleton attached to the index finger (digit II), or combined index and middle finger (digits II+III). ID: subject ID; θmcp,r: index finger MCP joint maximum extension angle; θmcp,e: index finger MCP joint maximum extension angle; II: index finger; III: middle finger; [1]: based on one trial.

ID	Without exo (# of blocks)	With exo (# of blocks)
S2	0	6
S4	0	5

Table 6.6 - Scores of the Box & Block Test, denoting the number of blocks transferred by the affected hand in 60 sec.

By comparing the maximum extension angles of Tables 6.4 and 6.5 it can be seen that the extension mechanism improved the finger extension. On average the extension angle increased with 46° (range 7 to 73) were achieved across all participants. For S1 and S4 the exoskeleton had a large effect on the MCP joint resting angle of the index finger.

6.6.4. Box & Block Test

Subjects should have sufficient proximal (arm) control to position their hand from one compartment to the other to complete the Box & Block Test. Only two of the four subjects (S2 and S4) were able to accomplish this. Therefore, the results from the test were only reported in Table 6.6 for these subjects. From our data it is observed that both subjects were able to successfully transfer several blocks with the exoskeleton mounted to their hand, compared to none without exoskeleton. In Fig. 6.8 three stills of the Box and Box Test of P02 are shown during grasping of one block.

6.7. Discussion

In this study we presented the mechanical design and evaluation of a novel hand exoskeleton that supports the finger extension of stroke patients. A technical evaluation of the device showed that the mechanical structure was able to counteract the passive flexion moments corresponding to the index finger of a severely affected stroke patient (with an MCP joint stiffness of k = 0.63Nm/rad). The maximum cable activation force that was measured during this evaluation was 58.8N. The device can achieve the desired grasp size of 7 cm when mounted to an average-sized hand of a healthy user. The device was also able to improve the extension of the index finger of four stroke patients when performing extension movements with the exoskeleton mounted to their hand. In a functional test (Box & Block Test) with two stroke patients, we demonstrated that the hand exoskeleton improved their ability to pick up 2.5 cm wooden blocks.

Fig. 6.8 - Stills from the Box & Block Test of P02 showing the initial hand opening (left), actual grasping (middle) and lifting (right) of one block.

Aspect	EXTEND exoskeleton	HERO Grip Glove [8]	SaeboFlex [13]	SaeboGlove (Saebo Inc., USA)
Design type [12]	Compliant	Compliant (glove)	Base-to-distal	Compliant (glove)
Actuation strategy	Not implemented yet	Active (pneumatic)	Passive (extension springs)	Passive (rubber bands)
Weight (g)	105	284	1587	453
Extension moment (Nm)	0.53	N/A (80N tensile force)	N/A (depends on spring stiffness)	N/A (depends on band stiffness)
Min. grasp size (cm)	0	0	6-7[1]	3-4[1]
Max. grasp size (cm)	>7	>7[2]	>7[2]	>7[2]
Dimensions (cm)	24x9x5	33x10	34x23x34	23x20x7
Active DOF (digits I-V)	II, or II+III	I to V	I to V	I to V
Wrist support (Yes/No)	Yes	Yes	Yes	Yes
Fingertip covered (Yes/No)	No	Yes	Yes	Yes

Table 6.7 – Comparison of the main aspects of the EXTEND hand exoskeleton with the state of the art. N/A: not available; [1]: estimation; [2]: estimation, but highly depending on user's grip strength and impairment level.

In Table 6.7 we present a brief comparison of the characteristics of our developed device with other devices found in literature. Compared to the state of art, our hand exoskeleton is lightweight, has a small volume and is easily mounted to the affected hand.

Several limitations regarding the design and test methods are addressed below.

In our device, the magnets that attach the extension mechanism to the finger connectors are subjected to forces parallel to the surface, which lowers the adhesive force to approximately 15-25% of their specified adhesive force. A raised brim on the edge of the finger connectors counteracts this effect partially. Still, the adhesive force is a limiting factor of the maximum force that can be applied to the finger. In the future we may consider using different magnets or a different magnet connector design.

In this study we focused on the technical aspects of the mechanical design. In a future study we will focus more on usability aspects such prolonged use during daily activities, and independent donning and doffing, and durability of the mechanism (e.g. of the cable and flexure). To be able to evaluate this, a portable actuation strategy should be implemented, such as body-powered actuation, or joint stiffness compensation based on a negative spring mechanism. Both strategies have the potential to be easy and simple to use, while they don't require complex, expensive and heavy components which are typically involved in electrically or hydraulically powered systems. Body movements directly control the hand opening as the cable of the extension. Body-powered actuation is commonly applied in upper

extremity prosthetics [22], where often contralateral shoulder movements control the prosthesis. In stroke patients using the contralateral side of the body may pose problems as it can lead to overstraining of the non-affected side. The application of body-powered control strategies should therefore be investigated further. Another actuation strategy is to use extension springs in a particular (so-called negative stiffness) configuration to compensate for the intrinsic stiffness of the finger joints [23]. Ideally, the passive flexion moment at each joint angle is perfectly counteracted by the energy stored in a normal extension spring. For the user to operate the device now only small voluntary finger flexion forces are required. A downside of this strategy is that it cannot compensate for hysteresis in the system.

The developed finger extension mechanism can be easily extended to the PIP joint, such that simultaneous control of the MCP and PIP joint is possible. We observed promising results of extending the finger with only active MCP control. Future work should also explore the finger kinematics of the finger when assisting both MCP and PIP extension.

The efficiency of Bowden cable transmissions largely depends on the geometric configuration of the system [24]. When evaluating the exoskeleton with users, the cable of the extension mechanism was attached to an operating handle through a Bowden cable. Even though the radius of curvature of the Bowden cable experimental setup was large (>30 cm), the frictional losses due to a wrap angle of 360° caused the force transmission to be less efficient. The cable activation forces will be lower if the wrap angle is decreased, e.g. when the cable is directed from the hand towards the actuation system in a straight line.

Increasing the height of the cable above the flexure can further decrease the required activation force, but will also increase the size of the mechanism.

In this design we secured the finger connectors to the proximal and middle phalanx of the finger, while the distal phalanx was left unsupported to not impede fingertip sensation. As the finger flexor tendon crosses multiple joints, the DIP joint will typically flex when extending the fingers. Therefore, in a future design, we might reconsider fixing the DIP joint to 15° flexion, as suggested by [19].

Also it will be worth investigating the possibilities of adding flexion assistance, especially for patients with limited grasp strength, by replacing the cable with a flexure.

References

[1] H. A. Wafa, C. D. Wolfe, E. Emmett, G. A. Roth, C. O. Johnson, and Y. Wang, "Burden of Stroke in Europe: Thirty-Year Projections of Incidence, Prevalence, Deaths, and Disability-Adjusted Life Years," Stroke, vol. 51, no. 8, pp. 2418–2427, 2020.

[2] B. H. Dobkin, "Rehabilitation after Stroke," New England Journal of Medicine, vol. 352, no. 16, pp. 1677–1684, apr 2005.

[3] A. J. Barry, D. G. Kamper, M. E. Stoykov, K. Triandafilou, and E. Roth, "Characteristics of the severely impaired hand in survivors of stroke with chronic impairments," Topics in Stroke Rehabilitation, vol. 29, no. 3, pp. 181–191, 2022.

[4] P. Raghavan, "Upper Limb Motor Impairment After Stroke," Physical Medicine and Rehabilitation Clinics of North America, vol. 26, no. 4, pp. 599–610, nov 2015.

[5] H. In, H. Lee, U. Jeong, B. B. Kang, and K.-j. Cho, "Feasibility study of a slack enabling actuator for actuating tendon-driven soft wearable robot without pretension," Icra, pp. 1229–1234, 2015.

[6] D. Popov, I. Gaponov, and J.-h. Ryu, "Portable Exoskeleton Glove With Soft Structure for Hand Assistance in Activities of Daily Living," IEEE/ASME Transactions on Mechatronics, vol. 22, no. 2, pp. 865–875, 2017.

[7] J. M. Ochoa, D. G. Kamper, M. Listenberger, and S. W. Lee, "Use of an electromyographically driven hand orthosis for training after stroke," IEEE International Conference on Rehabilitation Robotics, 2011.

[8] A. Yurkewich, I. J. Kozak, D. Hebert, R. H. Wang, and A. Mihailidis, "Hand Extension Robot Orthosis (HERO) Grip Glove: Enabling independence amongst persons with severe hand impairments after stroke," Journal of NeuroEngineering and Rehabilitation, vol. 17, no. 1, pp. 1– 17, 2020.

[9] C. E. Proulx, J. Higgins, and D. H. Gagnon, "Occupational therapists' evaluation of the perceived usability and utility of wearable soft robotic exoskeleton gloves for hand function rehabilitation following a stroke," Disability and Rehabilitation: Assistive Technology, vol. 0, no. 0, pp. 1–10, 2021.

[10] L. Connelly, Y. Jia, M. L. Toro, M. E. Stoykov, R. V. Kenyon, and D. G. Kamper, "A pneumatic glove and immersive virtual reality environment for hand rehabilitative training after stroke," IEEE Transactions on Neural Systems and Rehabilitation Engineering, vol. 18, no. 5, pp. 551–559, 2010.

[11] A. L. Coffey, D. J. Leamy, and T. E. Ward, "A novel BCI-controlled pneumatic glove system for home-based neurorehabilitation," 2014 36th Annual International Conference of the IEEE Engineering in Medicine and Biology Society, EMBC 2014, pp. 3622–3625, 2014.

[12] T. du Plessis, K. Djouani, and C. Oosthuizen, "A review of active hand exoskeletons for rehabilitation and assistance," Robotics, vol. 10, no. 1, 2021.

[13] J. F. Farrell, H. B. Hoffman, J. L. Snyder, C. A. Giuliani, and R. W. Bohannon, "Orthotic aided training of the paretic upper limb in chronic stroke: results of a phase 1 trial." NeuroRehabilitation, vol. 22, no. 2, pp. 99–103, 2007.

[14] T. Feix, I. M. Bullock, and A. M. Dollar, “Analysis of human grasping behavior: Object characteristics and grasp type,” IEEE Transactions on Haptics, vol. 7, no. 3, pp. 311–323, 2014.
[15] R. W. Bohannon and M. B. Smith, “Interrater Reliability of a Modified Ashworth Scale of Muscle Spasticity,” Physical Therapy, vol. 67, no. 2, pp. 206–207, feb 1987.
[16] X. Q. Shi, H. L. Heung, Z. Q. Tang, K. Y. Tong, and Z. Li, “Verification of Finger Joint Stiffness Estimation Method With Soft Robotic Actuator,” Frontiers in Bioengineering and Biotechnology, vol. 8, no. December, pp. 1–12, 2020.
[17] E. B. Brokaw, I. Black, R. J. Holley, and P. S. Lum, “Hand Spring Operated Movement Enhancer (HandSOME): A portable, passive hand Exoskeleton for stroke rehabilitation,” IEEE Transactions on Neural Systems and Rehabilitation Engineering, vol. 19, no. 4, pp. 391–399, 2011.
[18] J. R. Napier, “The Prehensile Movements Of The Human Hand,” The Journal of Bone and Joint Surgery. British volume, vol. 38-B, no. 4, pp. 902–913, nov 1956.
[19] G. Smit, D. H. Plettenburg, and F. C. T. Van Der Helm, “The lightweight Delft Cylinder hand: First multi-articulating hand that meets the basic user requirements,” IEEE Transactions on Neural Systems and Rehabilitation Engineering, vol. 23, no. 3, pp. 431–440, 2015.
[20] Q. A. Boser, M. R. Dawson, J. S. Schofield, G. Y. Dziwenko, and J. S. Hebert, “Defining the design requirements for an assistive powered hand exoskeleton: A pilot explorative interview study and case series,” Prosthetics and Orthotics International, 2020.
[21] V. Mathiowetz, G. Volland, N. Kashman, and K. Weber, “Adult Norms for the Box and Block Test of Manual Dexterity,” The American Journal of Occupational Therapy, vol. 39, no. 6, pp. 386–391, jun 1985.
[22] R. J. PURSLEY, “Harness patterns for upper-extremity prostheses.” Artificial limbs, vol. 2, no. 3, pp. 26–60, 1955.
[23] C. J. W. Haarman, E. E. G. Hekman, G. Prange, and H. van der Kooij, “Joint Stiffness Compensation for Application in the EXTEND Hand Orthosis,” in 2018 7th IEEE International Conference on Biomedical Robotics and Biomechatronics (Biorob), vol. 2018-Augus, 2018, pp. 677–682.
[24] A. Schiele, P. Letier, R. Van Der Linde, and F. Van Der Helm, “Bowden cable actuator for force-feedback exoskeletons,” IEEE International Conference on Intelligent Robots and Systems, pp. 3599–3604, 2006.

7. Design and feasibility of the T-GRIP thumb exoskeleton to support the lateral pinch grasp of spinal cord injury patients

Abstract— Improving the impaired hand function of spinal cord injury patients with a robotic exoskeleton can highly impact their self-management, and ultimately their quality of life. In this paper the design and evaluation of a new, lightweight (50g) robotic thumb exoskeleton, called T-GRIP, was presented that supports the lateral pinch grasp. The mechanism consists of a linear actuator that was mounted to the dorsal side of the hand, and a force transmission mechanism that flexes the thumb towards the side of the index finger. The thumb movement was controlled through contralateral wrist rotation. Experimental results from an evaluation with three spinal cord injury patients showed that the achieved grip force (~7N) was higher and the overall performance during the Grasp and Release Test was better with the T-GRIP than without device. The device shows great potential for improving the hand function of patients with cervical spinal cord injury by actuating only a single degree of freedom.

Haarman, C. J. W., Hekman, E. E. G., Maas, E.M., Rietman, J. S. & van der Kooij, H. (2022). Design and feasibility of the T-GRIP thumb exoskeleton to support the lateral pinch grasp of spinal cord injury patients. 2022 IEEE 17th International Conference on Rehabilitation Robotics.

7.1. Introduction

A spinal cord injury (SCI) can be traumatic (e.g. due to falls, road traffic accidents or sports) or non-traumatic (e.g. due to bleedings, infections, tumors or degenerative diseases). The incidence of traumatic SCI is estimated to be 14-16 per million per annum in Western Europe [1-2]. The incidence of non-traumatic SCI is unknown but assumed to be slightly higher than the incidence of traumatic SCI [3]. More than 69% of the traumatic cases are cervical lesions (tetraplegia) [1]. Depending on level and severity of injury, the motor and sensory function of the upper extremities might be affected. 77% of the tetraplegic subjects expect an important or very important improvement in their quality of life if their hand function would improve [4].

Several assistive, robotics devices are available to support the impaired hand function following SCI, including recent developments such as proposed in prior research [5–8]. Most of these devices support the hand by enabling a cylindrical grasp which requires at least two or more fingers to be actuated. An extensive review of the current state of the art is presented in [9].

Reconstructive surgery can (partially) restore impaired hand function by transferring tendons [10] or nerves [11]. However, this change is permanent and the procedure is invasive. In a survey study by Wagner et al., the factors of risks and recovery time have been shown to influence the desire to undergo surgical procedure among 62% and 52% of the interviewed SCI patients [12].

In this paper we present the design and evaluation of a new robotic thumb exoskeleton, called T-GRIP, that solely supports the lateral pinch grasp. For most spinal cord injury patients, this grasp is considered the most useful one to be restored [13]. In lateral pinch, objects are clamped between the thumb and the side of the index finger. Our design approach helps to deal with the most important factors to consider in assistive hand exoskeleton design such as wearability, low weight and comfort [9]. Compared to other assistive devices that support for example the cylindrical or tripod grasp, our new mechanism provides functional support with minimal hardware as only one degree of freedom (one thumb rotation) needs to be controlled. The other fingers are assumed to stay in place (or will be fixated).

First, an overview of the mechanical design including kinematic analysis is presented, followed by the experimental procedure and the results from an evaluation with 3 patients.

7.2. Thumb exoskeleton

7.2.1. Mechanical design

The hand-mounted part of the exoskeleton (see Fig. 7.1) consists of a thermoplastic hand bracket onto which an electric micro linear actuator (Actuonix Motion Devices Inc., Canada) is attached. This actuator has a weight of 15g, a stroke of 20mm and provides a maximum force of 40N. To accommodate a pinch grasp, the linear actuator pushes on a lever arm which moves a thumb ring to the index finger. The hand bracket and thumb ring can be adjusted to

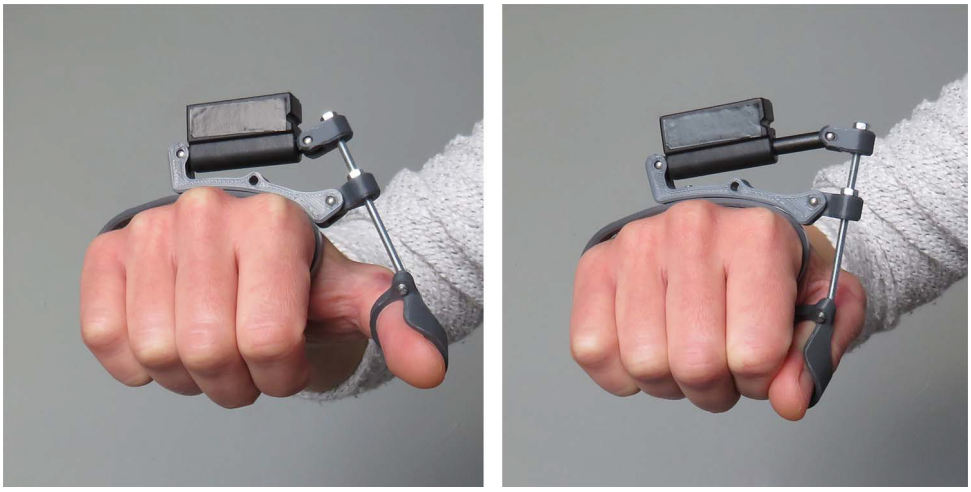

Fig. 7.1 - Overview of the T-GRIP thumb exoskeleton that supports the lateral pinch grip. The force transmission mechanism is shown with the thumb in extended (left) and flexed (right) position.

Fig. 7.2 - The T-GRIP enables grasping of various objects of different size and shape, including cylindrical, flat and irregular shaped objects.

fit the user's hand. Hyperextension of the distal joint of the thumb is prevented by the thumb ring design.

A lateral pinch grip requires a flexed index finger to provide a stable counterpart for the grasping movement. If the user is unable to maintain a flexed index finger position, or if the passive stiffness in medio-lateral direction is limited, an additional bracket can be used to stabilize the finger in the desired flexed position. The total weight of the hand-mounted part is 50g. The maximum height of the mechanism above the hand is 40 mm. The device accommodates grasping of objects of different size and shapes, see also Fig. 7.2.

The linear actuator is suspended on the dorsal side of the hand at point F, see Fig. 7.3A. The lever arm hinges around point P and is on one end connected to the actuator (at point A) and on the other end to the thumb ring (at point T).

To successfully grasp and manipulate thin objects with the lateral pinch grasp, the tip of the thumb should be able to touch the side of the index finger. Depending on the width of the index finger and thumb, the thumb extension angle θe (Fig. 7.3B) at which the thumb touches the side of the index finger is approximately 10°. The maximum extension of the actuator should therefore move the thumb to an extension angle of 10° or less, while the minimum extension of the actuator should not cause the thumb to exceed the maximum comfortable extension angle limit of approximately 40° to 50°. This is dependent on the maximum passive thumb extension of the patient.

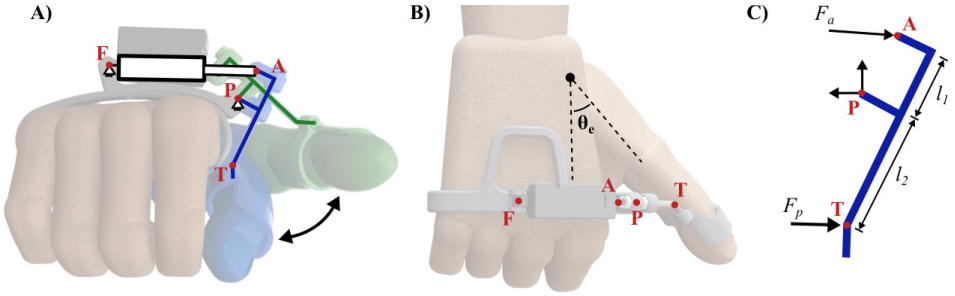

Fig. 7.3 – A) Schematic overview of the T-GRIP mechanism mounted on the hand while the lever arm causes the thumb to be in extended (green) and flexed (blue) position (frontal view). The lever arm rotates around the pivot point (P) and secures the tip of the actuator (A) to the thumb (T). The actuator is suspended on the hand at point (F). B) Top view of the hand in opened position, showing the thumb extension angle (θe). C) Free body diagram of the lever arm of the T-GRIP mechanism. Actuator force (Fa) causes the lever arm to rotate around the pivot point, resulting in a force (Fp) at the distal point of the lever arm. Varying the ratio between l_1 and l_2 will affect the resulting force Fp and the thumb range of motion.

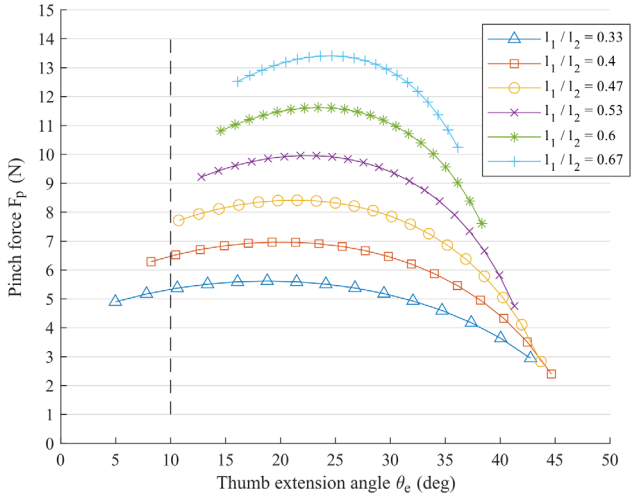

Fig. 7.4 - Plot showing the thumb extension angle θe (°) versus pinch force Fp (N) for different lever arm ratios (l_1 / l_2). The dashed line indicates the approximate thumb extension angle at which the thumb and index finger touch.

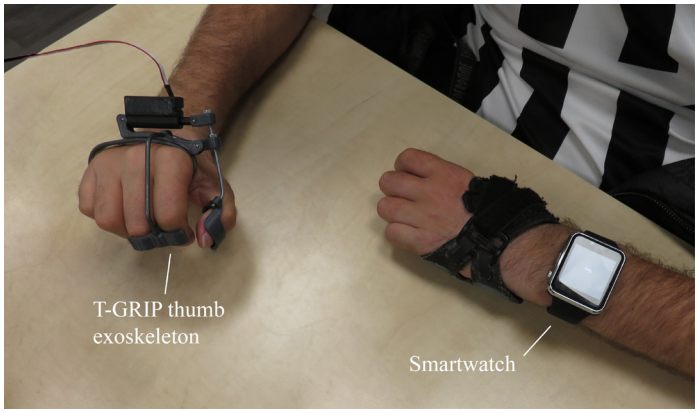

Fig. 7.5 – Flexion and extension of the T-GRIP thumb exoskeleton is controlled with the programmable smartwatch that is worn on the contralateral wrist.

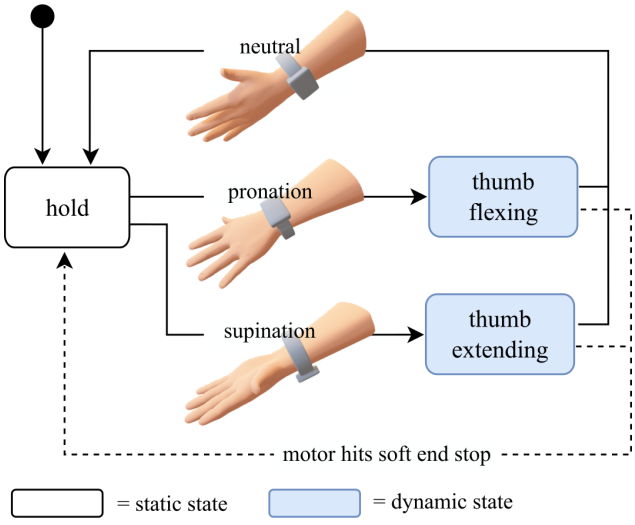

Fig. 7.6 – Discrete state machine of the exoskeleton control showing the possible transitions from the static state (hold) to the dynamic states ('thumb extending' and 'thumb flexing'). Actions to transition between these states are written next to the arrows. Pronation of the contralateral wrist controls thumb flexion. A neutral position stops the motor. Supination of the contralateral wrist controls thumb extension.

A kinematic model was derived (Appendix 7.1) to calculate the thumb range of motion and pinch force for any configuration of the mechanism. The range of motion of the mechanism can, among others, be adjusted by changing the lever arm ratio (l_1 / l_2), see Fig. 7.3C. As an illustration of this effect, in Fig 7.4 the pinch forces are plotted as a function of the thumb extension angle for varying lever arm ratios (l_1 / l_2) while keeping the total lever arm (l_1+l_2) length equal. The configuration that was used for this calculation was: Fa = 40N, l_1+l_2=50mm, l_{FX}=50mm, l_{FY}=25mm, l_A=8mm, l_P=10mm, β=15°. See also Appendix 7.1 for a detailed description of all relevant model parameters. From Fig. 7.4 it can be seen that decreasing the lever arm ratio will increase the total range of motion, and causes a smaller

minimum θe to be reached. Thus, for smaller lever arm ratios smaller objects can be grasped. However, the maximum pinch force (Fp) will decrease as the ratio decreases.

7.2.2. Control strategy

The actuator movement direction of the exoskeleton is controlled by rotating a 32-bit programmable smartwatch (LilyGo, CN) that is worn on the contralateral wrist, see Fig. 7.5. The smartwatch contains a digital, triaxial acceleration sensor that measures wrist orientation which is then sent over Bluetooth Low Energy to a discrete state machine (see Fig. 7.6) that is implemented on an ESP32 microcontroller (LilyGo, CN). Wrist pronation starts a flexion movement and wrist supination triggers thumb extension by sending a PWM signal to the motor that determines the average value of the output voltage. Thumb movement is stopped if the wrist is put into neutral position, or if the actuator soft end stop is reached. The electronics and battery are contained in an enclosure (170g, 80x150x35 mm). The exoskeleton is powered by a rechargeable 6V battery (Ni-MH, 350 mAh).

7.3. Experimental procedure

The goal of the feasibility study was to evaluate the technical viability of the T-GRIP thumb exoskeleton when used by SCI patients. During this session pinch force measurements, the Grasp and Release Test and the D-QUEST questionnaire about the user satisfaction with the device were conducted.

Three tetraplegic patients (AIS A/B) were recruited from Roessingh, Center for Rehabilitation (Enschede, the Netherlands). Other inclusion criteria included: ≥18 years, weakness of finger flexors (Medical Research Council muscle power ≤ 2, and normal passive range of motion of the thumb. Contra-indications for the participants were: increased tone or spasticity in the arm and hand, severe contractures or joint deformities in the fingers, open wounds and infected areas of the hand, recent arm or hand surgery (<6 months) or lack of active contralateral wrist pronation and supination. Ethical approval for this study was obtained from the Ethics Committee of the University of Twente (ref. number 2021.12995). Written informed consent was obtained from all participants before the study onset. During fitting, only lengths l_1 and l_2 of the lever arm were customized for each patient. The other parameters were kept the same.

7.3.1. Pinch force

The peak and sustained pinch grip force were assessed firstly without, and then with the thumb exoskeleton. Subjects were instructed to hold and squeeze an E-link Pinchmeter (Biometrics Ltd, USA) during a 10-second period. Each condition was repeated three times and the average peak force and average force over the last 60% of the measurement were reported per participant.

7.3.2. Grasp and Release Test

The Grasp and Release Test (GRT) measures the unilateral hand function during object manipulation and is validated for SCI patients [14-15]. For this study, three (out of six) objects of the GRT were chosen that require a lateral pinch grasp: peg, fork and weight (see

also Fig. 7.7). These objects vary in size, weight and surface texture. The sequence of movements for the peg and weight equals 'grasp', 'lift', and 'release'. The sequence of movements of the fork equals 'depress handle', 'lift' and 'release'. For each object, the corresponding sequence was executed by the subjects as many times as possible in 30 seconds and the number of successful completions were scored. In total three trials per object were performed. Between trials there was a 30-second resting period. For the peg a successful completion involved dropping the item in the test box (20x20x4.5cm) without touching the side of the box. The fork should be pressed down to the indicator line, while the weight should be placed upright on top of the test box for a successful completion. For each participant, the mean number of successful sequence completions performed in 30 seconds across three trials were reported per object.

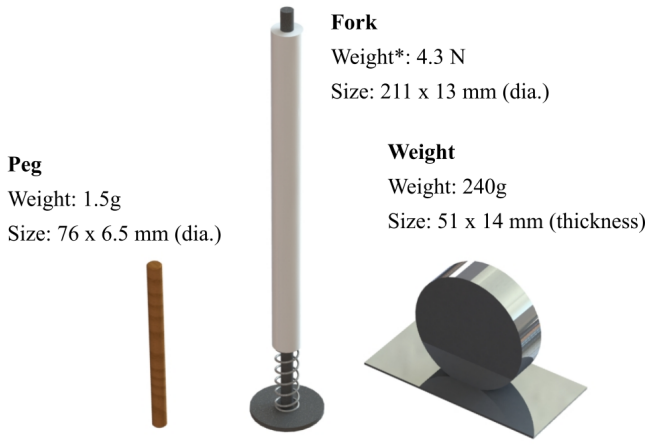

Fig. 7.7 - 3D representation including specifications of the three objects of the Grasp and Release Test that are handled with a lateral pinch grasp. These are: peg, fork and weight.

7.3.3. User satisfaction

The satisfaction of the participants with the assistive device was rated with the Quebec User Evaluation of Satisfaction with Assistive Technology (QUEST) questionnaire [16]. The first eight items of this questionnaire relate to the assistive device, and were scored on a scale from 1 (not satisfied at all) to 5 (very satisfied). The question related to the durability was left out of the investigation, because the use period was too short to rate this aspect.

	Age	Gender	Dominant hand	Exo	SCI level		
					AIS	Motor	Sensory
P1	39	M	Right	Right	B	C5	C6
P2	26	M	Right	Right	A	C5	C4
P3	39	F	Right	Left	A	C6	n/a

Table 7.1 – Baseline characteristics of participants. SCI: Spinal Cord Injury; AIS: American Spinal Injury Association Impairment Scale; M: male; Motor: motor level of injury; Sensory: sensory level of injury; F: female; C[1-7]: cervical vertebra that defines the level of injury.

	Maximum pinch force (N)		Sustained pinch force (N)	
	No exo Mean (SD)	With exo Mean (SD)	No exo* Mean (SD)	With exo Mean (SD)
P1	0.0 (0.0)	7.2 (0.5)	-	6.5 (0.5)
P2	0.7 (0.5)	7.8 (0.0)	-	6.5 (0.5)
P3	0.0 (0.0)	1.3 (0.5)	-	1.3 (0.5)

*Table 7.2 – Average maximum and sustained pinch grip strength measured without and with the exoskeleton across three measurements. Sustained pinch force is the mean pinch force over last 60% of 10s pinch force measurement. * Participants were unable to reach the threshold (1N) that triggered the start of the sustained force measurement with the E-Link pinchmeter. SD: standard deviation.*

7.3.4. Pinch force

The results of the maximum and sustained pinch force measurements are reported in Table 7.2. For all participants, the maximum pinch force measurement with exoskeleton was higher than without exoskeleton. For participant P3, the maximum pinch force measurement with exoskeleton was much lower than for the other two participants. All three participants were unable to reach a threshold of 1N that triggered the start of the sustained pinch force measurement with the E-Link Pinchmeter software. Still, it can be concluded that the sustained pinch force with exoskeleton was higher than without exoskeleton.

7.3.5. Grasp and Release Test

The Grasp and Release Test (see Fig. 7.8) was conducted to observe the difference in ability of participants to grasp and release standardized objects with and without the thumb exoskeleton. The mean number of successful completions across three trials (Nsuccess, see also Fig. 7.8) show that all participants were able to successfully grasp the pegs without exoskeleton. For two participants, the mean number of successful peg sequence completions was lower when the exoskeleton was used. None of the participants were able to successfully grasp the fork and weight without exoskeleton. In contrast, all participants were able to grasp the fork and weight with exoskeleton.

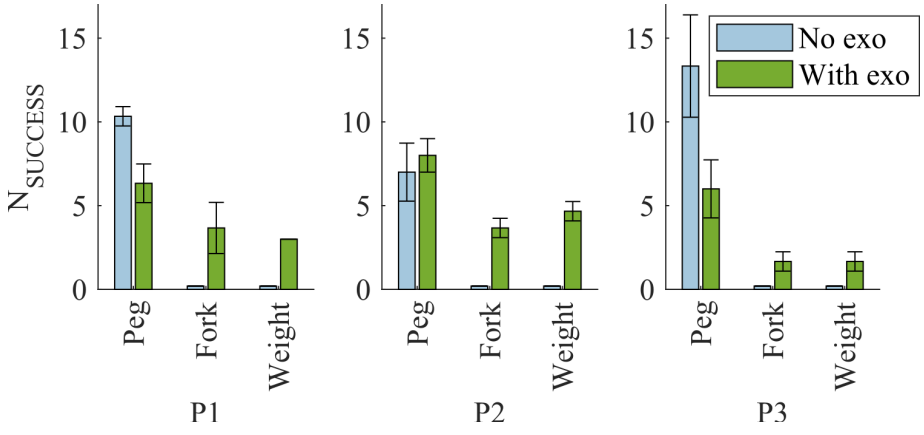

Fig. 7.8 - The results of the Grasp and Release Test for each participant and object showing the mean number of successful completions (Nsuccess) in 30 seconds across three trials without and in with the exoskeleton.

7.3.6. User satisfaction

To evaluate user satisfaction, the Quebec User Evaluation of Satisfaction with assistive Technology (QUEST), was conducted after the measurements. In Table 7.3 the questions and scores are reported per participant. Also a mean score per aspect was calculated. The results from the questionnaire reported a high level of satisfaction (range 3.7-4.3). Users are most satisfied with the safety (4.3) and effectiveness (4.3) of the device. Comfort was rated lowest (3.7). According to the participants, the most important aspects were weight, and effectiveness, followed by ease of use and comfort.

How satisfied are you,	P1	P2	P3	Mean score
1. With the dimensions (size, height, lengths, width) of your assistive device?	5	3	4	4
2. With the weight of your assistive device?	5*	3*	4	4
3. With the ease in adjusting (fixing, fastening) the parts of your assistive device?	5	4	3	4
4. How safe and secure your assistive device is?	5	4	4	4.3
5. How easy it is to use your assistive device?	5*	4	3	4
6. How comfortable your assistive device is?	5	3*	3	3.7
7. How effective your assistive device is (the degree to which your device meets your needs)?	5*	4*	4	4.3

*Table 7.3 – User satisfaction results from QUEST questionnaire. 1: not satisfied at all; 2: not very satisfied; 3: more or less satisfied; 4: quite satisfied; 5: very satisfied; * = most important aspects of an assistive device according to user.*

7.4. Discussion

Supporting the impaired hand function of SCI patients with a robotic exoskeleton can highly impact their self-management, and ultimately their quality of life. In this study, the design of a new, lightweight thumb exoskeleton, T-GRIP, was presented that supports the lateral pinch grasp. The mechanism consists of a force transmission mechanism that moved the thumb towards the side of the index finger. The exoskeleton focuses on enabling the core functionality required to regain basic functional performance.

Experimental results from an evaluation with three SCI patients showed that the pinch force improved when using the exoskeleton. Also, their ability to successfully grasp and manipulate objects of different sizes and weights was improved. The low weight (50g) of the hand-mounted part is another advantage of the device. The average weight of comparable hand exoskeletons found in literature is approximately 200g [9]. The evaluation revealed a high degree of satisfaction with the device. Although these conclusions are based on only three participants, the results still provide valuable insights and suggestions for improvements such as increasing the speed and personalize the fitting. A clinical study with more participants should be performed to further investigate the functionality and usability of the system.

Limitations of the study were a sub-optimal fitting procedure and a limited number of participants. A peak pinch force of more than 7N was measured for two participants. For participant P3, the measured force was much lower 1.3N. This may have been caused by the small hands of this patient. For participant P3, the fitting procedure might have been not optimal, leading to incomplete flexion of the thumb and therefore insufficient pinch force. This emphasizes that it is essential to personalize the thumb exoskeleton based on more parameters besides the lever arm ratio, for example the position of the mechanism with respect to the hand (l_{PX}, l_{PY}, l_{PZ}), the position of the actuator (l_{FX}, l_{FY}), or lever arm parameters (l_A, l_P, β), see Fig. 7.9. The order of the test execution was not randomized due to the small sample size. Potential fatigue could have biased the results. However, as the evaluation with the exoskeleton was always performed after the evaluation without exoskeleton, it is unlikely that the results were positively biased towards the exoskeleton. The additional bracket that may be used to help maintaining a flexed index finger also provides support of the index finger in medio-lateral direction. Not using a bracket thus could have affected the maximum grip force of the two participants that did not use the bracket, as the pinch force will be lower if the index finger is pushed medially by the thumb. Future work should include a larger and more diverse sample size to provide more conclusive results about the potential benefit of the T-GRIP exoskeleton.

Even with weak motor function, grasping and manipulation of lightweight objects is often still possible for SCI patients by utilization of the natural tenodesis effect [17]. In fact, the addition of the thumb exoskeleton decreased the performance for two participants during the peg object of the Grasp and Release Test, as the speed of the linear actuator (max. no-load speed of 10mm/s limited the speed of the test execution. For heavier objects such as the fork and weight during the Grasp and Release Test, the thumb exoskeleton improved the performance. In a future study the limiting effect of the actuator speed will be investigated.

Of all device aspects, comfort was rated lowest (3.7 out of 5) by the three participants. Improvements that could increase the comfort are to use padding between the hand bracket and the skin, and to further personalize the fitting procedure.

All three participants were able to easily control the thumb exoskeleton through contralateral wrist rotation after a 3-minute training period. This indicates that the used control strategy is intuitive. However, the strategy decreases the employability of their contralateral hand during bimanual tasks or trunk stabilization. For users with low residual hand function, or during unilateral tasks, this might not be a problem, but in other cases this is not desired. In the future, we will explore alternative control strategies such as voice control to bypass this problem. Also, it would be interesting to add a feedback modality, but this may be complicated due to a decreased sensitivity of the fingers.

Appendix 7.1

A kinematic model of the thumb and the exoskeleton was derived to calculate the pinch force (Fp) and the thumb angles (θe and θa) for any mechanism configuration. In Fig. 7.9, all relevant model parameters are shown. The closed-form expression of Fp was found from the moment equilibrium of forces Fa and Fp acting around point P:

$$F_p = F_a \frac{l_1}{l_2} \cos(\gamma - \alpha) \cos(\beta) \tag{7.1}$$

Actuator and pivot (α and γ) angles were numerically solved (using MATLAB's routine *fsolve*) by minimizing sum of the squared function values of the system of equations S_1:

$$S_1(\alpha, \gamma) = \begin{cases} -l_{fx} + (l_{act} + l_s)\cos(\alpha) - \left(l_p \cos(\gamma) - l_1 \sin(\gamma) - l_a \cos(\gamma)\right) = 0 \\ l_{fy} + (l_{act} + l_s)\sin(\alpha) - \left(l_p \sin(\gamma) + l_1 \cos(\gamma) - l_a \sin(\gamma)\right) = 0 \end{cases} \tag{7.2}$$

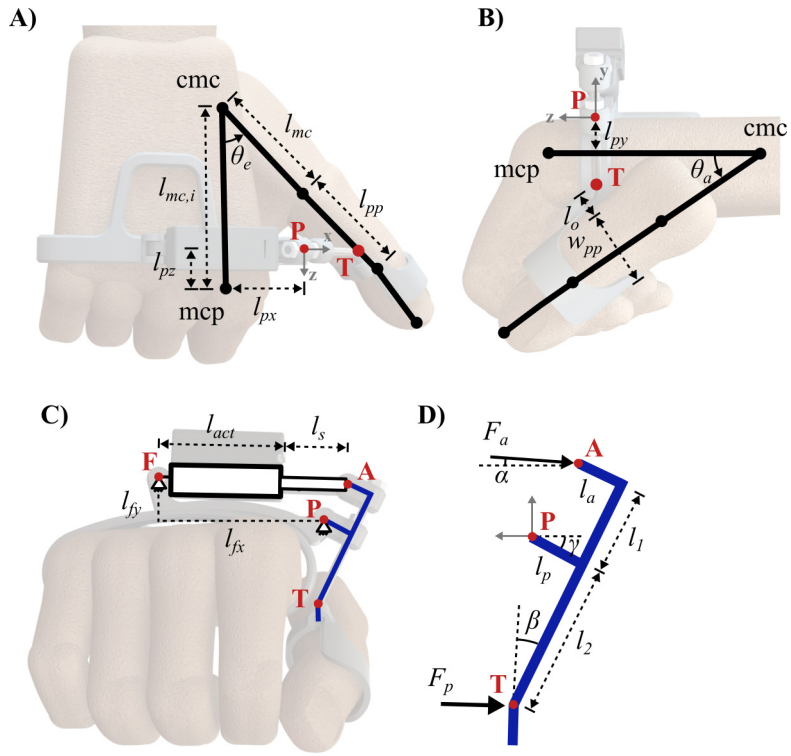

Fig. 7.9 - A) Top view of the hand with the thumb extended by angle θe. B) Side view of the hand with the thumb in flexed position, and abducted by angle θa. C) Front view of the hand with the actuator fully extended such that the lever arm (blue) flexed the thumb. The actuator (length lact and stroke ls) is suspended at a distance (lfx, lfy from pivot point P. D) Close-up of the lever arm. Actuator force (Fa) causes the lever arm to rotate around the pivot point (P), resulting in a force (Fp) at the distal point of the lever arm (T).

The thumb angles (θe and θa) were numerically solved (using MATLAB's routine *fsolve*) by minimizing sum of the squared function values of the system of equations S_2:

$$S_2(\theta_a, \theta_e) = \begin{cases} T_x - \left(l_p \cos(\gamma) + l_2 \sin(\gamma)\right) \\ T_y - \left(l_p \sin(\gamma) - l_2 \cos(\gamma)\right) \end{cases} \tag{7.3}$$

Here, T is the interface point between mechanism and thumb:

$$T = R_x(\theta_a) R_y(\theta_e) \begin{bmatrix} -\left(\frac{w_{pp}}{2} + l_0\right) \\ 0 \\ l_{mc} + r l_{pp} \end{bmatrix} + \begin{bmatrix} -l_{px} \\ -l_{py} \\ l_{pz} - l_{mc,i} \end{bmatrix} \tag{7.4}$$

R_x and R_y are the basic 3D rotation matrices around the x- and y-axis, w_{PP} is the thumb proximal phalanx width, l_0 is an offset from the skin, l_{MC} and l_{PP} are the metacarpal and proximal phalanx thumb lengths, and r is a fraction. l_{PX}, l_{PY}, l_{PZ} are the MCP joint coordinates relative to P, and $l_{MC,I}$ is the index finger metacarpal bone length.

References

[1] J. H. Nijendijk, M. W. Post, and F. W. Van Asbeck, “Epidemiology of traumatic spinal cord injuries in the Netherlands in 2010,” Spinal Cord, vol. 52, no. 4, pp. 258–263, 2014.

[2] B. B. Lee, R. A. Cripps, M. Fitzharris, and P. C. Wing, “The global map for traumatic spinal cord injury epidemiology: Update 2011, global incidence rate,” Spinal Cord, vol. 52, no. 2, pp. 110–116, 2014.

[3] R. Osterthun, M. W. Post, and F. W. Van Asbeck, “Characteristics, length of stay and functional outcome of patients with spinal cord injury in Dutch and Flemish rehabilitation centres,” Spinal Cord, vol. 47, no. 4, pp. 339–344, 2009.

[4] G. J. Snoek, M. J. Ijzerman, H. J. Hermens, D. Maxwell, and F. Biering-Sorensen, “Survey of the needs of patients with spinal cord injury: Impact and priority for improvement in hand function in tetraplegics,” Spinal Cord, vol. 42, no. 9, pp. 526–532, 2004.

[5] T. B¨utzer, O. Lambercy, J. Arata, and R. Gassert, “Fully Wearable Actuated Soft Exoskeleton for Grasping Assistance in Everyday Activities,” Soft Robotics, vol. 8, no. 2, pp. 128–143, 2021.

[6] L. Randazzo, I. Iturrate, S. Perdikis, and J. D. Mill´an, “Mano: A Wearable Hand Exoskeleton for Activities of Daily Living and Neurorehabilitation,” IEEE Robotics and Automation Letters, vol. 3, no. 1, pp. 500–507, 2018.

[7] Y. Yun, S. Dancausse, P. Esmatloo, A. Serrato, C. A. Merring, and P. Agarwal, “Maestro: An EMG-driven assistive hand exoskeleton for spinal cord injury patients,” Proceedings - IEEE International Conference on Robotics and Automation, pp. 2904–2910, 2017.

[8] H. In and K.-j. Cho, “Exo-Glove : Soft wearable robot for the hand using soft tendon routing system,” IEEE Robotics & Automation, vol. 22, no. March 2015, pp. 97–105, 2015.

[9] T. du Plessis, K. Djouani, and C. Oosthuizen, “A review of active hand exoskeletons for rehabilitation and assistance,” Robotics, vol. 10, no. 1, 2021.

[10] J. A. Dunn, K. A. Sinnott, A. G. Rothwell, K. D. Mohammed, and J. W. Simcock, “Tendon transfer surgery for people with tetraplegia: An overview,” Archives of Physical Medicine and Rehabilitation, vol. 97, no. 6, pp. S75–S80, 2016.

[11] N. van Zyl, B. Hill, C. Cooper, J. Hahn, and M. P. Galea, “Expanding traditional tendon-based techniques with nerve transfers for the restoration of upper limb function in tetraplegia: a prospective case series,” The Lancet, vol. 394, no. 10198, pp. 565–575, 2019.

[12] J. P. Wagner, C. M. Curtin, D. R. Gater, and K. C. Chung, “Perceptions of People With Tetraplegia Regarding Surgery to Improve Upper-Extremity Function,” Journal of Hand Surgery, vol. 32, no. 4, pp. 483–490, 2007.

[13] J. H. House, “Reconstruction of the thumb in tetraplegia following spinal cord injury,” Clinical Orthopaedics and Related Research, vol. 195, pp. 117–128, 1985.

[14] K. S. Wuolle, C. L. Van Doren, G. B. Thrope, M. W. Keith, and P. Peckham, "Development of a quantitative hand grasp and release test for patients with tetraplegia using a hand neuroprosthesis," The Journal of Hand Surgery, vol. 19, no. 2, pp. 209–218, 1994.
[15] L. A. Harvey, J. Batty, R. Jones, and J. Crosbie, "Hand function of C6 and C7 tetraplegics 1-16 years following injury," Spinal Cord, vol. 39, no. 1, pp. 37–43, 2001.
[16] L. Demers, R. Weiss-Lambrou, and B. Ska, "Development of the Quebec User Evaluation of Satisfaction with assistive Technology (QUEST)." Assistive technology, vol. 8, no. 1, pp. 3–13, 1996.
[17] L. Harvey, "Principles of conservative management for a non-orthotic tenodesis grip in tetraplegics," Journal of Hand Therapy, vol. 9, no. 3, pp. 238–242, 1996.

8. General discussion

Many daily activities, such as reading hard-copy of this thesis, require the use of one's arms and hands: First the arm must reach to the thesis on the shelf. Then, the hand must be opened sufficiently to encompass the object, followed by a suitable grasping pattern of the fingers and adequate forces to grasp the book, while stabilizing the arm. Finally the thesis must be lifted and placed in front of the body, in order to read it. If one does not suffer from any upper extremity motor impairments, then all steps above can be performed without much effort. However, motor impairments of the shoulder and/or hand can largely affect the execution of daily activities and restrict participation of the person in society. Assistive devices aimed at reducing impairments can reduce disability and improve the quality of life of its users.

The main contribution of this thesis was the development and evaluation of novel assistive devices that support patients with impaired shoulders or hands. The research focused on improving the state of the art, by exploring alternative mechanical design strategies that can provide functional benefit to the patient by assisting them during daily activities. Three assistive devices were developed, one for the shoulder (Chapters 2-5) and two for the hand (Chapters 6 and 7). In this discussion we look back on our achievements. Furthermore, we expanded the toolkit of orthotists therapists with two new methods to improve orthosis alignment and to objectively assess orthosis wear time. We will discuss the potential of these procedures for enhancing treatment personalization. Each section is accompanied with some directions for future research. Finally a short conclusion is presented.

8.1. Improving the state of the art

The extent to which assistive devices aid in reducing disability largely depends on their perceived benefit. To be adopted by patients, assistive devices should not only reduce body impairments, but also ease daily activities and promote participation in society by removing performance barriers. Both the health condition and contextual factors (Fig 1.2) influence the degree of disability and should be taken into account during assistive device selection. However, suitable technology that matches the users' characteristics and needs does not always exist. In previous research, researchers often tend to focus on the development one or more technological (e.g. mechanical) aspects without considering the context in which the device will be used, as well as critical user requirements. Devices that originate from this approach, therefore often lack the subtleties that are required when designing assistive devices that are worn by their users during prolonged periods of time. Several gaps were identified in the current state of the art of assistive devices for the upper extremity (Chapter 1), mostly concerning aspects such as effectiveness, reliability and comfort. For example, a shoulder orthosis should not limit the remaining range of motion of patients with residual arm function, and hand orthoses should be lightweight, comfortable and should allow for independent donning an doffing without help from caregivers, while providing a sufficient degree of functionality to support daily activities. Our work differs from existing research as we specifically targeted problems that require technological advancements, but kept track of core user needs.

Requirements were gathered by means of interviews, questionnaires, observations made during the use of competitive devices, and literature searches. The feasibility of the developed prototypes were repeatedly evaluated throughout the design process with different stakeholders, by showing the design iterations and gathering feedback about the performance and the satisfaction with the proposed devices during use. In our effort to improve the state of the art, we explored the use of (passive) spring-based, and (active) underactuated approaches to support the impaired shoulder and hand.

8.1.1. Shoulder orthosis

The main objective of the shoulder orthosis was to support the impaired shoulder to decrease shoulder pain without limiting the user's functional arm movements. In this way secondary symptoms such as muscle atrophy and increased joint stiffness resulting from non-use can be prevented. Existing orthoses typically use non-elastic bands to support the arm. This static design (i.e. the arm is kept in a fixed position) creates significant restrictions during the execution of daily tasks. We therefore decided to focus on the development of a dynamic design (i.e. the arm can freely move). Additionally, a passive system consisting of elastic materials to store and release energy was preferred over an active system, due to its simplicity and cost-effectiveness. The amount of energy required to support the arm is easily stored in passive springs. Active systems would require the use of many (heavy, complex or expensive) components to store and release the energy which will potentially limit the wearability and comfort of the solution.

Our dynamic orthosis is based on a passive spring-balancing system that does not restrict the functional range of motion of the user. The shoulder orthosis features two elastic bands, located anteriorly and posteriorly of the shoulder, that are arranged in a special configuration between the shoulder and upper arm to create a spring-to-spring balancer. In Chapter 2 the conceptual design of this orthosis was presented. The first prototype included an aluminum bracket to suspend the elastic bands proximally (Fig. 8.1A). The elastic bands were distally attached to an upper arm cuff that was held in place by friction between the silicone liner material and the human skin. The magnitude of the supporting force can be adapted by

Fig. 8.1 – Evolution of the prototypes of the shoulder orthosis. A) First prototype that was used during the pilot evaluation (Chapter 2). B) Improved prototype that was used during the clinical trial (Chapter 5).

changing the tension of the elastic bands. The prototype was evaluated in a pilot study with two patients, assessing, among others, the glenohumeral stability, restriction during movement, and comfort. Promising results were reported regarding stability and unrestricted movement, which encouraged us to continue with our investigation. However, both users reported high pressures on the shoulder arc due to the rigid aluminum construction. Also, one participant mentioned discomfort due to the rigid parts pressing on the spine during seating. To improve comfort, the aluminum construction was replaced with a wire-frame construction that was positioned laterally on the torso to prevent interference with the body and the environment (e.g. back rest of a chair), see Fig. 8.1B. The wire-frame can be easily modified to follow the contours of the human body. The aluminum construction on the shoulder arc was replaced by a padded liner to further increase the level of comfort. Perspiration and warmth, caused by the silicone liner material of the arm cuff, were issues frequently mentioned by shoulder orthosis users in a previous study [1]. Therefore, the upper arm cuff of the first prototype was substituted by an arm cuff made of fabric that locks itself around the forearm due to its conical shape. The improvements made to the construction and arm cuff reduced the total weight of the original prototype from 650g to a weight of 274g for the improved prototype.

The clinical effects of the improved shoulder orthosis were then assessed in a clinical trial (Chapter 5) with 10 patients who suffered from chronic shoulder pain. After two weeks of use, participants were most satisfied with the weight of the device, the safety, the ease in adjusting and the effectiveness. The improved prototype was well-tolerated by the patients who participated in the clinical trial. The results provide strong evidence that the shoulder orthosis is capable of supporting the impaired shoulder to decrease this shoulder pain. As none of the participants in our study suffered from glenohumeral subluxation we concluded in Chapter 5 that a reduction of the stress on the glenohumeral structures was primarily responsible for this achievement, not the restoration of joint alignment.

Similar designs have less functionality. For example the Omo Neurexa (Otto Bock, Germany) and Neuro-lux II (Sporlastic, Germany) limit the existing range of motion due to the use of non-elastic straps, while the GivMohr sling requires elbow extension to create an upward force to support the shoulder, which limits the use of the arm during functional tasks. In Chapter 5 we showed that our orthosis did not affect the remaining range of motion. Users felt less restricted by the dynamic orthosis during their daily activities compared to other, previously worn orthoses, which can potentially break the vicious cycle of shoulder pain, non-use and muscle atrophy. The weight (~250g) and physical appearance of our design was comparable or better to other devices (ranging from 250g to 900g), but provides an additional benefit as the level of supporting force provided to the arm can be controlled more precisely by changing the tension of the elastic bands. As the duration of our clinical trial was only two weeks, the clinical effects of the orthosis should be further explored in an extended study.

Based on the results of the clinical study we conclude that the newly developed dynamic shoulder orthosis has a higher degree of functionality while providing a comparable or higher degree of effectiveness than existing shoulder orthoses.

8.1.2. Hand exoskeletons

By focusing on core user needs we aimed to improve the state of the art of assistive hand exoskeletons. Two uses cases were defined at the start of this project for which the state of the art could be improved:

(1) Hand opening may be compromised if patients do not have sufficient muscle strength to overcome the effects of increased muscle tone of the finger flexors. The objective of the hand orthosis presented in Chapter 6 was to support finger extension of stroke patients.
(2) Performing grasping tasks is complicated if patients do not have sufficient muscle strength to grasp objects. The objective of the hand orthosis presented in Chapter 7 was to support spinal cord injury patients with grasping during daily activities.

The first prototype of a hand exoskeleton to support hand opening (Fig. 8.2A) explored the idea of using negative stiffness springs to compensate for the increased finger joint stiffness without the need for external actuators and sensors [2]. With this particular spring arrangement, we aimed to improve the commercially available spring-based extension devices that typically require large voluntary flexion torques in order to grasp objects. The pilot feasibility study seemed promising, as the system was able to increase the range of motion. However, the resulting mechanical design was considered too heavy to be useful during daily activities. Also, the digit caps blocked fingertip sensation during object grasping and the stiffness tuning was considered too impractical. Therefore, we decided to focus on alternative mechanical designs to support hand opening of severely affected stroke patients. Multiple prototype iterations have resulted in the hand exoskeleton shown in Fig. 8.2B. Compared to existing devices such as developed by [3] and [4], the mechanical design was reduced significantly in terms of size and weight (105g, instead of >350g of competitive devices). This was mainly due to the remote actuation strategy that reduces the need for actuators to be mounted close to the hand. Also, we decided to actuate only the index (and middle) finger, while stabilizing the thumb in an opposed position. The state of the art features many gloves, either cable-driven or pneumatically actuated [5-7]. These gloves are difficult to don and doff for patients with a clenched fist. In an attempt to further improve the state of the art, we chose to stay away from glove-like designs and split the donning procedure in two steps. First, the connectors are attached to the thumb and index finger with medical

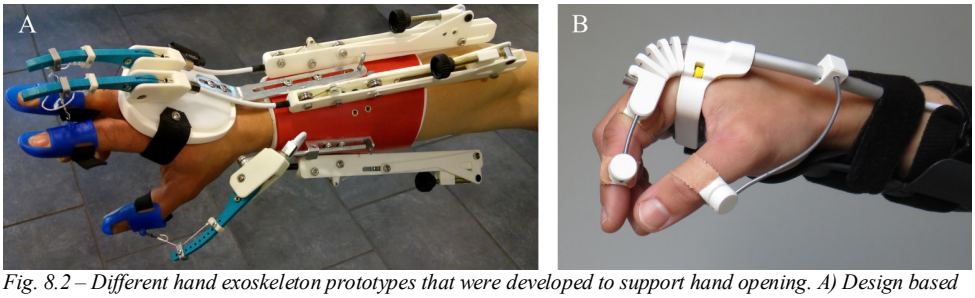

Fig. 8.2 – Different hand exoskeleton prototypes that were developed to support hand opening. A) Design based on a negative stiffness mechanism, to passively compensate joint stiffness of the thumb, index and middle finger [2]. B) Mechanical design of the hand orthosis to support extension of the index finger (Chapter 6).

adhesive tape after which the device is magnetically fastened to the connectors from the lateral side. A technical characterization of the system showed that the device can compensate for large joint stiffness associated with severely affected stroke patients. A feasibility study with four stroke patients revealed that the exoskeleton was able to increase the range of motion of the MCP joint of the index finger.

The results of Chapter 6 prove that our novel mechanical design has the potential to support hand opening of patients with high finger joint stiffness values. However, the usability evaluation was not extensive. We recommend to increase the sample size in a future evaluation, and focus more on usability aspects such as one-handed donning and doffing. During the development process, parts were designed to support easy customization of the exoskeleton. By simply changing the number of flexible segments and the size of the hand splint, the mechanism can be easily fitted to different hand sizes. The resulting mechanical design is able to withstand high forces, but was only tested for a relatively short period. Its suitability for everyday use needs yet to be explored.
The aim of Chapter 7 was to develop an assistive device that supports grasping of bimanually

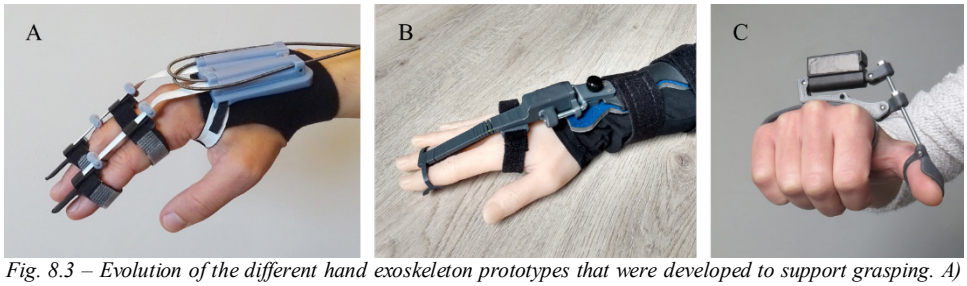

Fig. 8.3 – Evolution of the different hand exoskeleton prototypes that were developed to support grasping. A) Underactuated mechanism based on the actuation of curved leaf springs [10]. B) Underactuated mechanism* in which the index and middle finger are simultaneously flexed by pushing a leaf spring outwards with the linear actuator mounted on the dorsal side of the hand. C) T-GRIP exoskeleton (Chapter 7) to actuate the lateral pinch grasp. (* prototype does not include thumb stabilization.)*

affected patients (e.g. spinal cord injury patients). The combination of task, object and hand constraints often cause a particular grasping task to be impossible for these patients. A small increase in hand function may already represent a clinically meaningful change in performance as the assistive device can allow particular grasps to be feasible.

During the initial generation of conceptual designs to support the hand during grasping, we focused on actuating multiple fingers, while stabilizing the thumb in an opposed position. This design approach is commonly used in other exoskeletons. Conveying large forces to the fingertip to provide sufficient output force is possible with underactuated mechanisms that span multiple joints. Although the resulting designs were slim (Fig. 8.3A and 8.3B), the underactuated nature of these mechanisms may result in unpredictable behavior, especially when attached to the impaired hand. In our effort to develop a lightweight yet effective device that enables users to perform basic activities of daily living, we therefore decided to invert the role of the thumb and fingers during object grasping. Instead of actuating the fingers, we decided to actuate the thumb while keeping the fingers stable. This way, the complexity of the hardware can be reduced significantly. The resulting exoskeleton presented in Chapter 7

(see also Fig. 8.3C) supports the impaired hand by restoring the lateral pinch grip such that objects of different size and weight can be successfully grasped. In lateral pinch, the object is clamped between the thumb and the side of the index finger. This grasp is considered the most useful grasp to be restored [8]. Our design approach has resulted in a lightweight device of only 50g. Comparable exoskeletons that support grasping weigh approximately 200g [9]. Compared to commercial cable driven systems such as NeoMano (Neofect, South Korea) and Carbonhand (BioServo, Sweden), the mechanical structure of our hand exoskeleton guides the forces to the desired location without affecting safety. Compared to the RELab tenoexo, our minimalistic approach resulted in reduced hardware complexity. Still, the lateral pinch grip allowed for sufficient functionality such that objects of different weight and size could be grasped. Both the patients and involved clinicians were highly satisfied by the added functionality provided by the device during manipulation tasks. The results from the pilot study with three spinal cord injury patients (Chapter 7) showed that patients were able to provide pinch forces up to 7N, and objects of different size and weight could be successfully manipulated. The suitability of this technology for other target populations, such as for patients with unimanual impairments, remain yet to be investigated.

8.1.3. Directions for future research

Performance in daily life – All three assistive devices presented in this thesis were tested by patients suffering from various conditions. The clinical trial of the shoulder orthosis was the most extensive investigation, including unsupervised use at home for a duration of two weeks. A next step would be to investigate the long-term effects of the orthosis on outcome measures such as shoulder pain and shoulder function in an extended clinical trial. Both hand orthoses were only tested in a controlled environment during one session that lasted for approximately one hour. The tasks performed during this short evaluation included grasping of standardized objects. Although the results of these evaluations provided insight in the potential benefit of the developed hand exoskeletons, the actual performance of patients when using the device in an unsupervised setting remains to be investigated. Therefore, additional clinical evaluations are required.

Sample size – A total of 12 patients were included during the evaluations of the shoulder orthosis and 7 patients evaluated the hand exoskeletons. The small sample size caused the statistical power of these studies to be low. In future trials, the number of participants should therefore be increased.

Target population – Inclusion criteria of the patients that participated evaluations were deliberately kept broad during these initial evaluations. This allowed us to investigate the feasibility of the technology in a broad group of patients and identify potentially limiting contextual factors and health conditions for the application of the assistive device. For example, we found that the shoulder orthosis reduced shoulder pain, even in patients with no objectively established subluxation. Future work should investigate whether application of the orthosis to support the shoulders of patients with (large) subluxations will lead to a further reduction of shoulder pain and improvement in arm function. Spinal cord injury patients with limited wrist extension capabilities that used the thumb exoskeleton may require a static wrist splint, whereas other participants required stabilization of the index finger during lateral

pinch grasp. The thumb exoskeleton was only evaluated in a select group of spinal cord injury patients. Bimanually affected patients would require little improvement in hand function to gain a significant improvement in performance. On the other hand, patients with a unimanual impairment (e.g. stroke patients) will only use their affected hand during bimanual tasks to stabilize objects. As the lateral pinch grasp is very different from their normal grasping strategy (e.g. cylindrical grasp), the added benefit of the device for other target populations remains to be investigated. Future clinical investigations should take these findings into account.

Control strategies – Although Chapter 7 and 8 were (primarily) devoted to advancing the mechanical design of the state of the art, we acknowledge that intuitive control plays a significant role in the usage of assistive devices. Due to individual characteristics and preferences a modular approach should be pursued such that different control strategies could be easily deployed in a particular device. Future investigations should focus on the implementation and personalization of different control strategies.

8.2. Treatment personalization

As every patient is unique, treatments involving assistive devices should be tailored to each individual as much as possible. This includes personalization of the assistive device itself including the fitting procedure. Our design approach resulted in modular systems with easily customized parts that allow for simple customization of the orthosis' shape and dimensions, to fit a wide variety of patients. Besides personalization of the assistive device, the treatment plan should be optimized to match the user's needs as well. Effectiveness and comfort are among the major factors contributing to satisfaction of patients with assistive technology, as explained before. As an example, the shoulder orthosis developed in this thesis should be correctly aligned to the shoulder joint, to achieve its desired functionality. Also, misalignment of the orthosis can create undesired forces acting on the body that may contribute to discomfort. Improvement of the fitting procedure of this assistive device thus may improve the functionality and level of comfort. Additionally, gaining insight in device use may contribute to tailoring the treatment plan, as knowledge about the actual wear time could to help understand (the lack of) device efficacy. Reported numbers on the non-use of assistive technology are as high a one-third of all provided devices. Non-use may prevent an assistive device from mitigating the effects of disability, and may also result in wasted financial resources. In many cases, nonuse is caused by a lack of perceived benefit due to a mismatch between user expectations and technical features of the device. Personal and environmental factors play a big role in this. Revealing patterns of non-use could identify potential gaps in the user's knowledge, or could serve as feedback for medical professionals that are responsible for the delivery to improve their service.

The two methods developed in this thesis to assess the glenohumeral center of rotation (Chapter 3) and assess the wear time of upper extremity orthoses (Chapter 4) could be used to improve shoulder orthosis alignment and objectively determine the actual use by patients in an unsupervised setting. The center of rotation estimation method was not applied to the clinical trial of Chapter 5 due to a lack of time, but the wear time estimation method was

successfully deployed obtain the estimated wear time after two weeks of unsupervised use of the shoulder orthosis.

8.2.1. Directions for future research

Transfer to other joints – Currently available methods to estimate the glenohumeral center of rotation and the orthosis wear time are far below the desired degree of usability and therefore not (often) adopted in clinical practice. There is reason to believe that our proposed methods have significant advantages over other systems based on the results presented in Chapters 3 and 4. Both tools currently focus on a limited use-case, i.e. the shoulder. However, many use cases could potentially benefit from our technology, as orthosis misalignment is a common problem resulting in discomfort and undesired forces acting on the body [11-13]. Also, wear time assessment of other types of orthoses such as spinal correction braces, orthopedic footwear, hand splints, etc. may be beneficial. To this end, the tools developed in this thesis must be transferred to other body parts.

Transfer from lab to clinic – In Chapter 5 we assessed the ability to objectively assess the wear times of a shoulder orthosis during a clinical study. However, the developed methods can not only help researchers, but can also help medical professionals in a clinical setting, to gain more insight in the usage of the devices that they provide to patients. A next step would thus be to transfer the methodology to the clinical practice. Similar remarks can be made for the shoulder orthosis alignment procedure. We recommend to implement and test this method with patients. Potential issues concerning the applicability of the proposed method may be encountered if the humeral head is not aligned with the glenoid due to an inferior shift in patients with glenohumeral subluxation. This means that the apparent center of rotation of the shoulder joint is different from the true center of rotation (resembling 'healthy' shoulder motion). The method presented in Chapter 3 can only estimate the apparent center of rotation. Without knowing the degree of subluxation, the true center of rotation can thus not be determined. In case of large subluxations, the proposed method may therefore not suffice. In other cases it might be safe to assume that the humeral head is located a few millimeters superiorly from the apparent center of rotation. Another option might be to passively support the arm with help from a second person such that joint alignment is temporary restored during the assessment.

Additional analyses – From the ICF model of disability (Fig 1.2) can be seen that contextual factors contribute to disability, for instance personal factors such as cognitive abilities and motivation, but also environmental factors such as domestic situation. However, these same contextual factors may also affect a patient's decision to use certain assistive devices in a particular situation. So far, we used the technology from Chapter 4 solely to assess the wear time, but the available data permits more analyses to be done. For example patterns of (non)use may be identified based on the logged data which can help to further personalize treatment plans.

8.3. Conclusion

The goal of this thesis was to develop and evaluate novel assistive devices that support patients with impaired shoulders or hands. Existing technologies often do not meet basic user

requirements regarding effectiveness and comfort, leading to high rejection rates of these assistive devices. We investigated which essential degrees of freedom should be represented in the device to improve the user's performance during daily activities. By exploring underactuated and modular design approaches, we were able to develop effective, comfortable and easy to use devices that advance the state of the art. We developed and evaluated three assistive devices, one to reduce disability caused by impaired shoulder function and two to reduce disability caused by impaired hand function by following a user-centered design approach. The shoulder orthosis reduced shoulder pain after two weeks of unsupervised used while it did not impede remaining arm movement. The hand exoskeleton improved the hand opening of stroke patients with increased flexor muscle tone. Also, spinal cord injury patients were able to restore basic grasping function by using the hand exoskeleton. Besides these advancements in hardware, two methods were developed to assist with the personalization of assistive devices. The first method includes a procedure to determine the center of rotation of the glenohumeral joint. This can improve the alignment of shoulder orthoses which may improve functionality and comfort. Secondly, a procedure was established to objectively assess the wear time of upper limb orthoses. With this information therapists can tailor a treatment plan and could to help understand (the lack of) device efficacy. In this thesis it was demonstrated that the developed assistive devices were effective in mitigating the effects of disability and succeeded in improving the current state of the art. Future studies have to further explore the added value of the technologies in clinical trials.

References

[1] Verloop, W. R. G., Haarman, C. J. W., van Vliet, R. O., de Koning, J. L., & Rietman, J. S. (2021). A newly designed shoulder orthosis for patients with glenohumeral subluxation: a clinical evaluation study. Prosthetics & Orthotics International, 45(4), 322–327.

[2] Haarman, C. J. W., Hekman, E. E. G., Prange, G.B., & van der Kooij, H. (2018). Joint Stiffness Compensation for Application in the EXTEND Hand Orthosis. 2018 7th IEEE International Conference on Biomedical Robotics and Biomechatronics (Biorob), 2018-Augus, 677–682.

[3] Conti, R., Meli, E., & Ridolfi, A. (2016). A novel kinematic architecture for portable hand exoskeletons. Mechatronics, 35, 192–207.

[4] Li, M., He, B., Liang, Z., Zhao, C. G., Chen, J., Zhuo, Y., … Althoefer, K. (2019). An attention-controlled hand exoskeleton for the rehabilitation of finger extension and flexion using a rigid-soft combined mechanism. Frontiers in Neurorobotics, 13(May), 1–13.

[5] In, H., Lee, H., Jeong, U., Kang, B. B., & Cho, K. (2015). Feasibility study of a slack enabling actuator for actuating tendon-driven soft wearable robot without pretension. Icra, 1229–1234.

[6] Popov, D., Gaponov, I., & Ryu, J. (2017). Portable Exoskeleton Glove With Soft Structure for Hand Assistance in Activities of Daily Living. IEEE/ASME Transactions on Mechatronics, 22(2), 865–875.

[7] Yurkewich, A., Kozak, I. J., Hebert, D., Wang, R. H., & Mihailidis, A. (2020). Hand Extension Robot Orthosis (HERO) Grip Glove: Enabling independence amongst persons with severe hand impairments after stroke. Journal of NeuroEngineering and Rehabilitation, 17(1), 1–17.

[8] House, J. H. (1985). Reconstruction of the thumb in tetraplegia following spinal cord injury. Clinical Orthopaedics and Related Research, 195, 117–128.

[9] du Plessis, T., Djouani, K., & Oosthuizen, C. (2021). A review of active hand exoskeletons for rehabilitation and assistance. Robotics, 10(1).

[10] Haarman, C. J. W., Hekman, E. E. G., Rietman, H. S., & van der Kooij, H. (2019). Pushing the Limits: A Novel Tape Spring Pushing Mechanism to be Used in a Hand Orthosis. In Biosystems and Biorobotics (Vol. 22, pp. 475–479).

[11] Schiele, A., & Helm, F. C. T. Van Der. (2006). Kinematic Design to Improve Ergonomics in Human Machine Interaction. 14(4), 456–469.

[12] Zanotto, D., Akiyama, Y., Stegall, P., & Agrawal, S. K. (2015). Knee Joint Misalignment in Exoskeletons for the Lower Extremities: Effects on User's Gait. IEEE Transactions on Robotics, 31(4), 978–987.

[13] Bessler-Etten, J., Schaake, L., Prange-Lasonder, G. B., & Buurke, J. H. (2022). Assessing effects of exoskeleton misalignment on knee joint load during swing using an instrumented leg simulator. Journal of NeuroEngineering and Rehabilitation, 19(1), 13.

Summary

To be able to independently perform daily activities, it is important that humans can use their arms and hands to a sufficient extent. The positioning of the arm and the execution of grasping tasks play an essential role in this. Disability caused by impairments of arm and hand function can lead to activity limitations and participation restrictions. Assistive devices can contribute to reducing the effect of disability. However, these devices must meet users' expectations regarding effectiveness, reliability, durability, comfort and ease of use to reduce the risk of device abandonment. In this thesis we developed and evaluated three novel assistive devices that support patients with impaired shoulders or hands. During the design process we focused on restoring performance (i.e. on the activity and participation level) rather than restoring capacity (i.e. on the impairment level). Therefore, all device functionality that did not contribute to this goal was omitted from the design.

The shoulder plays an important role in positioning the arm. When the passive structures around the shoulder joint are continuously stretched, pain often occurs that prevents patients to actively engage their arm in daily activities. In **Chapter 2**, a dynamic shoulder orthosis has been developed with the aim of reducing the stress on the shoulder joint and thereby reducing pain without impeding the retaining range of motion of the shoulder. This orthosis works by statically balancing the arm with two elastic bands. In a clinical study with 10 patients (**Chapter 5**), the effects of the orthosis on shoulder pain and arm function were investigated after two weeks of use. The results show that the orthosis supports the shoulder and that patients can use the shoulder orthosis well during daily activities.

For an optimal functioning of the balancing principle of the shoulder orthosis, the orthosis must be aligned with the glenohumeral joint. There is currently no easy method to do this. Therefore, in **Chapter 3** a new method was developed to determine the center of rotation of the glenohumeral joint using only one camera and two printed markers. Experiments with a test bench have shown that the method is accurate. Experiments with 5 healthy subjects have shown that the method is reproducible.

An orthosis can only be effective if it is worn by the user. It is therefore important to determine the wearing time objectively. Subjective methods such as diaries or questionnaires are often used in the current clinical practice, but these frequently lead to an overestimation of the actual use. In **Chapter 4** an algorithm has been developed that provides an objective estimate of the wearing time of orthoses for the upper extremities using miniature temperature loggers. The algorithm was trained and validated with data from 15 healthy subjects who repeatedly put the temperature loggers on and off during a 24h period.

In order to perform grasping tasks, it is important that the hand can be opened far enough to grasp objects, and then sufficient force can be applied to stabilize or lift objects.

Hand opening may be compromised if patients do not have sufficient muscle strength to overcome the effects of contractures or hypertonia of the finger flexors. In these cases it may be necessary to support the hand opening with an assistive device. In **Chapter 6**, a hand exoskeleton has been developed that supports finger extension of stroke patients. The device

is controlled by a cable and can actively stretch the index and middle finger. The feasibility of the exoskeleton has been investigated in a pilot test with four stroke patients. Results show that the exoskeleton was able to improve finger extension of severely affected stroke patients.

Performing grasping tasks is also complicated if patients do not have sufficient muscle strength to grasp and lift objects. In **Chapter 7**, an active orthosis has been developed to support the hand function of spinal cord injury patients. The developed thumb orthosis is lightweight and supports the lateral grip (key grip) of the hand by means of a miniature linear actuator. A study with three spinal cord injury patients showed that the orthosis improved the grip force which enabled patients to regain basic hand function.

In conclusion, the work presented in this thesis showed the significant steps that were made in improving assistive devices to support shoulder and hand function during daily activities.

Samenvatting

Om dagelijkse activiteiten zelfstandig uit te kunnen voeren, is het van belang dat mensen hun armen en handen in voldoende mate kunnen gebruiken. De positionering van de arm en het uitvoeren van grijptaken spelen daarbij een essentiële rol. Aandoeningen aan de arm- en handfunctie kunnen leiden tot activiteits- en participatiebeperkingen. Hulpmiddelen kunnen bijdragen aan het verminderen van het effect van een handicap. Deze apparaten moeten echter voldoen aan de verwachtingen van gebruikers met betrekking tot effectiviteit, betrouwbaarheid, duurzaamheid, comfort en gebruiksgemak om het risico op het afstoten van hulpmiddelen te verminderen. In dit proefschrift hebben we drie nieuwe hulpmiddelen ontwikkeld en geëvalueerd die patiënten met aangedane schouder- of handfunctie ondersteunen. Tijdens het ontwerpproces hebben we ons gericht op het herstellen van prestaties (op het activiteiten- en participatieniveau) in plaats van op het herstellen van capaciteit (op het niveau van beperkingen). Daarom is alle functionaliteit die hier niet aan bijdraagt weggelaten uit het ontwerp.

De schouder speelt een belangrijke rol bij het positioneren van de arm. Wanneer de passieve structuren rond het schoudergewricht continu worden uitgerekt, treedt vaak pijn op waardoor patiënten hun arm niet actief kunnen betrekken bij dagelijkse activiteiten. In **hoofdstuk 2** is een dynamische schouderorthese ontwikkeld met als doel de belasting van het schoudergewricht te verminderen en daarmee pijn te reduceren zonder het bewegingsbereik van de schouder te belemmeren. Deze orthese werkt door de arm statisch te balanceren met behulp van twee elastische banden. In een klinische studie met 10 patiënten (**hoofdstuk 5**) werden de effecten van de orthese op schouderpijn en armfunctie onderzocht na twee weken gebruik. De resultaten laten zien dat de orthese de schouder ondersteunt en dat patiënten de schouderorthese goed kunnen gebruiken tijdens dagelijkse activiteiten.

Voor een optimale werking van het evenwichtsprincipe van de schouderorthese moet de orthese uitgelijnd zijn met het glenohumerale gewricht. Er bestaat momenteel geen simpele methode om dit te doen. Daarom is in **hoofdstuk 3** een nieuwe methode ontwikkeld om het rotatiecentrum van het glenohumerale gewricht te bepalen met slechts één camera en twee gedrukte markers. Experimenten met een proefopstelling hebben aangetoond dat de methode nauwkeurig is. Experimenten met 5 gezonde proefpersonen hebben aangetoond dat de methode reproduceerbaar is.

Een orthese kan alleen effectief zijn als deze door de gebruiker wordt gedragen. Het is daarom belangrijk om de draagtijd objectief vast te stellen. In de praktijk worden veelal subjectieve methoden zoals dagboeken of vragenlijsten gebruikt, maar deze leiden vaak tot een overschatting van het daadwerkelijke gebruik. In **hoofdstuk 4** is een algoritme ontwikkeld dat een objectieve schatting maakt van de draagtijd van orthesen voor de bovenste extremiteiten met behulp van miniatuur temperatuurloggers. Het algoritme is getraind en gevalideerd met gegevens van 15 gezonde proefpersonen die de temperatuurloggers gedurende een periode van 24 uur herhaaldelijk om- en af hebben gedaan.

Om grijptaken uit te voeren, is het belangrijk dat de hand ver genoeg kan worden geopend om objecten vast te pakken, en dat vervolgens voldoende kracht kan worden uitgeoefend om objecten te stabiliseren of op te tillen.

Het openen van de hand wordt bemoeilijkt als patiënten niet voldoende spierkracht hebben om de effecten van contracturen of hypertonie van de vingerflexoren te overwinnen. In deze gevallen kan het nodig zijn om de handopening te ondersteunen met een hulpmiddel. In **hoofdstuk 6** is een handexoskelet ontwikkeld dat vingerextensie van patiënten met een beroerte ondersteunt. Het apparaat wordt bestuurd door een kabel en kan de wijs- en middelvinger actief strekken. De haalbaarheid van het hulpmiddel is onderzocht in een pilottest met vier CVA-patiënten. De resultaten tonen aan dat het hulpmiddel de vingerextensie van ernstig getroffen patiënten met een beroerte kan verbeteren.

Het uitvoeren van grijptaken wordt ook bemoeilijkt als patiënten niet voldoende spierkracht hebben om objecten vast te pakken en op te tillen. In **hoofdstuk 7** is een actieve orthese ontwikkeld om de handfunctie van patiënten met dwarslaesie te ondersteunen. De ontwikkelde duimorthese is lichtgewicht en ondersteunt de laterale greep (sleutelgreep) van de hand door middel van een miniatuur lineaire actuator. Een studie met drie dwarslaesiepatiënten heeft aangetoond aan dat de orthese de grijpkracht verbetert, waardoor patiënten de handfunctie deels wordt hersteld.

De onderzoeken die gedaan zijn in het kader van dit proefschrift laten de significante stappen zien die zijn gezet bij het verbeteren van hulpmiddelen ter ondersteuning van de schouder- en handfunctie tijdens dagelijkse activiteiten.

About the author

Claudia Haarman was born on the 18th of November 1987 in Raalte, the Netherlands. She received her M.Sc. degree in Biomedical Engineering from the University of Twente, Netherlands (2012), and a Professional Doctorate in Robotics (2016), also from the University of Twente.

In 2016 she started her PhD at the University of Twente under the supervision of prof. dr. ir. Herman van der Kooij, prof. dr. Hans Rietman and ir. Edsko Hekman. Since 2016 she is working at Hankamp Rehab where she is the head of the research and development department.

Journal publications

- **Haarman, C. J. W.**, Hekman, E. E. G., Haalboom, M. F. H., van der Kooij, H., & Rietman, J. S. (2021). A New Shoulder Orthosis to Dynamically Support Glenohumeral Subluxation. IEEE Transactions on Biomedical Engineering, 68(4), 1142–1153.
- **Haarman, C. J. W.**, Hekman, E. E. G., Rietman, J. S. & van der Kooij, H. (2022). Feasibility of reconstructing the glenohumeral center of rotation with a single camera setup. Prosthetics and Orthotics International - *Online ahead of print*.
- **Haarman, C. J. W.**, Hekman, E. E. G., Rietman, J. S., & van der Kooij, H. (2022). Accurate Estimation of Upper Limb Orthosis Wear Time Using Miniature Temperature Loggers. Journal of Rehabilitation Medicine, 54(SE-Articles), jrm00277
- **Haarman, C. J. W.**, Hekman, E. E. G., van der Kooij, H., & Rietman, J. S. Evaluating the clinical effects of a dynamic shoulder orthosis. (*under review*)
- **Haarman, C. J. W.**, Hekman, E. E. G., Rietman, J. S. & van der Kooij, H., Mechanical design and feasibility of a hand exoskeleton to support finger extension of severely affected stroke patients. (*under review*)
- Bos, R. A., **Haarman, C. J. W.**, Stortelder, T., Nizamis, K., Herder, J. L., Stienen, A. H. A., & Plettenburg, D. H. (2016). A Structured overview of trends and technologies used in dynamic hand orthoses. Journal of neuroengineering and rehabilitation, 13(1), 62-62.
- Ates, S., **Haarman, C. J. W.**, & Stienen, A. H. A. (2017). SCRIPT passive orthosis: design of interactive hand and wrist exoskeleton for rehabilitation at home after stroke. Autonomous Robots, 41(3), 711-723.
- Ciullo, A. S., Veerbeek, J. M., Temperli, E., Luft, A. R., Tonis, F.J., **Haarman, C. J. W.**, Ajoudani, A., Catalano, M. G., Held, J. P. O., & Bicchi, A. (2020). A Novel Soft Robotic Supernumerary Hand for Severely Affected Stroke Patients. IEEE transactions on neural systems and rehabilitation engineering, 28(5), 1168-1177.
- Verloop, W. R. G. & **Haarman, C. J. W.**, van Vliet, R. O., de Koning, J. L., & Rietman, J. S. (2021). A newly designed shoulder orthosis for patients with

glenohumeral subluxation: a clinical evaluation study. Prosthetics and orthotics international, 45(4), 322-327.

- van der Velden, L. L., Benner, J. L., Onneweer, B., **Haarman, C. J. W.**, Selles, R., Ribbers, G., & Roebroeck, M. E. (2022). Reliability and Validity of a New Diagnostic Device for Quantifying Hemiparetic Arm Impairments: An Exploratory Study. Journal of rehabilitation medicine, 54(12), jrm00283.
- van der Velden, L. L., Onneweer, B., **Haarman, C. J. W.**, Benner, J. L., Roebroeck, M. E., Ribbers, G. M., & Selles, R. W. (2022). Development of a single device to quantify motor impairments of the elbow: proof of concept. Journal of neuroengineering and rehabilitation, 19(1), 77.

Conference contributions

- **Haarman, C. J. W**., Hekman, E. E. G., Prange, G. B., & van der Kooij, H. (2018). Joint Stiffness Compensation for Application in the EXTEND Hand Orthosis. 2018 7th IEEE International Conference on Biomedical Robotics and Biomechatronics (Biorob), 677-682.
- **Haarman, C. J. W**., Hekman, E. E. G., Maas, E.M., Rietman, J. S. & van der Kooij, H. (2022). Design and feasibility of the T-GRIP thumb exoskeleton to support the lateral pinch grasp of spinal cord injury patients. 2022 IEEE 17th International Conference on Rehabilitation Robotics.
- **Haarman, C.J.W.**, Hekman, E.E.G., Rietman, H.S., van der Kooij, H. (2019). Pushing the Limits: A Novel Tape Spring Pushing Mechanism to be Used in a Hand Orthosis. In: Carrozza, M., Micera, S., Pons, J. (eds) Wearable Robotics: Challenges and Trends. WeRob 2018. Biosystems & Biorobotics, vol 22. Springer, Cham.
- Hekman, E. E. G., **Haarman, C. J. W.**, Haalboom, M. F. H., & Rietman, J. S. (2019). A free-motion shoulder subluxation orthosis. XXVII Congress of the International Society of Biomechanics, ISB 2019, Calgary, Alberta, Canada.

Dankwoord

Met het schrijven van dit dankwoord is er (bijna) een einde gekomen aan mijn promotietraject. De afgelopen jaren heb ik veel inspirerende mensen ontmoet en met veel mensen samen mogen werken. Jullie hebben stuk voor stuk een belangrijke bijdrage geleverd aan de totstandkoming van dit proefschrift. Enkele mensen wil ik in dit dankwoord specifiek bedanken.

Mijn promotoren Herman van der Kooij en Hans Rietman, en dagelijks begeleider Edsko Hekman, zonder wie ik dit proefschrift niet had kunnen realiseren, ben ik bijzonder veel dank verschuldigd. Herman, de afgelopen jaren heb ik ontzettend veel van je geleerd. Je inhoudelijke kennis is van onschatbare waarde en onze meetings waren zeer constructief. Dank voor al je opbouwende kritiek die mij in staat zelfde om nog meer uit het onderzoek te halen. Hans, jij bent de verbindende schakel tussen de techniek en de patiënt. Door jouw vakkennis en ervaring vanuit de praktijk kon je het onderzoek vaak een duw in de goede richting geven. Met jouw enthousiasme en positiviteit wist je mij te keer op keer te motiveren. Dank voor al je vertrouwen in mijn gekke ideeën. Edsko, sinds 2011 kruisen onze paden elkaar. Eerst tijdens mijn afstuderen, daarna toen ik werkzaam was op de UT als onderzoeker, tijdens mijn PDEng traject, en nu tijdens mijn promotieonderzoek. Je bent onlosmakelijk verbonden aan mijn onderzoek, en dankzij jou is mijn voorliefde voor mechanische oplossingen gegroeid. Samen hebben we vele mooie dingen bedacht en ontwikkeld. Dank voor je al je hulp de afgelopen jaren. Hopelijk volgen er met jullie allemaal nog veel mooie samenwerkingen in de toekomst.

Verder wil ik prof. dr. ir. Gabrielle Tuijthof, prof. dr. ir. Geke Ludden, prof. dr. Ruud Selles, prof. em. Klaas Postema en dr. Judith Fleuren hartelijk danken voor het beoordelen van dit proefschrift en het plaatsnemen in mijn promotiecommissie.

Ik ben enorm veel dank verschuldigd aan alle proefpersonen die hebben meegeholpen tijdens het onderzoek. Dank voor jullie geweldige inzet. De belangrijkste inzichten heb ik opgedaan tijdens de vele testen waarbij jullie geduldig mijn aanwijzingen opvolgden. Door jullie besef ik me ook hoe waardevol je gezondheid is en hoe kleine verbeteringen aan arm- en handfunctie al een groot verschil kunnen maken in iemands leven.

Dank aan alle collega's van Hankamp Rehab en Gears. Freek, je gaf mij de kans om de bijdrage van Hankamp Rehab aan het Softpro project in te vullen middels een promotieonderzoek. Je frisse kijk op het vakgebied en ons onderzoek heeft erg geholpen om buiten de gebaande paden te denken. Dank voor al je steun de afgelopen jaren. Koen en Annelies, dank dat jullie mijn paranimfen willen zijn. Fijn dat ik alle kleine successen (en mislukkingen) tijdens mijn promotietraject met jullie heb mogen delen. Koen, vanaf het begin konden we het al erg goed met elkaar vinden. Naast de goede gesprekken die we afgelopen jaren hebben gevoerd over flenslagers, toleranties en 7075 aluminium, hebben we ook ontzettend veel gelachen. En stiekem ben je net zo'n grote fan van boybands als ik. Annelies, je werkt nu iets meer dan twee jaar bij Hankamp, maar het voelt alsof je er altijd al bent geweest. Onze samenwerking gaat bijna vanzelf en ik hoop dat we nog veel leuke projecten gaan doen de komende tijd. Marion en Britt (en Susan), dank voor jullie luisterend oor. Ik

bewonder de manier waarop jullie de mannen op kantoor en in de fabriek in het gareel houden. Verder heb ik de afgelopen jaren heel wat studenten mogen begeleiden. Dat zijn er teveel om op te noemen, ik tel er 28, maar weet dat ik jullie tomeloze inzet, gekke ideeën, en positieve bijdrage aan de sfeer op kantoor zeer heb gewaardeerd.

Dank ook aan alle (oud-)collega's van de vakgroep Biomedische Werktuigbouwkunde, in het bijzonder Mark, Arvid, Lianne, Jeanine, Yolanda, Wouter, Niek, Kostas, Victor, Heidi, Amber, Vera, Denise, Hielke, René, Bob, Stergios, Simone, Joan, Serdar, Martijn, Quint, Kyrian en natuurlijk de hele Biomechatronics groep. Dank voor alle gezelligheid tijdens de pauzes en daarbuiten! Michelle, Ander en Alejandro: ondanks dat ik de afgelopen jaren niet veel op kantoor was, hielden jullie toch altijd een plekje voor mij vrij. Bedankt daarvoor!

Dit promotietraject is deels voortgekomen uit het Softpro-project. We hebben met z'n allen heel wat afgereisd (en gegeten), met elk half jaar een overleg in een andere Europese stad. De Twentse delegatie was hierbij altijd goed vertegenwoordigd. Gerjan, Martin, Gijs, Peter, Frodo, Bert-Jan, Ed, Stefano, Anne, Jeremia, Olivier, Raffaele, Christoph, Andrea and Manuel, thank you for the very pleasant times we had during these meetings and the cool projects we did together.

Zonder de hulp van artsen, therapeuten en onderzoekers van het Roessingh, en Roessingh Research and Development zou dit onderzoek veel minder relevant zijn geweest. Ellen, Reinout, John-John, Anke, Gerdienke en Leendert, hartelijk dank voor jullie adviezen en hulp.

Familie en vrienden, bedankt voor jullie interesse in mijn werk en bijdrage aan belangrijke momenten van ontspanning tijdens het sporten, gezellige avonden en uitjes, vakanties, en de vriendenweekenden in alle uithoeken van het land.

Pap en mam. Fijn dat jullie er altijd voor mij zijn en mij hebben geleerd dat alles mogelijk is. Bedankt voor al jullie onvoorwaardelijke steun. Ik hou van jullie.

Juliet, waar moet ik beginnen met jou te bedanken? De speciale band die we hebben is eigenlijk niet te beschrijven en alles wat je voor me hebt gedaan ook niet. We zijn volgens mij een tweeling, maar dan met één jaar ertussen. Je hebt aan een half woord genoeg om te weten wat ik denk en je staat altijd voor mij klaar. Ik ben ongelooflijk trots op het feit dat ik nu in jouw voetsporen kan treden.

Otis en Juna, ook jullie verdienen hier een plekje. Het duurt nog een paar jaar voor jullie dit kunnen lezen, maar ik wil jullie bedanken voor de gezelligste afleiding die er bestaat. Door jullie besef ik me dat zo'n proefschrift eigenlijk maar weinig voorstelt vergeleken bij alles wat iemand in de eerste paar jaar van zijn leven moet leren. Dat relativeert enorm!

Lieve Jolanda. Zonder jouw steun en oneindige vertrouwen had ik nooit zo ver kunnen komen. Bedankt ook voor alle keren dat je me achter mijn computer hebt weggetrokken om een rondje te fietsen of wandelen. En dat je een oogje in het zeil hield als de 3D printer weer eens aan stond. Ik kan niet wachten om nog meer mooie dingen samen te beleven. It's always better when we're together!